Aston University

Some pages of this thesis have been removed for copyright restrictions.

If you have discovered material in AURA which is unlawful e.g. breaches copyright, (either yours or that of a third party) or any other law, including but not limited to those relating to patent, trademark, confidentiality, data protection, obscenity, defamation, libel, then please read our Takedown Policy and contact the service immediately

GAS EXCHANGE STUDIED IN A MATHEMATICAL MODEL OF THE LUNG

A thesis submitted to

THE UNIVERSITY OF ASTON IN BIRMINGHAM

for the degree of

DOCTOR OF PHILOSOPHY

by

KHURSHID AHMAD NAQVI

NOVEMBER 1984

THE UNIVERSITY OF ASTON IN BIRMINGHAM

GAS EXCHANGE STUDIED IN A MATHEMATICAL MODEL OF THE LUNG

KHURSHID AHMAD NAQVI

A thesis submitted to the University of Aston in Birmingham for the Degree of Doctor of Philosophy

NOVEMBER, 1984

SUMMARY

A mathematical model is presented to represent gas exchange in the lung during steady and unsteady state conditions in order to simulate gas uptake in a lung. From the literature survey it is apparent that the majority of work carried out on multigas exchange considers the exchange of Oxygen, Carbon Dioxide, Carbon Monoxide and Nitrogen, during elimination rather than uptake or steady state.

The model sets out to examine in a systematic way the overall gas exchange in a heterogeneous lung for both uptake and elimination under steady and unsteady state conditions. Arterial pressure (P_{aG}) against inspired alveolar ventilation perfusion ratio ($\dot{V}_{IA}/\dot{Q}$) curves for a number of gases are examined in a series of simulations and comparison between uptake and elimination is made for various degrees of solubility. The resulting gas equations are solved by using various numerical techniques and curves representing these relationships are plotted.

Finally a set of inequalities are proposed to give the conditions under which enhancement of uptake takes place.

Solubility

Enhancement

Arterial Pressure

Uptake.

DECLARATION

No part of the work described in this thesis has been submitted in support of an application for another degree or qualification of this or any other University or other institute of learning.

No part of the work described in this thesis has been done in collaboration with any other person.

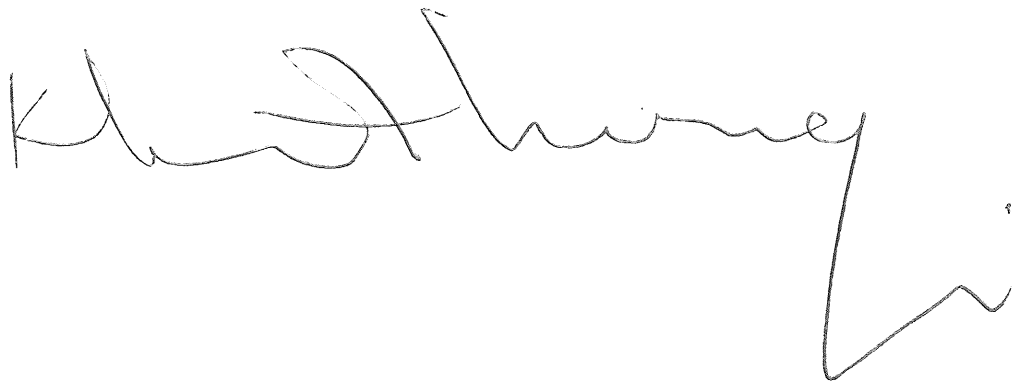

ACKNOWLEDGEMENTS

I would like to express my gratitude to Dr. D.A. Scrimshire for his guidance and supervision, and to Professor R.H. Thornley for enabling the work to be carried out in the Department of Production Technology and Production Management.

I am very grateful to the time given by Professor R. Green and Dr. E.M. Evans of the University of Manchester Medical School for the useful discussion on this topic.

I am also very grateful for the financial support given by the Science Research Council.

Finally, sincere thanks are expressed to my Mother, Brothers and Niece, Huma, for their support and encouragement throughout the project.

CONTENTS

SUMMARY

DECLARATION

ACKNOWLEDGEMENTS

LIST OF FIGURES

LIST OF SYMBOLS

DEFINITIONS

LIST OF TABLES

CHAPTER I INTRODUCTION

1.1 Background of research 1

1.2 An overview of the thesis 3

1.3 Conclusions 4

CHAPTER 2 LUNG STRUCTURE AND FUNCTION

2.1 Architecture of the human lung 5

2.2 Ventilation (breathing) 7

2.3 Transport of gases by the blood 8

2.3.1 Carbon Dioxide exchange 8

2.3.2 Oxygen exchange 10

CHAPTER 3 GENERAL LITERATURE SURVEY

3.1 Inert gas exchange 14

3.2 Inert gas and ventilation perfusion in-homogeneity 14

3.3 Earlier models 20

3.3.1 The Böhr equations 20

3.3.2 The Haldane and Krögh controversy 21

3.3.3 Inhomogeneity 22

	3.3.4	Rileys method	22
	3.3.5	Farhis model	23
	3.3.6	Farhi and Yokoyama	24
	3.3.7	The Evans model	25
	3.4	Other models	26
	3.5	Regional Inequalities	26
CHAPTER 4		THE MATHEMATICAL MODEL	
	4.1	Inert gas elimination	39
	4.2	Derivation of equations	40
	4.2.1	Gas exchange in a homogeneous lung	40
	4.2.2	Exchange of two gases	41
	4.2.3	Multigas exchange in a lung model	42
	4.3	Elimination and uptake in a lung model	42
	4.3.1	Elimination phase	42
	4.3.2	Uptake phase	42
	4.4	Model for overall gas exchange	43
	4.4.1	Generation of ventilation and perfusion data	43
	4.4.2	Data options	44
	4.5	$\dot{V}_A/\dot{Q}$ model	44
	4.5.1	$\dot{V}_A/\dot{Q}$ model for homogeneous lung	44
	4.5.2	$\dot{V}_A/\dot{Q}$ model for two gases	44
	4.5.3	$\dot{V}_A/\dot{Q}$ model for multigas exchange	45
	4.5.4	$\dot{V}_A/\dot{Q}$ model (elimination phase)	47
	4.5.5	$\dot{V}_A/\dot{Q}$ model (uptake phase)	47

4.6	Gas exchange in a two compartment model	48
4.6.1	Gas exchange in a multicompartment lung model	49
4.6.2	Elimination in a multicompartment lung model	51
4.6.3	Uptake in a multicompartment lung model	52
4.7	Analysis of uptake and elimination	54
4.8	The Newton Raphson method	55
CHAPTER 5	RESULTS OF SIMULATION	
5.1	Independent $\dot{V}_A$ and $\dot{Q}$ distribution	59
5.2	Effect of increasing the solubility of uptake	60
5.2.1	Solubility of uptake $\lambda_1 = 0.001$	60
5.2.2	Solubility of uptake $\lambda_1 = 0.01$	61
5.2.3	Solubility of uptake $\lambda_1 = 0.1$	61
5.2.4	Solubility of uptake $\lambda_1 = 1.0$	61
5.2.5	Solubility of uptake $\lambda_1 = 10.0$	62
5.3	Effect of increasing the solubility of elimination by a factor of ten	62
5.3.1	Solubility of uptake $\lambda_1 = 0.001$	62
5.3.2	Solubility of uptake $\lambda_1 = 0.01$	62
5.3.3	Solubility of uptake $\lambda_1 = 0.1$	63
5.3.4	Solubility of uptake $\lambda_1 = 1.0$ and $\lambda_1 = 10.0$	63
5.4	Effect of increasing the solubility of elimination from 0.001 to 10.0	63
5.5	Effect of changing the degree of inequality B	64
5.6	Overall gas exchange	64

5.6.1 Effect of changing the solubility of uptake (λ) from 0.001 to 10.0 64

5.6.2 Effect of increasing the solubility of elimination (λ) by a factor of 10. 64

5.7 Individual uptake 65

5.7.1 Constant ventilation λ_2 = 0.01,0.1 65

5.7.2 Constant perfusion λ_2 = 0.01,0.1 65

5.7.3 Constant ventilation λ_2 = 1,10 65

5.7.4 Constant perfusion λ_2 = 1,10 66

5.7.5 Constant ventilation λ_2 = 1.00,0.1 for λ_3 = 0.01 66

5.7.6 Constant perfusion λ_2 = 1.00,0.1 for λ_3 = 0.01 66

5.8 Comparison for all the uptake curves 67

5.8.1 Constant ventilation 67

5.8.2 Constant perfusion 67

5.9 Uptake curves for $\dot{V}_{A/\dot{Q}}$ model 67

CHAPTER 6 DISCUSSIONS

6.1 Calculation of alveolar tension of one inert tracer gas 106

6.1.1 Farhis equations 106

6.1.2 Evans equations 107

6.2 Gas exchange of two inert gases, expressed in terms of $\dot{V}_{A/\dot{Q}}$ ratio 108

6.3 Acute effect of ventilation perfusion inequality on gas exchange 112

6.4 Effect of increasing ventilation 114

6.5	Effect of increasing blood flow	114
6.6	Critical inspired ventilation perfusion ratio	116
6.7	Enhancement in uptake	117
6.7.1	Constant ventilation λ_2 = 0.01,0.1	117
6.7.2	Constant perfusion λ_2 = 0.01,0.1	118
6.8	Enhancement in uptake for $\dot{V}_{A/Q}$ model	118
6.9	General conditions for enhancement in uptake	118
CHAPTER 7	CONCLUSIONS	121
CHAPTER 8	FUTURE WORK	122
APPENDIX A	COMPUTER SIMULATION OF THE MODEL	124
A.1	List of variables used in the simulation	125
A.2	Flowchart for the simulation of the model	127
A.3	Computer Hard Copy	134
APPENDIX B	SOLUTION OF THE CUBIC EQUATION	148
B.1	List of variables	149
B.2	Flowchart	150
B.3	Hard Copy	152

LIST OF FIGURES

1.	Schemetic representation of the trachea	12
2.	Model of the bronchial tree of Horsfield, Relea and Cumming	13
3.	Interaction between ventilation-perfusion ratio and partition coefficient in the elimination of inert gases	31
4.	Relative role of ventilation and perfusion in gas exchange	32
5.	Ventilation-perfusion lines for two tracers	33
6.	Effect of inert gas exchange on O_2 and CO_2 tensions	34
7.	Oxygen-Carbon Dioxide diagram showing ventilation-perfusion ratio lines	35
8.	Three compartment lung model	36
9.	Log normal distribution curves for a large degree of ventilation-perfusion ratio inequality	37
10.	Ten compartment lung model	38
11.	Elimination of gas via the alveolous in a multi-compartment lung model	58
12.	Uptake of gas in a multicompartment lung model	58
13.	Uptake-elimination process, where two gases are being taken up while the third is being eliminated	69
14.	Elimination-uptake curves for solubility of uptake 1 = 0.001, elimination = 0.001.	70
15.	Elimination-uptake curves for solubility of uptake 1 = 0.01, elimination = 0.001	71

16. Elimination-uptake curves for solubility of uptake 1 = 0.1, elimination = 0.001 — 72

17. Elimination-uptake curves for solubility of uptake 1 = 1.0, elimination = 0.001 — 73

18. Elimination-uptake curves for solubility of uptake 1 = 10.0, elimination = 0.001 — 74

19. Effect of increasing the solubility of elimination by a factor of ten; uptake 1 = 0.001, elimination = 0.01 — 75

20. Uptake-elimination curves for solubility of elimination = 0.01, uptake 1 = 0.01 — 76

21. Uptake-elimination curves for solubility of elimination = 0.01, uptake 1 = 0.1 — 77

22. Uptake-elimination curves for solubility of elimination = 0.01, uptake 1 = 1.0 — 78

23. Uptake-elimination curves for solubility of elimination = 0.01, uptake 1 = 10.0 — 79

24. Effect of increasing the solubility of elimination = 0.1, by a factor of ten; 1 = 0.001, elimination = 0.1 — 80

25. Elimination-uptake curves for solubility of uptake 1 = 0.01, elimination = 0.1 — 81

26 Elimination-uptake curves for solubility of uptake 1 = 0.1, elimination = 0.1 — 82

27 Elimination-uptake curves for solubility of uptake 1 = 1.0, elimination = 0.1 — 83

28. Elimination-uptake curves for solubility of uptake 1 = 10.0, elimination = 0.1 — 84

29.	Effect of increasing the solubility of elimination by a factor of ten; uptake 1 = 0.001, elimination = 1.0	85
30.	Elimination-uptake curves for solubility of uptake 1 = 0.01, elimination = 1.0	86
31.	Elimination-uptake curves for solubility of uptake 1 = 0.1, elimination = 1.0	87
32.	Elimination-uptake curves for solubility of uptake 1 = 1.0, elimination = 1.0	88
33.	Elimination-uptake curves for solubility of uptake 1 = 10.0, elimination 1.0	89
34.	Effect of increasing the solubility of elimination by a factor of ten; uptake 1 = 0.001, elimination = 10.0	90
35.	Elimination-uptake curves for solubility of uptake 1 = 0.01, elimination = 10.0	91
36.	Elimination-uptake curves for solubility of uptake 1 = 0.1, elimination = 10.0	92
37.	Elimination-uptake curves for solubility of uptake 1 = 1.0, elimination = 10.0	93
38.	Elimination-uptake curves for solubility of uptake 1 = 10.0, elimination = 10.0	94
39.	Uptake-Elimination curve for various degrees of inequality using a log linear scale	95
40.	Uptake/Elimination curve for various degrees of inequality using a log linear scale	96

41. Individual uptake curves for constant ventilation, solubility of uptake 2 = 0.001,0.1 — 97

42. Individual uptake curves for constant perfusion, solubility of uptake 2 = 0.01,0.1 — 98

43. Individual uptake curves for constant ventilation, solubility of uptake 2 = 1.0,10 — 99

44. Individual uptake curves for constant perfusion solubility of uptake 2 = 1.0,10 — 100

45. Individual uptake curves for constant ventilation, solubility of uptake 2 = 1.0,0.1 for elimination = 0.01 — 101

46. Individual uptake curves for constant perfusion, solubility of uptake 2 = 1.0,0.1 for elimination = 0.01 — 102

47. Comparison of all the uptake curves for constant ventilation — 103

48. Comparison of the uptake curves for constant perfusion — 104

49. Uptake curves for $\dot{V}_A/\dot{Q}$ model — 105

LIST OF SYMBOLS

	Symbol	Definition
I General variables	V	Gas volume
	$\dot{V}$	Gas volume per unit time (ventilation).
	P	Gas pressure
	F	Fractional concentration of gas indry phase
	C	Concentration in blood phase
	R	Respiratory exchange ratio (volume CO_2/volume O_2)
	$\dot{Q}$	Volume flow of blood
II Symbol for the gas phase (small capitals)	I	Inspired gas
	E	Expired gas
	A	Alveolar gas
	T	Tidal gas
	D	Dead space gas
	B	Barometric
III Symbol for the blood phase	b	Blood in general
	a	Arterial
	v	Venous
	c	Capilliary
	$\bar{v}$	Mixed venous
IV Special symbols and abbreviations	$\bar{X}$	Dash above any symbol indicates a mean value
	$\dot{X}$	Dot above any symbol indicates a time derivative

	Symbol	Definition
	S	Subscript to denote the steady state
(small capitals)	STPD	Standard temperature pressure, dry ($0\,^{\circ}C$, 760 mmHg)
V Other symbols	λ	Blood gas partition coefficient (Ostwald partition coefficient Farhi (12)).
	α	Bunsen solubility coefficient $\lambda = 1.136\ \alpha$

DEFINITIONS

DIFFUSION HYPOXIA	dilution of Oxygen when Nitrous Oxide is eliminated from the blood.
HYPOXIA	deficiency of Oxygen
HYPOXEMA	deficiency of Oxygen in the blood
INERT	the gas which does not react with blood
HYPERCARBIA	deficiency of Carbon Dioxide

LIST OF TABLES

1. Gases suitable for uses in simulation 57

2. Approximate composition of the Atmosphere 120

CHAPTER 1

INTRODUCTION

1.1 Background of Research

Theoretical developments in the quantitative description of the physiology of gas exchange within the lung have helped to clarify and systematize much existing information as well as suggesting new concepts and experimental investigation. The increasing use of computers in analysing data and the development of new instrumentation have helped the analysis of respired gas. So far the respiratory physiologists have considered the organ as a 'black box' Nunn (1) and produced mathematical models in order to gain insight in this organ. These models were simulated using numerical techniques and conclusions were drawn which failed to give an accurate and complete picture. As these models have been in use for a few decades, most students have grown up to regard the model as the real lung. When actual pulmonary structure is discussed, senior workers regard Miller (2) as the final authority. The first quantitative analysis was that of Böhr (3) who assumed the lungs have only two compartments; a dead space and an alveolar space. The simple Böhr equation describes respiratory gases moving in and out of the lung model, which is now defined as alveolar ventilation. This analysis was improved in the field of aviation medicine by Brink (4), Helmholz et al (5) and Riley and Cournand (6) to produce the well known alveolar gas equation.

There are two reasons for the fact that the regional ($\dot{V}_{A/Q}$) (gas volume per unit time/volume flow of blood) inequality always reduces the efficiency of pulmonary gas exchange.

1. Multicompartment models based on the (classical) analysis of Riley and Cournand (6) and Rahn (7) invariably give rise to Hypoxia (deficiency of Oxygen) and Hypercarbia (deficiency of Carbon Dioxide) when subjected to unequal ventilation ($\dot{V}_A$) or perfusion ($\dot{Q}$) irrespective of the form assumed e.g. Farhi and Rahn (8), West (9), Kelman (10), Scrimshire (11). The consideration of Oxygen (O_2) and Carbon Dioxide (CO_2) exchange was viewed as a special case.

2. By considering the exchange of a single physiological inert * gas, it has been demonstrated by Farhi (12), Shah et al (13), Farhi and Olszwka (14), Dantzker et al (15), West (16, 17) and Wagner (18) that both elimination and uptake will be <u>impaired</u> when $\dot{V}_{A/\dot{Q}}$ ratios within the lung become unequal.

The majority of work carried out on multigas so far considers the gas exchange in a theoretical lung model; the gases exchanged being limited to O_2, CO_2 and CO (and much later) N_2. Other gases were studied in isolation but mainly by anaesthesiologists or toxicologists and it was only a decade ago that other respiratory gases were used as indicators, such as Krypton by Gurtner et al (19), Briscoe and Cournand (20) and Rochester et al (21). <u>All</u> the work points to the fact that only one gas at a time was considered (taken up or eliminated) in the human lung.

The majority of the workers, such as Scrimshire and Tomlin (22), Scrimshire (23), and Wagner (18) considered the exchange of O_2 and CO_2 due to its physiological implications in the real situation.

* A gas which does not react chemically with blood, Farhi (12)

Wagner (18) agreed with the findings of West (16) and Scrimshire (11) that the maldistribution of blood flow but not of ventilation tends to affect CO_2 more, whereas maldistribution of ventilation has a more pronounced effect on O_2.

The reason for studying inert gas exchange during elimination Farhi (12) rather than uptake or steady state was that it was possible to deal with each gas as if its transport were independent of that of the other gases in question, even though exchange of any one gas is always affected by the other inert gases, as well as by the exchange of Oxygen (O_2) and Carbon Dioxide (CO_2). The term "second gas effect" Stoelting (24) is used to describe and explain what happens when two inert gases are inhaled. As the transfer of the gases not normally present in respired air has such a profound effect on arterial oxygen levels and because these changes are functionally linked to $\dot{V}_{A/Q}$ ratios, it is interesting to speculate whether $\dot{V}_{A/Q}$ inequalities will have the same influence in situations in which one or more inert gases are present in the inspirate.

1.2 An Overview of The Thesis

A new mathematical model will be presented in this thesis which will set out to examine in a systematic way the overall gas exchange in a hetrogenous lung model. The model is based upon the original gas exchange equations of Riley and Cournand (6), Rahn (7) and Farhi (12). The mathematical model developed in Chapter 4 was simulated using techniques described elsewhere by Scrimshire and Naqvi (71) for inspired alveolar ventilation to perfusion ratio ($\dot{V}_{IA/Q}$) and arterial pressure of the gas (P_{aG}). The gas equations are solved using the Newton Raphson method. Arterial pressure (P_{aG}) against inspired alveolar ventilation to per-

fusion ratio ($\dot{V}_{IA/\dot{Q}}$) curves are examined for a series of simulations and a comparison is made between the variation of (P_{aG}) for various degrees of solubilities (λ). A series of uptake against various degrees of inequality (B) curves are plotted, and the comparison between uptake and elimination curves for various degrees of solubilities (λ) made. Finally a set of inequalities are derived to give the conditions under which enhancement of uptake will take place.

1.3 Conclusions

A number of important conclusions result from analysis of the simulated gas exchange equations. They may be stated as follows:

(a) That the presence of regional ($\dot{V}_{IA/\dot{Q}}$) inequality <u>does not</u> always reduce the efficiency of pulmonary gas exchange confirming the classical analysis of Riley and Cournand (6) and Rahn (7).

(b) That both elimination and uptake are <u>not</u> always impaired when the $\dot{V}_{A/\dot{Q}}$ ratios within the lung became unequal. Demonstrated by Farhi (12), Scrimshire (11) and West (16, 17).

(c) Under certain conditions, the uptake is <u>enhanced</u> for a given parameter set.

In conclusion,this study of a ten compartment lung model,Figure (10) for gas exchange, questions all the previous findings, and in future a practical study under clinical conditions should be considered.

CHAPTER 2

LUNG STRUCTURE AND FUNCTION

2.1. Architecture of the Human Lung

The lungs communicate via the trachea, or windpipe which has a flexible tubular structure that extends from the larynx downward through the midline of the neck and into the thorax. It has a mean diameter of 1.8 cm and length of 11 cm Nunn (25), and lies in front of the esophagus. Despite the flexibility of the trachea, it's walls are very strong because of the presence of 16 to 20 U shaped tracheal cartilages. These cartilages are placed horizontally, one above the other, at very close intervals (Figure 1). The open end of the U is at the back, facing the esophagus, and the gap is bridged by connective tissue and smooth muscle. The cartilage rings keep the trachea open at all times for the passage of air to and from the lungs.

The trachea ends by dividing into right and left primary bronchi which extend to the lungs. Each bronchus enters the lung of its own side through a slit, called the Lilus. The right, primary bronchus is more nearly vertical, shorter, and wider than the left. As soon as each primary bronchus enters its respective lung it branches to form smaller or secondary bronchi. Each lobar bronchus continues to branch dichotomously for approximately twelve generations down to the terminal bronchioles (25). The branching network of respiratory tubes resemble the branches of a tree; thus it is referred to as the bronchial tree, (Figure 2). The lungs are cone-shaped organs, Weibel and Gomez (26) which fill their own halves of the thorax. The total number of alveoli present in a healthy adult is of the order of 300×10^6 (27, 28) which collectively provide for a total internal surface area of $100m^2$ West (17). The right

lung is shorter and broader than the left. The concave base of each lung rests as the diaphragm and the apex extend into the root of the neck for a distance of about 2.5 cm above the first rib. The medial surface of each lung is also concave and shows the imprint of the heart. Above and behind the cardiac imprint is the helius, or slit, through which pass those structures that make the root of the lung. The root structure includes the primary bronchus, the pulmonary and the bronchial blood vessels, the lymphatics, and the nerves. The lungs are freely moveable except at the hilus where they are anchored by the root and the pulmonary ligaments.

Each lung is invested by a transparent, serous membrane called the pleura. This membrane is arranged in the form of a closed sac and consists of two layers - a visceral layer and a parietal pleura lines the inner surface of the chest wall, covers the upper surface of the diaphragm, and is reflected over the structures of the midiastinum. The two layers of the pleura are continuous with one another around the root of each lung. The pleural layers are held in close contact with one another by the cohesive effect of a thin film of serous fluid; this fluid also serves to lubricate the surfaces so that they can glide smoothly, one over the other.

The lungs are light, porous, and spongy in texture. Within the spongy tissue are the secondary bronchi and the bronchioles which pipe air to and from the respiratory units of the lung. An important feature of lung tissue is its great elasticity; this property is of fundamental importance during the act of breathing.

Deep tissues divide each lung into lobes, the right lung has three lobes (superior, middle and inferior) while the left lung has only two lobes (superior and inferior). The individual lobes are further sub-divided into small lobules.

The lobules are irregular in shape and size, but each is supplied with a bronchial. As a bronchial enters a lobule it branches repeatedly to form terminal bronchioles. Each terminal bronchiole, in turn, branches into two or more respiratory bronchioles, to which alveolar ducts and sacs are attached. Alveolar sacs are clusters of cup-shaped, thin walled alveoli which share a common opening. Each alveolar is surrounded by a network of capilliaries and supported by elastic and relicular fibres. Gas is exchanged between the lungs and the blood by diffusion through the thin walls of the alveoli and the capilliaries.

2.2 Ventilation (Breathing)

The process of ventilation is sub divided into inspiration (breathing in) and expiration (breathing out).

During inspiration,the upward-curving diaphragm contracts, pulling downward, and increasing the vertical length of the thoracic cage. The intercostal muscles pull the ribs upward and outward. Thus the thoracic cage is increased in size laterally and vertically. It is this active increase in size of the cage that causes lung expansion and the "pulling" in of air.

Expiration is passive; all the contracted muscles relax. The surface tension of fluid lining the alveoli causes a continual tendency of the alveoli to collapse, as does the elasticity of the lung tissue. Therefore with relaxation of respiratory muscles, the lung recoils and air is pushed

out of the lungs.

2.3 Transport of Gases by the Blood

2.3.1 Carbon Dioxide Exchange

Carbon Dioxide is carried in three ways by the blood, dissolved carbon dioxide (CO_2), bicarbonate ion, and haemoglobin carbonate compounds, Klocke (29). The latter two compounds are not exchanged across the alveolar capilliary membrane and must be converted into free carbon dioxide prior to excretion in the lungs.

About 64 percent is carried in the form of bicarbonate ion according to the equation

$$CO_2 + H_2O \longrightarrow H_2CO_3 \longrightarrow H^+ + HCO_3^-$$

part of the bicarbonate ion is formed within the plasma by the above reaction; part is formed within the erythrocyte; HCO_3^- concentration, increases within the red cell until it begins to diffuse out of the cell into the plasma, and to maintain electrical neutrality, plasma chloride ion moves into the cell (the chloride shift). Up to about 27 percent of the carbon dioxide is carried, attached to the globin portion of the haemoglobin molecule, in the form of carbaminohaemoglobin.

About 9 percent is carried in physical solution in the plasma and the chemical reaction can be explained by the following equation:

$$CO_2 + H_2O \longrightarrow H_2CO_3 \longrightarrow HCO_3^- + H^+$$

$$+$$

$$CO_2 + HgbO_2 + HgbCO_2 + O_2$$

$$\downarrow$$

$$H\,Hgb + O_2 + O_2$$

Hydrogen ion produced from the dissociation of carbonic acid is buffered by haemoglobin and by the plasma buffering system to resist changes in PH.

At the tissues, carbon dioxide (CO_2) dissolves in plasma water or enters the erythrocytes to react with cellular water. In each case, carbonic acid is formed, which dissociates into hydrogen ion and bicarbonate ion. The hydrogen ion produced in the plasma is buffered by reacting with plasma proteins, but the hydrogen ion produced within the erthrocytes does not pass through the cell membrane and is buffered by haemoglobin. Bicarbonate ion accumulates within the erythrocytes and soon begins to diffuse out of the cell into plasma. A loss of negative charge occurs, and to return electrical neutrality, chloride ion moves from the plasma into the erythrocytes (chloride shift). Some carbon dioxide (CO_2) displaces oxygen (O_2) from the haemoglobin and the excess H^+ in the erythrocyte drops the PH and also drives oxygen (O_2) from the haemoglobin. This accounts for two thirds of the total CO_2 uptake. Holland and Forester (30).

At the lung, the action of carbonic anhydrose liberates carbon dioxide (CO_2) from erythrocyte carbonic acid. To reform carbonic acid requires that the hydrogen ion from within the cell chemically reacts with bicarbonate ion from the plasma. As bicarbonate ion moves into the erythrocyte, an excess of negative charge accumulates and chloride ion moves back into the plasma. The high oxygen levels in this region cause displacement of carbon dioxide (CO_2) from the haemoglobin and the formation of oxyhaemoglobin occurs. Hydrogen ion is released from its combination with protein as bicarbonate enters the erythrocyte, and protein is made available to buffer more H^+. The above processes show an interrelationship between gas transport and the buffering system of the body.

2.3.2 Oxygen Exchange

Oxygen (O_2) is carried in the blood in two forms, the greater part is in the form of a reversible chemical combination with haemoglobin, while a smaller part is in physical solution in plasma and intracellular fluid. The ability to carry large quantities of oxygen (O_2) in the blood is of great importance to the body, since without haemoglobin, the amount carried would be so small that the cardiac output would need to be increased by a factor of 20 to give an adequate oxygen flux. This would require a considerable increase in blood volume. Each gram of haemoglobin carries 1.34 ml of oxygen (31).

Thus 98.5 percent of the oxygen transported in the blood stream is carried in haemoglobin as a compound called oxyhaemoglobin. Oxygen combines with the iron atoms of the four heme molecules found in a molecule of haemoglobin. Since oxygen (O_2) combines as a molecule with the haemoglobin, each haemoglobin molecule can carry eight atoms of oxygen. The four atoms of iron in a haemoglobin molecule do not become oxygenated or deoxygenated simultaneously. Oxygen is taken up in steps, with each step having its own constant (K). Thus oxygen (O_2) uptake can be represented as: (haemoglobin Hb) using Adair's hypothesis (32).

$$Hb_4 + O_2 \underset{K_1}{\overset{K_1'}{\rightleftharpoons}} Hb_4O_2 \qquad K_1 = \frac{K_1'}{K_1}$$

$$Hb_4O_2 + O_2 \underset{K_2}{\overset{K_2'}{\rightleftharpoons}} Hb_4O_4 \qquad K_2 = \frac{K_2'}{K_2}$$

$$Hb_4O_4 + O_2 \underset{K_3}{\overset{K_3'}{\rightleftharpoons}} Hb_4O_6 \qquad K_3 = \frac{K_3'}{K_3}$$

$$Hb_4O_6 + O_2 \underset{K_4}{\overset{K'_4}{\rightleftharpoons}} Hb_4O_8 \qquad K_4 = \frac{K'_4}{K_4}$$

The velocity constant of each dissociation is indicated by a small k. The addition of a prime ('), defining the velocity constant of the forward reaction K'_3 is thus the velocity constant of the reaction Hb_4O_4 with O_2 to yield Hb_4O_6. The ratio of the forward velocity constant to the reverse velocity constant equals the equilibrium constant of each reaction in the series (K) as mentioned above.

The separate velocity constants have been measured Nunn (25) and it is now known that the last reaction has a forward velocity constant (K'_4) which is much higher than that of the other reactions. During the saturation of the last 75 percent of reduced haemoglobin, the last reaction will predominate and the high velocity counteracts the effects of the ever diminishing number of oxygen-receptors which would otherwise slow the reaction rate by the law of mass action, Staub (33). In fact the reaction proceeds at much the same rate until saturation is completed. The significance of this in relation to oxygen transfer in the lung has been presented by Staub (34).

The gas exchange (uptake and elimination), in the model presented in this thesis follows exactly the same principles as described above.

FIGURE 1

Schemetic Representation of Trachea

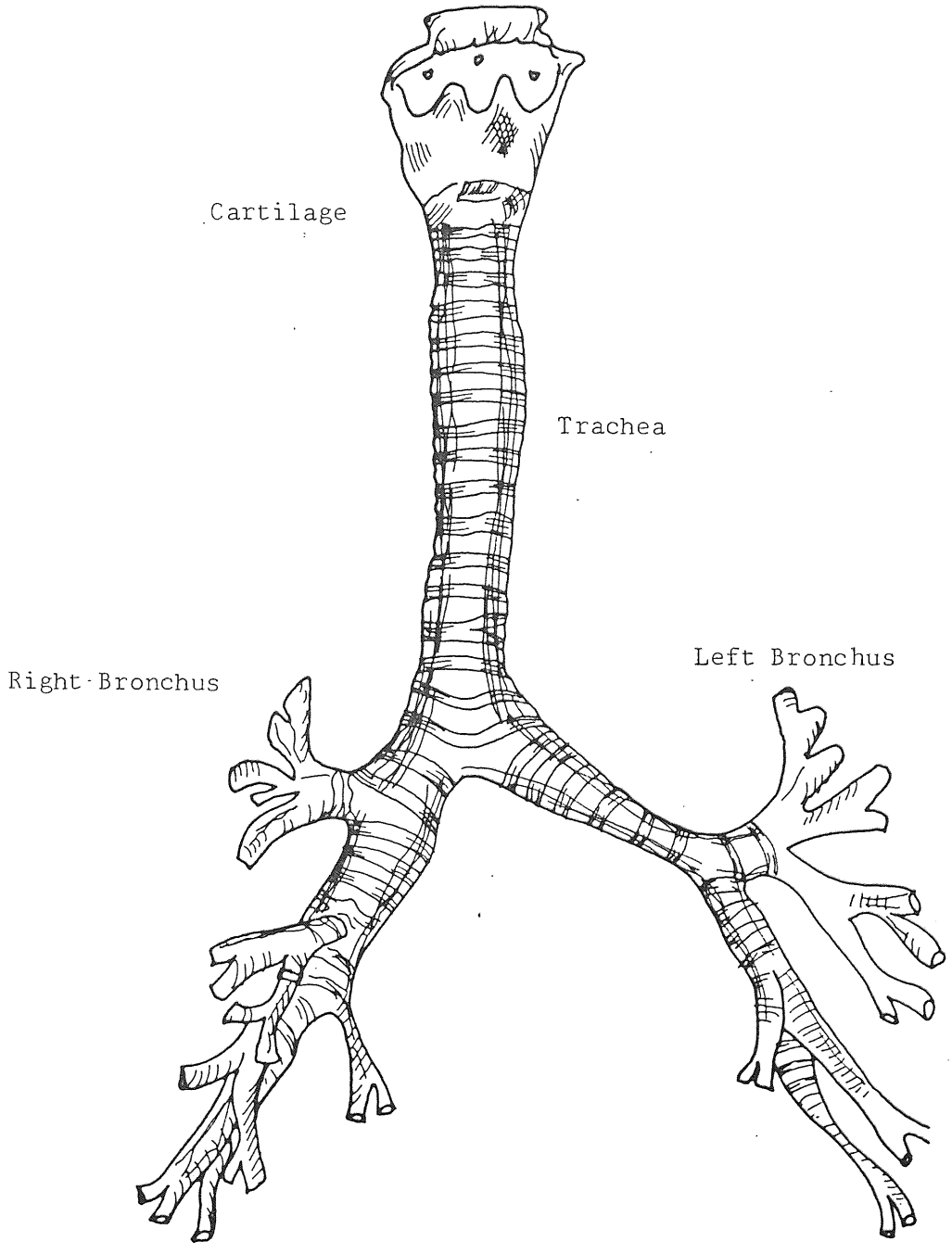

FIGURE 2

Model of The Bronchial Tree of Horsfield, Relea and Cunning

Showing Symmetrical Branching

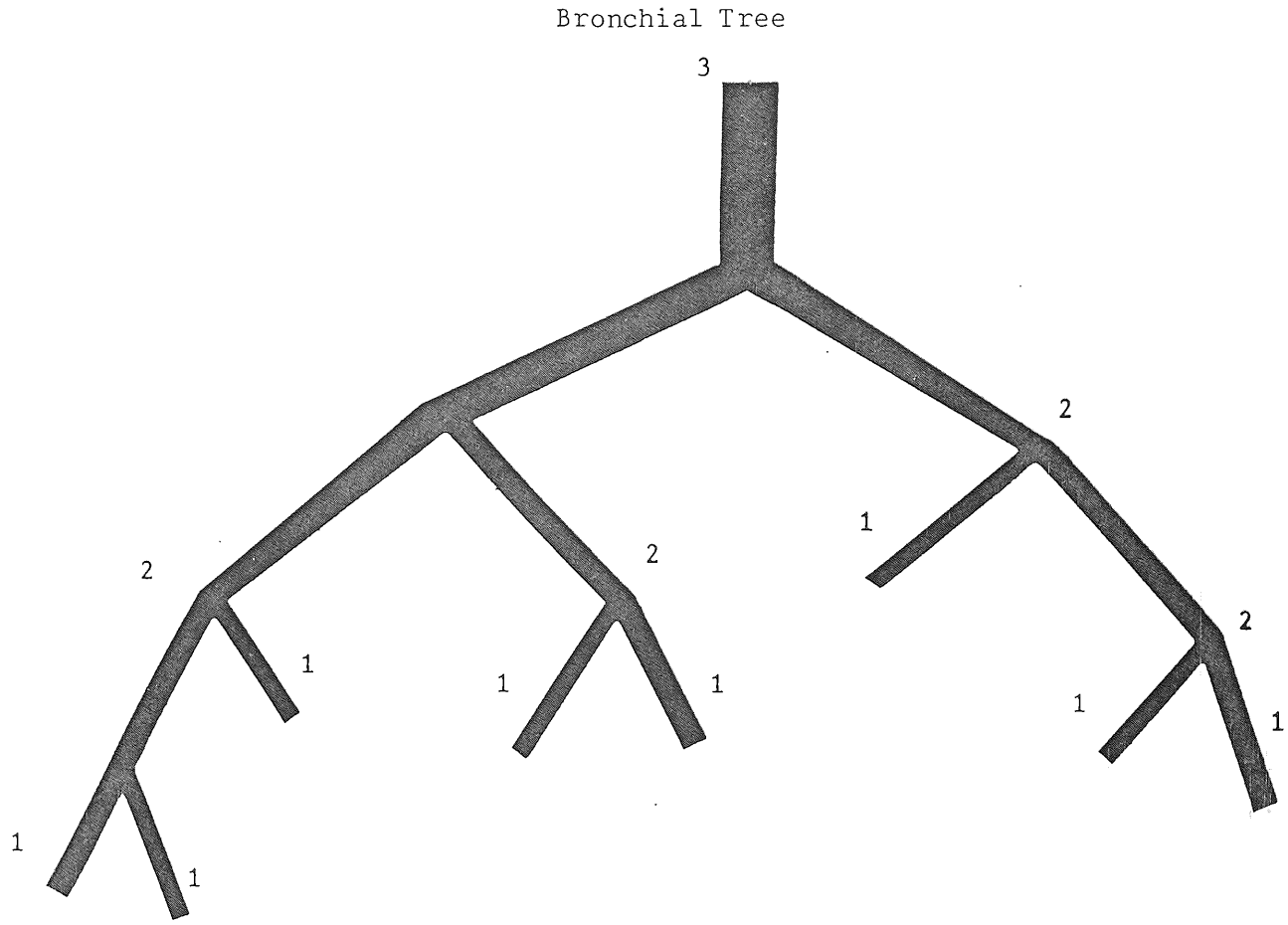

CHAPTER 3

GENERAL LITERATURE SURVEY

3.1 Inert Gas Exchange

Respiratory physiologists have been interested in transport of oxygen (O_2) and carbon dioxide (CO_2) only and have excluded other gases for more than a hundred years. Nitrogen (N_2) and other inert gases were considered simply as "filler gases" until it became clear that inert gases could further the understanding of oxygen (O_2) and carbon dioxide (CO_2) exchange. Another disadvantage is that inert gases have a wide range of solubilities, i.e. a factor of approximately 10^5 is presented between the solubilities of acetane and sulphur hexafluoride (SF_6) in blood.

3.2 Inert Gases and Ventilation Perfusion In-homogeneity

It is recognised that the unequal distribution of ventilation perfusion ($\dot{V}_A/\dot{Q}$) ratio throughout the lung, must effect the efficiency of gas exchange, Colburn et al (35), Evans et al (36), Scrimshire (11) and Farhi and Yokoyama (37). It is also obvious that all gases that exchange across the alveolar epithelium must similarly be effected.

Inert gas reaching the lung in solution in the pulmonary arterial blood must leave this organ either in the expired alveolar gas, or in the pulmonary venous blood. Partition of the tracer gas between the two exit rates will depend on the relative size of the two sinks. It is easy to assume that if ventilation increases, the amount of inert gas eliminated in the gas phase will rise, whereas an increase in either blood flow ($\dot{Q}$) or solubility of the inert gas will boost the fraction of the tracer retained in the blood. Thus the gas will be partitioned between expirate

and blood flow according to their relative flows and to the relative affinity of the two media for the gas. This qualitative statement is expressed mathematically by Farhi (12). Considering the condition where the inert gas is not present in the inspirate, the total amount of gas presented to the lung must be equal to the sum of the two outputs giving

$$\dot{Q} \; C_{\bar{P}_{v_n}} = \dot{Q} \; C_{P_{a_n}} + \dot{V}_A \; (P_{a_n} / 863) \qquad (1)$$

Where $\dot{Q}$ is the pulmonary blood flow, C stands for the concentration, P_a and P_v indicate pulmonary artery and pulmonary vein respectively, n represents the inert gas, P_a is the alveolar pressure. The correction factor 863 is used to express $\dot{V}_A$ at S.T.P.D.

The above equation can also be expressed slightly differently reflecting the fact that the blood that reaches the lung is systemic mixed venous blood and that the blood leaving the lung is usually sampled in a peripheral artery, and by introducing the blood gas partition coefficient, this leads to

$$\dot{Q} \; \lambda \; P_{\bar{v}_n} = \dot{Q} \; \lambda \; P_{a_n} + \dot{V}_A \; P_{a_n} \qquad (2)$$

$$P_{a_n} = P_{\bar{v}_n} \; \dot{Q} \; \lambda / (\dot{Q} \; \lambda + \dot{V}_A) \qquad (3)$$

where $P_{\bar{v}_n}$ is the mixed venous pressure of the gas.

It is convenient to look at the retention of the tracer (second gas), which is defined as the fraction of amount presented to the lung that remains in blood after it has equilibrated with alveolar gas. Since the value of the inert gas reaching the lung is $\dot{Q} \; \lambda \; P_{\bar{v}}$ while the volume retained is $\dot{Q} \; \lambda \; P_a$ the retention R must equal $P_a / P_{\bar{v}}$. Combining with the above equation (3) this gives

$$R = \dot{Q}\lambda / (\dot{Q}\lambda + \dot{V}_A) \quad (4)$$

Where the term $\dot{Q}\lambda$ gives effective blood flow, i.e. the blood flow considered as a sink for the tracer, which takes into account both the actual perfusion and the ability of blood to start the inert gas exchange.

Dividing both sides by $\dot{Q}$ gives

$$R = \lambda / (\lambda + \dot{V}_A/\dot{Q}) \quad (5)$$

Which separates the relative affinity and the relative flows, and brings into focus the ratio of ventilation to perfusion (Figure 3) as described by Farhi (12).

A complementary equation deals with "clearance", i.e. the virtual blood flow from which a complete washout of the tracer would have resulted in the same tracer elemination. This is calculated as

$$\text{Clearance} = \dot{Q}(\dot{V}_A/\dot{Q}) / (\lambda + \dot{V}_A/\dot{Q}) \quad (6)$$

The above equation is of great importance in predicting elimination of anaesthetic or toxic gases from the organism. When such a gas is poorly soluble, its elimination by the lung is practically complete, and a sizeable increase in the output of the gas can be produced only by raising pulmonary perfusion, i.e. transport of inert gases of low solubility is perfusion dependant. Fractional elimination of very soluble, inert, gases is relatively low and can only be boosted by an increase in ventilation. Elimination of these gases is therefore said to be ventilation dependant (Figure 4).

Extending this analysis to study the simultaneous elimination of two gases by the same lung or part of the lung, as described by Farhi (12),

(Figure 5). If $\dot{V}_A/\dot{Q}$ is extremely low, the elimination of both gases will be small. As the values of $\dot{V}_A/\dot{Q}$ are gradually increased, elimination rises. Farhi found that the retention of more soluble gas is always greater. The difference again seems to disappear when $\dot{V}_A/\dot{Q}$ is so high that the retention of either gases is practically zero.

Farhi and Yokoyama (37) found that the $\dot{V}_A/\dot{Q}$ line will be straight if the two gases have the same value of λ and will show an increased deviation from linearity as the ratio of $\dot{V}_A/\dot{Q}$ deviates from unity. The standard $\dot{V}_A/\dot{Q}$ line, i.e. the one drawn for O_2 and CO_2 is found similarly to that calculated for two theoretical gases, the λ of which would be equal to the slope of the O_2 and CO_2 dissociation curve.

Yokoyama and Farhi (38) used the simultaneous elimination of two inert gases to divide the lung into two equivalent compartments. The basic principle was that both expired gas and the arterial blood are influenced by the composition of blood returning from each of the two compartments, but to a different degree, reflecting the fact that the alveoli, with a high $\dot{V}_A/\dot{Q}$ must effect mixed alveolar gas compositions more than mixed pulmonary venous blood, with the converse being true for alveoli with low $\dot{V}_A/\dot{Q}$.

Yokoyama and Farhi (38) used the simultaneous elimination of two inert gases in animal lungs and their results described three equivalent sets of two compartments each. This concept leads to the conclusion that under identical conditions in the same lung, different pairs of tracers will yield a different set of compartments. In a hypothetical lung there would be three types of alveoli: X with $\dot{V}_A/\dot{Q} = 0.01$, Y with $\dot{V}_A/\dot{Q} = 1$, and Z with $\dot{V}_A/\dot{Q} = 100$. If the two inert gases in question have a very low solubility, of the order of 0.1, then they will both

be eliminated by type Y and Z alveoli, and the resulting model will divide the lung into X and (Y + Z). If the value of $\dot{V}_A/\dot{Q}$ is chosen about 10 then both X and Y will retain the tracers, and the mathematical analysis will yield a lung model made up of (X + Y) and Z.

Wagner et al (39) developed a better technique for blood analysis allowing one to measure accurately the level of several inert gases and also the improved mathematical treatment of data so as to allow progress in two directions. This helped in expanding the above concept to a more realistic representation of the lung. Wagner et al (40) showed that one can use a set of six different inert gases to expand the basic concept into multidimensional analysis. It was also possible to break down the arterial compartments which was criticized by Olszowka (41) and Jaliwala et al (42). This was later answered by Evans and Wagner (43) but they came to a conclusion that complicating factors such as common respiratory dead space, series ventilation inequality and diffusion disequilibrium impaired inert gas exchange. The reason for studying inert gases during elimination rather than uptake or steady state is that it is possible to deal with each gas as if its transport were independent of that of the other gases in question, even though exchange of any one gas is always effected by the other inert gases, as well as by the exchange of Oxygen (O_2) and Carbon Dioxide (CO_2).

Considering the effect of Oxygen (O_2) and Carbon Dioxide (CO_2) on an inert gas exchange in a subject breathing air, the volume of inspired gas normally exceeds that of expired gas, because the amount of Carbon-

dioxide (CO_2) added by the pulmonary circulation is less than the volume of oxygen (O_2) uptake. Hence nitrogen (N_2) represents a higher fraction of the alveolar gas, where fractional concentration of nitrogen F_{N2} is commonly 1 percent higher than in inspired gas. This was pointed out by Canfield and Rahn (44) because the gas exchange ratio of elements has a low $\dot{V}_A/\dot{Q}$ and is lower than that of the whole lung, the F_{N2} in these units must be higher than in the lung as a whole. There are a number of logical extensions to this statement:

1. Since the alveoli contribute proportionately more to the blood leaving the lungs than to mixed alveolar gas, they will raise the arterial pressure of nitrogen (P_{N_2}) more than the alveolar, i.e. if there is a $\dot{V}_A/\dot{Q}$ inhomogeneity, there must be an arterial - alveolar nitrogen (N_2) difference and this has been used to quantitate maldistribution.

2. There must be a continuous nitrogen (N_2) exchange in the lungs even though there is no net nitrogen (N_2) transport. With low $\dot{V}_A/\dot{Q}$ the alveoli force some nitrogen (N_2) into the blood, while with high $\dot{V}_A/\dot{Q}$ the alveoli are responsible for an equal and opposite nitrogen (N_2) elimination.

Considering an example in which mixed venous pressure of Nitrogen is 570 mmHg and alveolar pressure of Nitrogen is 630 mmHg, then each unit of blood passing through the capillaries will only take up a thousandth of its volume of Nitrogen(N_2). It has been shown by Farhi and Olszowka (14) that it is only at extremely low $\dot{V}_A/\dot{Q}$ that oxygen (O_2) pressure or uptake is effected. Since inert gas Nitrogen (N_2) movement is impaired

by the combination of low solubility and a small alveolar mixed venous pressure difference, it is useful to investigate the effects of changes in either one or both parameters.

Fink (45) reported on the effects of exchange of a 'soluble' inert gas on Oxygen, he also defined a phrase of "diffusion hypoxia" to describe the dilution of Oxygen (O_2) when Nitrous Oxide (N_2O) is eliminated from the blood. Farhi and Olszowka (14) presented a more comprehensive analysis of the situation using Nitrous Oxide (N_2O) as an example, and indicated that during Nitrous Oxide (N_2O) uptake when the effects of inert gas are magnified by the high solubility and by a large alveolar mixed venous Nitrous Oxide (N_2O) difference, the alveolar Oxygen (O_2) tension may actually exceed that of the inspired gas, Figure (6).

Epstein et al (46) showed that when one, poorly soluble gas is concentrated as a result of uptake of a more soluble one, the second gas effect is observed, i.e. during induction of anaesthesia, Stoelting (24).

3.3 Earlier Models

This section describes earlier models upon which the model proposed in this thesis is based. Initially, all the gas exchange equations originated from the Böhr equations. Later a controversy between Haldane (47) and Krogh (48) increased the awareness of these equations and acted as catalyst for further work, and led to the models of Farhi (12), Farhi and Yokoyama (37) and eventually that of Evans (49).

3.3.1 The Böhr Equations

Böhr (3) introduced mixing equations from which the dead space (V_D) can be calculated if the expired tidal volume (V_T) and functional concentration of any component in inspired, expired and alveolar gases

(F_{I_x} F_{E_x} F_{A_x}) are known. They were derived as follows:

The total amount of any gas expired is equal to the amount in the dead space, plus the amount expired from the alveoli, i.e.

$$V_T \; F_{E_x} = V_D \; F_{I_x} + (V_T - V_D) \; F_{A_x} \qquad (7)$$

$$\frac{V_D}{V_T} = \frac{F_{A_x} - F_{E_x}}{F_{A_x} - F_{I_x}} \qquad (8)$$

3.3.2 The Haldane and Krogh Controversy

Both investigators believed that the lung behaved essentially as a large volume of alveoli in which gas exchange took place and that it connected to the atmosphere by a system of airways in which no gas exchange occurred. This is now defined as respiratory dead space.

There was substantial agreement between Krogh and Haldane on the magnitude of dead space volume during quiet breathing. The average value was found to be about 150 ml which agreed with the earlier results of Zuntz (50) and also those of Rührer (51), who had experimented on a cadaver lung.

The controversy, which continued for many years, was that the dead space volume was a static property of the lungs that varied little with large tidal volumes (hyperventilation) or exercise. Krogh (48) and Haldane (47) saw it as much more functional and entirely capable of physiological adaptation.

The controversy emphasized the difference in the measurement of dead space between the use of an exchanging gas such as Carbon Dioxide (CO_2) and a gas such as Hydrogen (H_2), which is in diluted form in the alveolar

gas. A later distinction was drawn between the physiological dead space, which is the volume of the lung that does not eliminate Carbon Dioxide (CO_2) and the anatomic dead space which is the volume of the conducting airways down to the level where the rapid dilution of an inspired, insoluble gas occurs with gas already in the lung. This reflects the geometry of the airways system. Fowler (52) describes the now accepted method for measuring the anatomic dead space by his use of the single breath Nitrogen (N_2) washout test. The term "physiological" was introduced for the dead space. Enghöff (53) used arterial P_{CO_2} rather than the alveolar P_{CO_2} value in the Böhr equation. This modification was further developed by Riley et al (54).

3.3.3 Inhomogeneity

Much of the research on pulmonary gas exchange since the second world war has been directed at a better understanding and expression of the inhomogeneity of alveolar gas and capillary blood. The Haldane - Krogh controversy acted as a catalyst to prompt research in the last thirty years on gas exchange.

3.3.4 Riley's Method

In the Riley and Cournand (6) method the P_{O_2} and P_{CO_2} of arterial blood and mixed expired gas are used to construct a three compartment model of the lung, as shown in Figure 8. One compartment (physiological shunt) is considered to be perfused but unventilated; ($\overline{V}$ on Figure 7) another (physiologic dead space) ventilated but unperfused (I on Figure 7) and the third compartment (ideal) contains the remaining portion of the ventilation and blood flow (point i on Figure 7).

The elegance of Riley's model lay in its simplicity. In 1946 Lillienthal and Riley (55) made an assumption that the percentage of various ad-

mixtures remained unchanged during low Oxygen (O_2) breathing. Using this assumption they devised a method for determining the diffusion capacity of Oxygen (O_2). This was accepted for two decades until it was shown to be simplistic by West (17) and Riley and Permutt (56).

This was the model which formed the basis for Farhi (12), Farhi and Yokoyama (37), Evans (49).

3.3.5 Farhi's Model

Farhi (12) considers a theoretical lung in which the ventilation perfusion ratio is equal in all elements, or to any single respiratory unit, and it is acknowledged due to Ball et al (57) and West and Dollery (58) that the normal lung does not fulfil these conditions. It is used, however, to establish the following relationship in which assumptions are made:

1. Blood leaving the lungs is in equilibrium with the alveolar gas

$$P_{aG} = P_{AG} \tag{9}$$

as described by Forster (59), Bates and Christie (60).

2. The amount of inert gas remaining in the alveolar gas volume is constant Nöehren (61), using Fick's equation 12. The amount of gas eliminated from the blood as it traverses the lungs is given by:

$$\dot{V}_{bG} = \dot{Q} (C\bar{V}_G - Ca_G) \tag{10}$$

α is the Bunsen solubility coefficient

$$\dot{V}_{bG} = \dot{Q} \frac{\alpha}{760} (P_{\bar{V}G} - P_{aG}) \tag{11}$$

since

$$P_{aG} = P_{AG}$$

$$\dot{V}_{bG} = \dot{Q} \frac{\alpha}{760} (P_{\overline{V}G} - P_{AG}) \quad (12)$$

$$\dot{V}_{AG} = \dot{V}_A F_{AG} \quad (13)$$

$$\dot{V}_{AG} = \dot{V}_A \frac{P_{AG}}{863} \quad (14)$$

$$\dot{Q} \frac{\alpha}{760} (P_{\overline{V}G} - P_{AG}) = \dot{V}_A \frac{P_{AG}}{863} \quad (15)$$

$$P_{AG} = P_{\overline{V}G} \frac{1.136\,\alpha}{1.136\,\alpha + \dot{V}_{A/\dot{Q}}} \quad (16)$$

$$P_{AG} = P_{\overline{V}G} \frac{\lambda}{\lambda + \dot{V}_{A/\dot{Q}}} \quad (17)$$

Similar gas equations were developed by Kety (62) Nöehren (61) and Severinghaus (63).

The conclusion drawn is that a greater increase in elimination is obtained when $\dot{Q}$ is increased than when $\dot{V}_A$ is increased by the same amount.

In this case it is seen that whatever the gases chosen (O_2 and CO_2) in this case, the uptake is impaired. Our findings clearly contradict their conclusions.

3.3.6 Farhi and Yokoyama (37)

The model presented is very similar to the one of Farhi (12) with certain modifications, i.e.

$$P_A = P_{\overline{V}} \frac{\lambda}{\lambda + \dot{V}_{A/\dot{Q}}} \quad (18)$$

P_A is defined in relation to $P_{\overline{V}}$ by

$$\frac{P_A}{P_{\bar{V}}} = \frac{\lambda}{\lambda + \dot{V}_{A/\dot{Q}}} \qquad (19)$$

The elimination of two gases is considered and a two compartmental equivalent model is used.

According to equation (18) the conclusion drawn is that whenever the $\dot{V}_{A/\dot{Q}}$ of alveolar is higher than that of the lungs, the partial pressure of the gas eliminated by this element must be lower than that prevailing in the rest of the lung.

He concludes that the shape of the $\dot{V}_{A/\dot{Q}}$ curve is dictated by the ratio λ_1/λ_2 regardless of the absolute value of λ_1 (partition coefficient of the inert gas 1) and λ_2 (partition coefficient of the inert gas 2).

3.3.7 The Evans Model (49)

This model is an extension of Farhi's model (12) and Farhi and that of Yokoyama (37), i.e. compartmental model. It is assumed that the lung is composed of a large number of compartments receiving continuous ventilation and perfusion at fixed rates and that there is complete equilibrium of the inert gas (no diffusion impairment) within each compartment.

The problem posed is of parallel equivalence to that of Wagner and Evans (64).

In the case of steady state exchange of an inert gas in parallel ventilation and perfusion models, the assumption is made that the carrier is not exchanged - a statement which we have found to be untrue. In our model the exchange of test gas is considered similar to the exchange of the gas in a homogeneous (one compartment) model with the same total

ventilation and perfusion and the same inspiratory and venous partial pressures of the inert gas.

3.4 Other Models

Briscoe (65, 66) developed a model with two compartments, one of which was poorly ventilated and this slow compartment was identified by inert gas studies. Briscoe's model accounts for the hypoxemia (Oxygen deficiency in blood) in patients with chronic, obstructive pulmonary disease better than the venous admixture of the three compartment model, and it predicts the effects of oxygen therapy better.

West and Dollery (58) introduced a radioactive gas technique that added spatial localization of $\dot{V}/\dot{Q}$, thus enhancing the information available from analysis of expired gas and arterial blood.

Wagner et al (67) devised a multiple inert gas technique that gives the complete distribution of ventilation and perfusion throughout the lungs. This technique answered all the questions of uneven distribution in the lungs.

3.5 Regional Inequalities

All the previous work concerned with the study of regional inequalities upon overall gas exchange has assumed that the variation in ventilation and blood flow in the lungs is such, that the pattern of ventilation-perfusion ratios so produced is compatible with the log normal distribution. This concept was first introduced by Rahn (7) who showed that an $(A - a)D_{O_2}$ of 8 mmHg would be developed in a lung if the standard deviation of the distribution was log 1.3. At a later stage Farhi and Rahn (68) demonstrated that progressively larger $(A - a)D_{O_2}$ values would result if the range of ventilation-perfusion ratios was widened by in-

creasing the standard deviation. Kelman (69) and West (16) carried out similar studies. They assumed a fixed body metabolism to simulate the changes in mixed venous blood gases in the steady state and to show that the output of carbon dioxide was affected nearly as much as the uptake of Oxygen (O_2) by inequalities in regional $\dot{V}_{IA}/\dot{Q}$ ratios, while the former study confirmed the earlier findings of higher $(A - a)D_{O_2}$ values when the range of $\dot{V}_{IA}/\dot{Q}$ ratios is increased; and also defined the changes in P_{aCO_2} and P_{aN_2} (arterial nitrogen and carbon dioxide pressures).

West (16) used a log-normal distribution of ventilation per unit volume with constant blood flow per unit volume to generate data. He observed that the impairment of gas exchange resulting from inequalities was identified with that found with perfusion inequalities and he attributed this to the feature of a log-normal distribution. The data generated from the log-normal distribution of ventilation and blood flow for a six compartment lung model is shown in Figure 9. There is very little difference seen in the $\dot{V}_{IA}/\dot{Q}$ ratios generated for the majority of the compartments regardless of the fact that uneven distribution of ventilation or blood flow is assumed. The only major difference in $\dot{V}_{IA}/\dot{Q}$ ratios are in the two compartments at the extreme ends of the range; since these compartments are poorly perfused their influence on mixed arterial blood gas content is negligible.

The difference between the $\dot{V}_{IA}/\dot{Q}$ ratios generated from the distributions will increase as the number of compartments increase.

The lung model is considered here which consists of ten equal volume alveolar compartments Figure (10) with an uneven distribution of ventilation and an even distribution of blood flow as described by Scrimshire

(11). The assumption made by Scrimshire (11) was that the parameters under consideration; be it ventilation or perfusion, follow a geometric progression. The same assumptions are made here.

The most commonly used distribution is log-normal due to its simplicity, West (16). Recently Scrimshire (11) generated ventilation and blood flow data by using a particular 'geometric progression distribution' and showed that models having unequal ventilation produce more hypoxia and less hypercarbia than unequal blood flow models.

West's (16) model using log-normal distribution failed to show any differences in gas exchange irrespective of whether ventilation or blood flow was assumed to be uneven. The reason was that the distribution generated by West, assuming uneven ventilation per unit volume, is identical to the one generated assuming uneven blood flow per unit volume. The result was proved by Scrimshire (11).

As Scrimshire (11) argued that there is no experimental evidence to support the contention that a log-normal distribution with large standard deviation represents the conditions existing in a diseased lung. The work of Briscoe and Cournand (20) has shown that Nitrogen washout data obtained from subjects with emphysema are not comparable with such distribution patterns, in that too great a proportion of the lung volume is too poorly ventilated. Scrimshire (11) suggested that the true frequency distribution would have to be very much skewed with its peak well to one side. Scrimshire (11) agreed that no physiological meaning is attached to the forms he used, but he found that uneven distributions of ventilation conformed to this general specification.

Finally as many naturally occurring phenomena take the form of a geometric progression it would not, therefore, be unreasonable to postulate a geometric series model.

In general the relative magnitude of ventilation or blood flow to any alveolar compartment (I) is expressed as $A^{(R + (I-1)b)}$ by Scrimshire (11). From this equation, it is obvious that the range of magnitude of blood flow or ventilation is dependant upon the parameters A and b, and upon the equal number of compartments. The number of compartments (I) is taken as equal to ten due to the analysis of West (16) which states that very little change occurs in accuracy of models of this type on increasing the number of compartments beyond ten.

The value of b (degree of inequality) determines the range of distribution where the value of b has been taken from 0 to 2.0 in steps of 0.25.

To generate data for a lung model having an uneven distribution of ventilation and an even distribution of blood flow, a particular value must be assigned to parameter b so that the values for compartmental ventilation may be calculated. For the blood flow data b is set equal to zero to produce identical blood flows for each compartment. Similarly, an uneven distribution of blood flow and an even distribution of ventilation may be generated by interchanging the assigned values of b. The two separate distributions thus formed will be said to possess the same degree of inequality and so the range of compartmental ventilation in the first distribution is equal to the range of compartmental blood flow in the second. Appendix A shows the ranges of $\frac{\dot{V}_{IA}}{\dot{Q}}$ ratios generated for a ten compartment model are increased as the degree of inequality (i.e. parameter b) of uneven distribution of ventilation and even distribution of blood flow is increased, and uneven distribution of blood flow and an even distribution of ventilation is increased. The relative increase in $\frac{\dot{V}_{IA}}{\dot{Q}}$ ratios over the range was found to be identical for distributions having uneven ventilation and distributions having uneven

blood flow with the same value of parameter b. For example, with b equal to 1.0 there was found to be a five hundred-fold increase in the $\frac{\dot{V}_{IA}}{\dot{Q}}$ ratios for both distributions. Although the relative changes in $\frac{\dot{V}_{IA}}{\dot{Q}}$ ratio are equal for uneven distribution of ventilation and even distribution of blood flow, and uneven distribution of blood flow and even distribution of ventilation, generated with the same value b it can be seen that the distributions embodying uneven ventilation consistently have lower $\frac{\dot{V}_{IA}}{\dot{Q}}$ ratios than the corresponding distributions having uneven blood flow. It is also noted that the difference between the two types of distribution becomes more marked as the degree of inequality increases. This further endorses the findings of Scrimshire (11).

FIGURE 3

Interaction Between Ventilation - Perfusion Ratio and Partition Coefficient

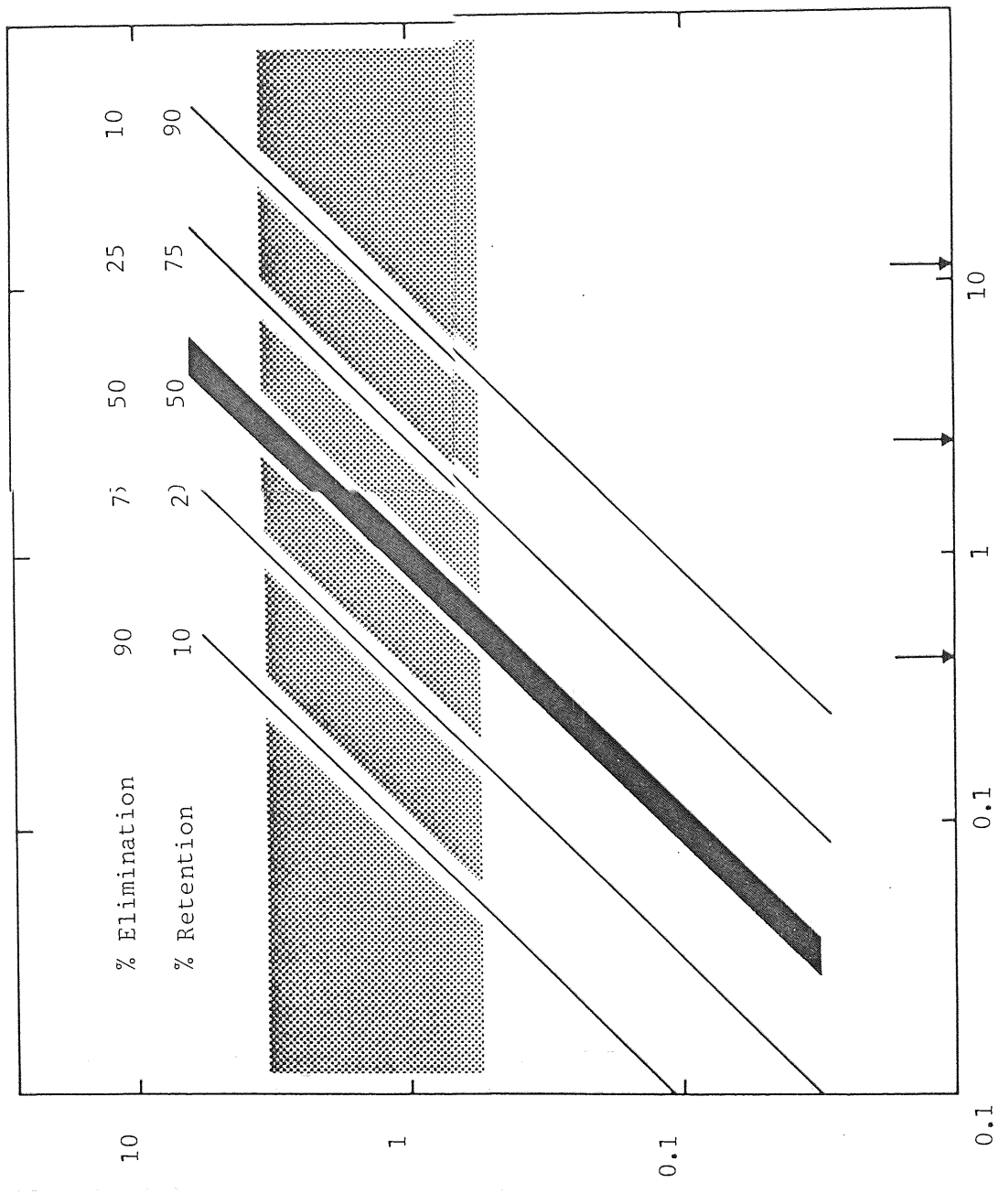

FIGURE 4

Relative Rule of Ventilation and Perfusion In Gas Exchange

Xenon Clearance

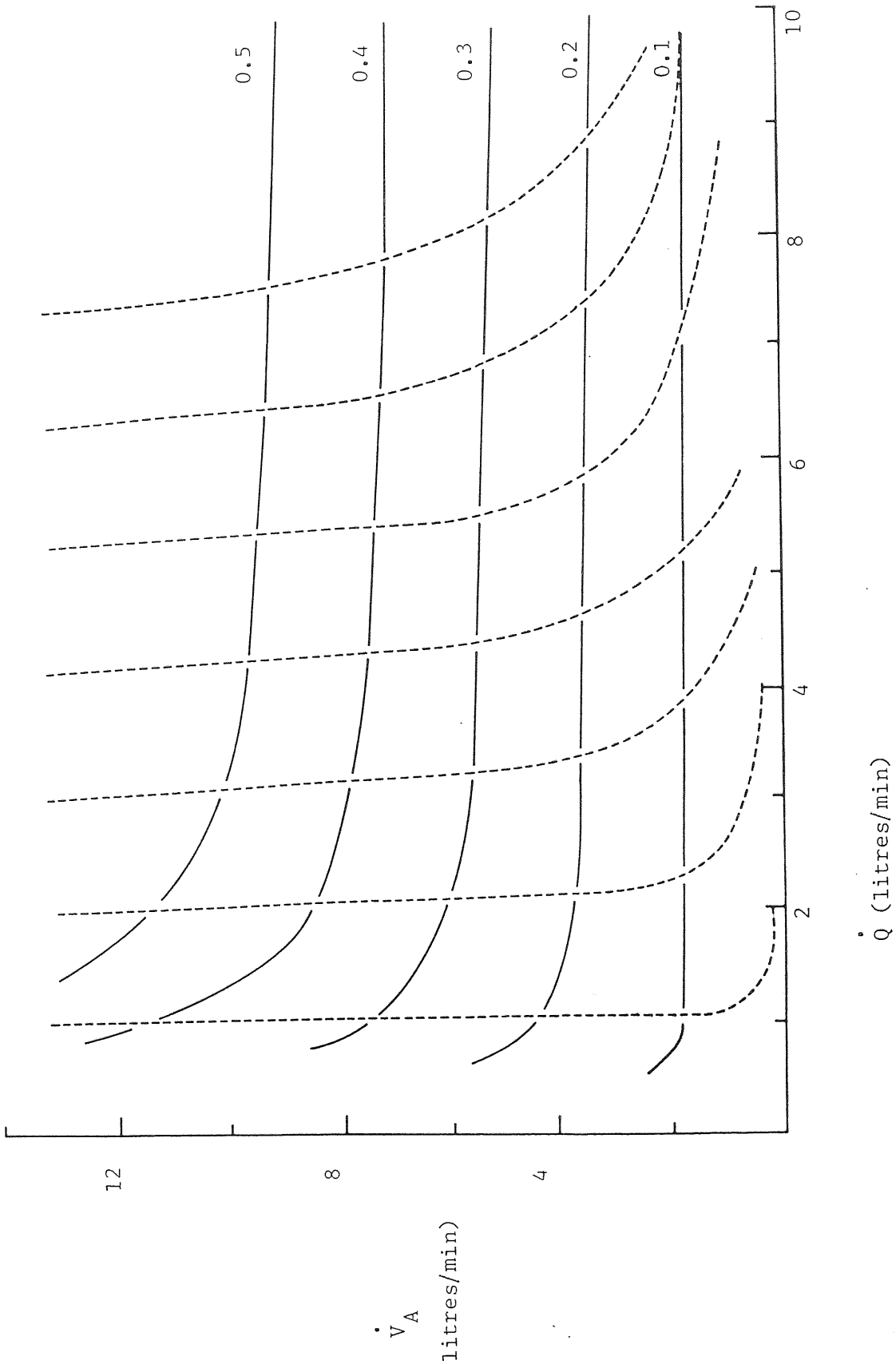

FIGURE 5

Ventilation Perfusion Lines for Two Tracers

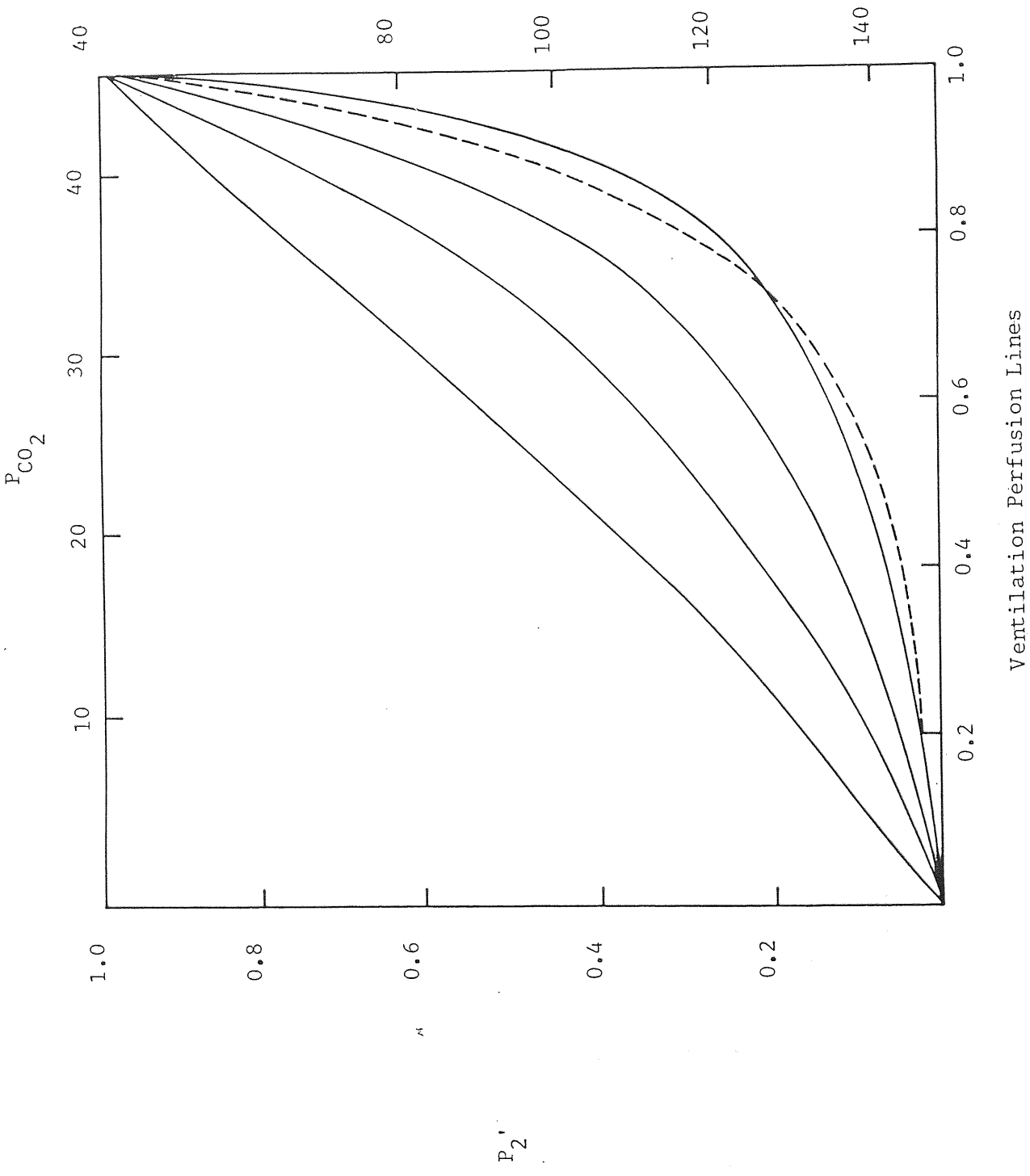

FIGURE 6

Effect of Inert Gas Exchange On O_2 and CO_2 Tensions

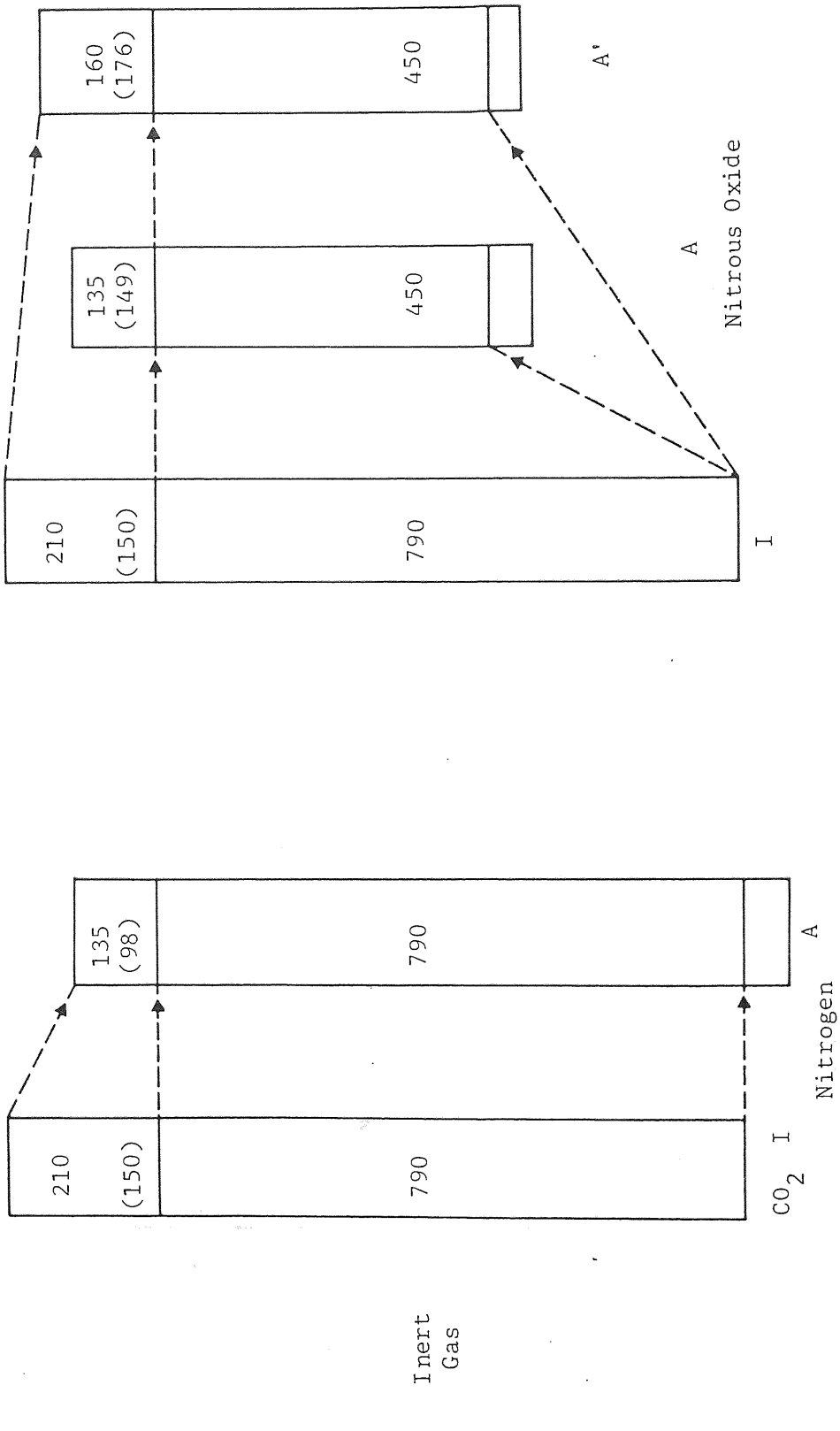

FIGURE 7

Oxygen Carbon Dioxide Diagram

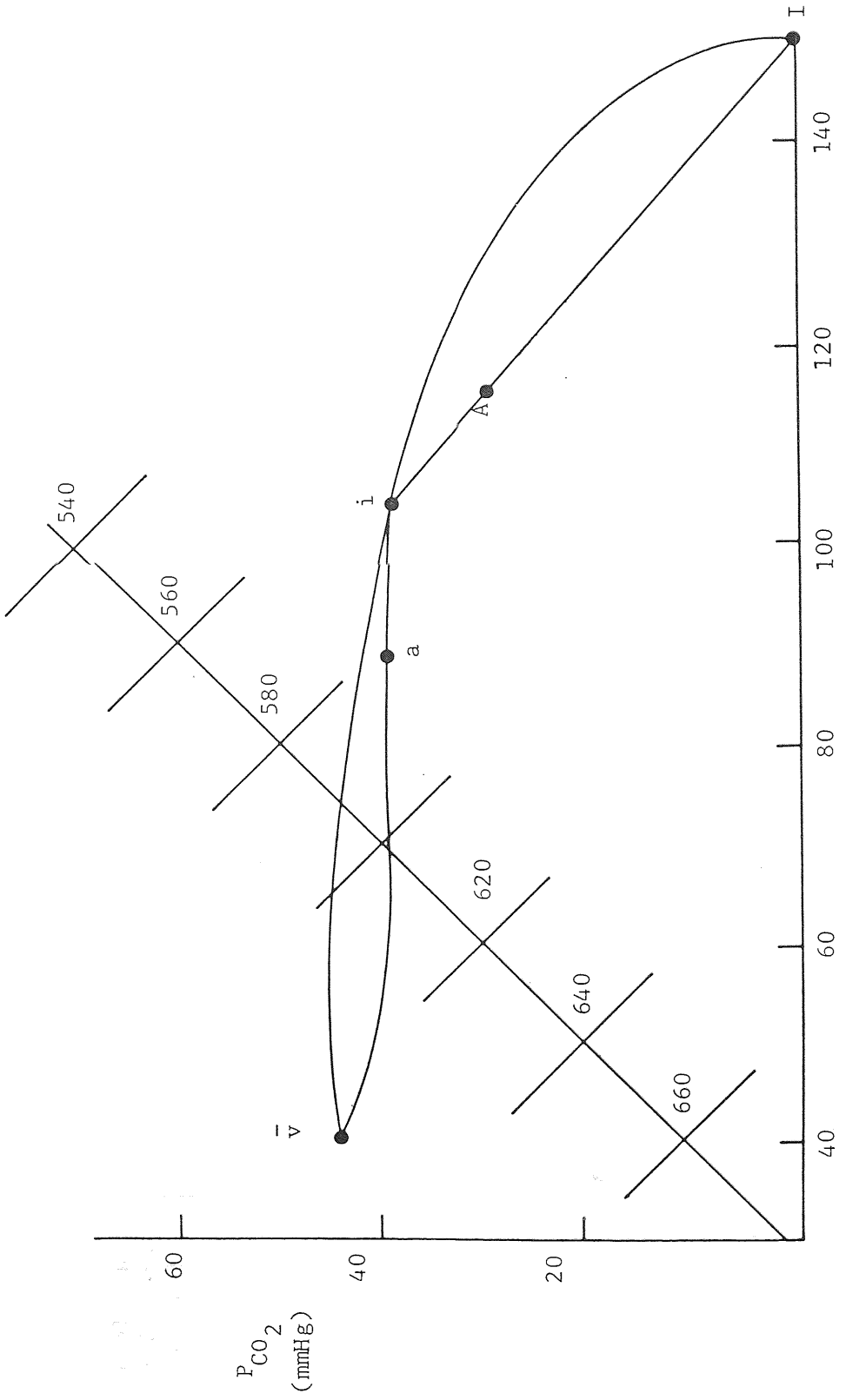

FIGURE 8

Analysis of Riley and Cournand. The Lung is Presented As Three Compartments.

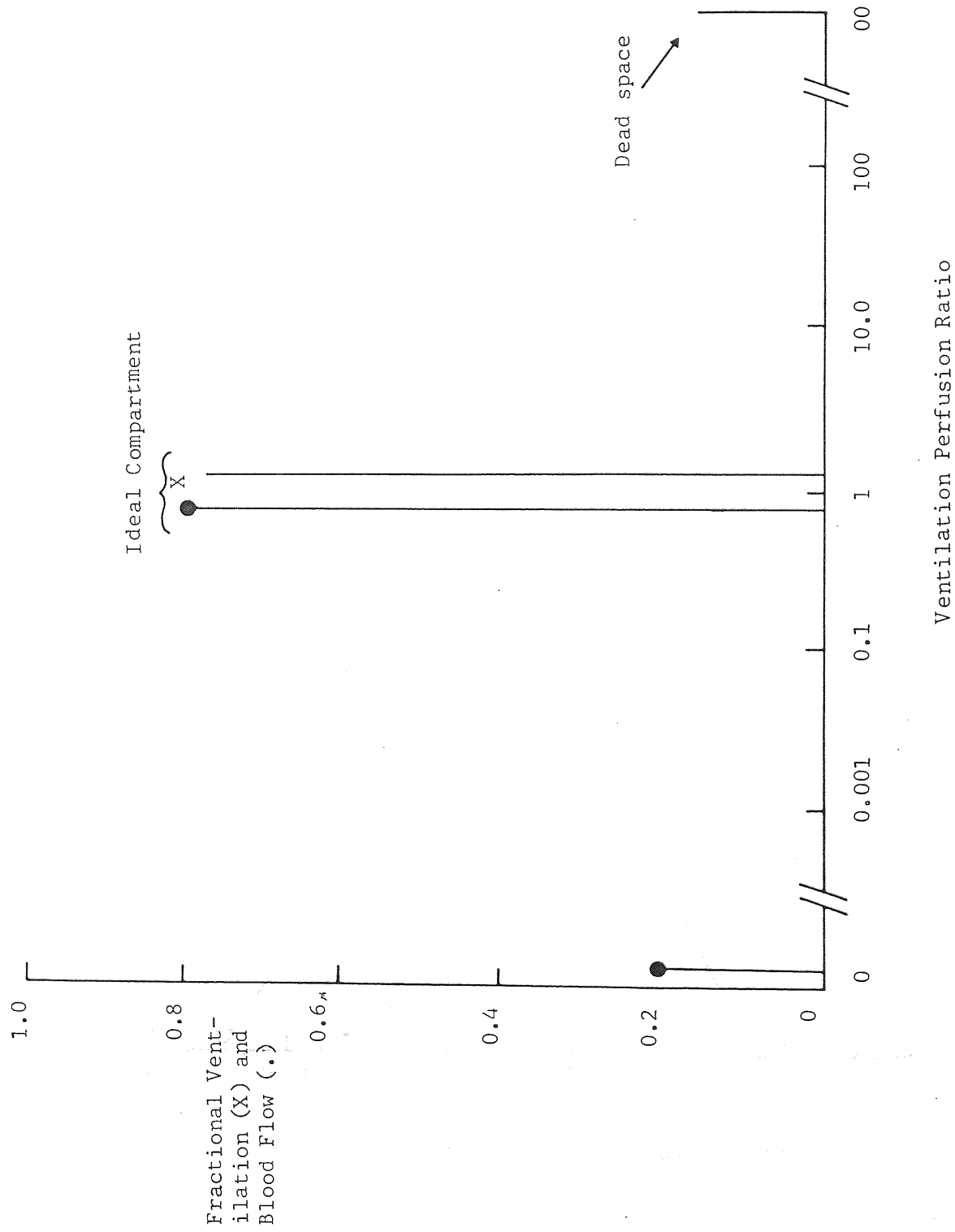

FIGURE 9

Example Of A Log Normal Distribution For A Fairly Large Degree Of Ventilation - Perfusion Ratio Inequality

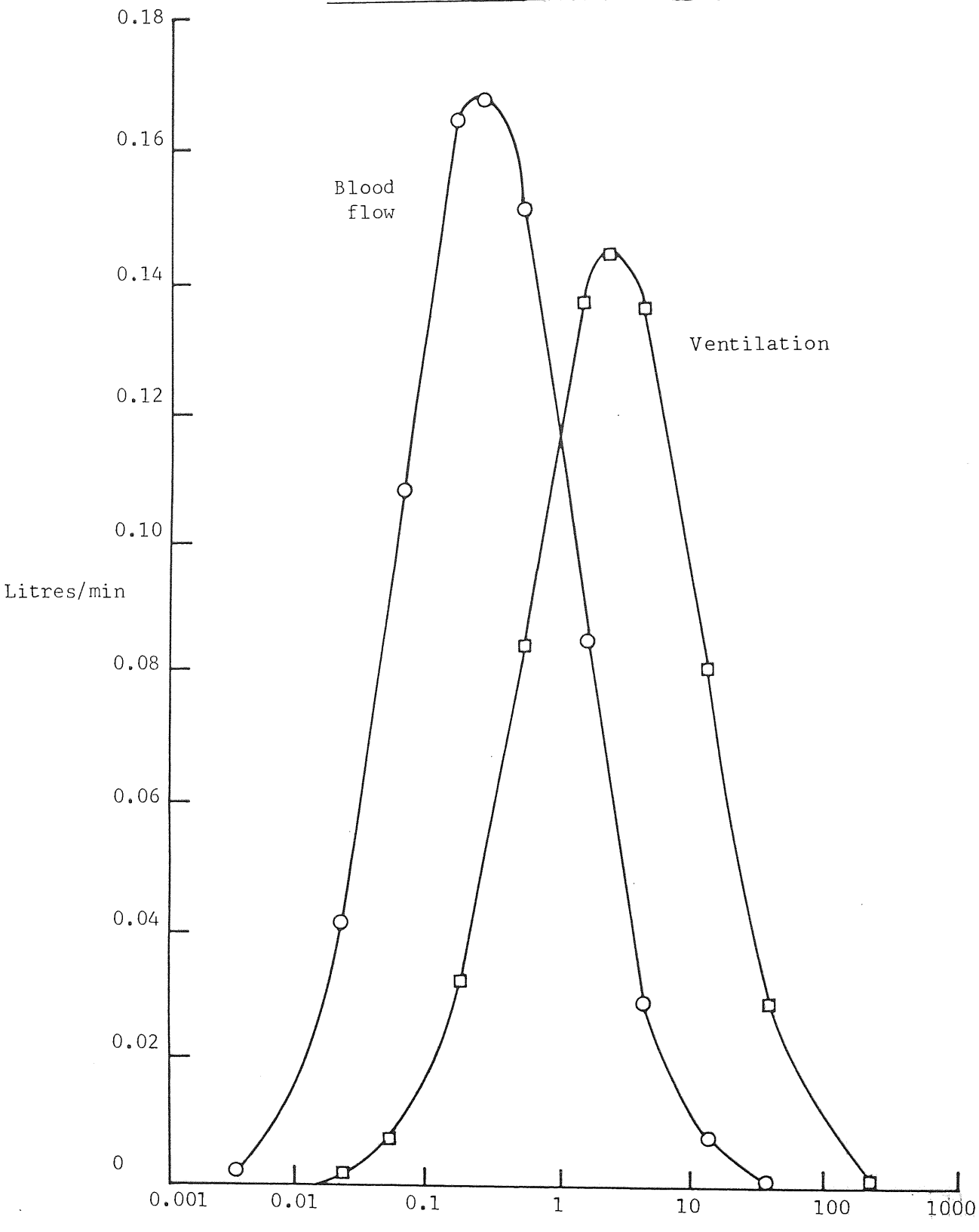

FIGURE 10

10 Compartment Lung Model

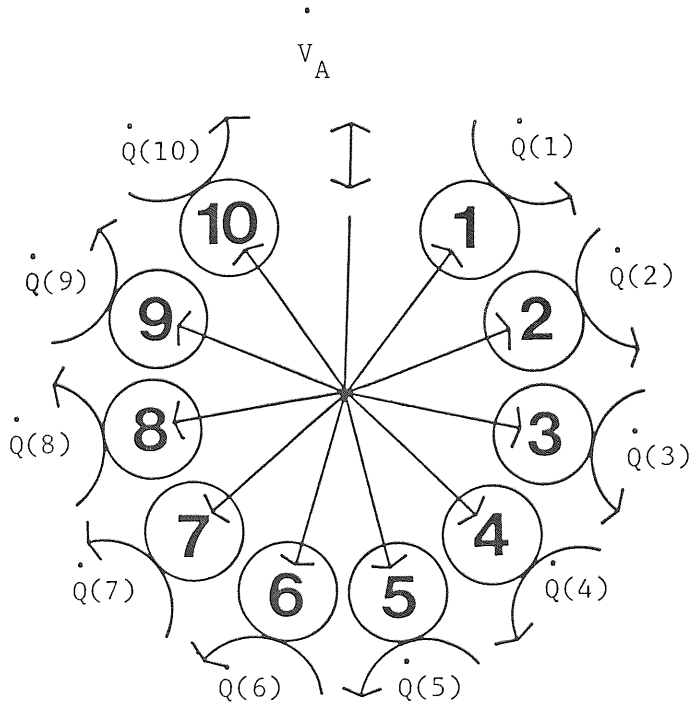

CHAPTER 4

THE MATHEMATICAL MODEL

This chapter describes a mathematical model developed during the course of this research to represent pulmonary gas exchange under "steady-state" conditions, using tracers of various solubilities under constant perfusion or constant ventilation; it determines the overall gas exchange and ventilation/blood flow ratio ($\dot{V}_{A/\dot{Q}}$).

4.1 Inert Gas Elimination

Table (1) gives the list of inert gases suitable for elimination studies. The inert gas elimination method rests on the mass balance principle which relates alveolar pressures of inert gases in the lung to the solubility of the gas and the ventilation - perfusion ratio ($\dot{V}_{A/\dot{Q}}$) of the area of lung under consideration. The general equation has been derived and described previously,Kety (62) and Farhi (12).

The inert gas exchange can be studied during uptake, elimination or steady state conditions and involves the transport of Oxygen (O_2) and Carbon Dioxide (CO_2). Most previous researchers have only considered the elimination of an inert gas and ignored uptake and steady state conditions.

The assumption in arriving at the basic equations for such a case were those stated in Chapter 3, Sections 3.3.5 and 3.3.6.

If the inert gas is present in the inspirate, then P_{IG} is different from zero. Then equation 19 becomes:

$$\frac{P_{AG} - P_{IG}}{P_{VG} - P_{IG}} = \frac{\lambda}{\lambda + \frac{\dot{V}_A}{\dot{Q}}} \qquad (20)$$

4.2 Derivation of Equations

The model used in this research is the ten compartment model shown in Figure (10). A geometric progression is used Scrimshire (11), to generate alveoli and all the equations are based upon Fick's equation, Farhi (12).

All symbols used in deriving relationships will follow the Pappenheimer nomenclature (70).

4.2.1 Gas Exchange In A Homogenous Lung

Consider an alveolus, or homogenous lung containing one gas and having a finite solubility. The pressure of this gas must always be atmospheric, hence it follows that:

$$P_T = P_{A1} = P_{BAR} = 760 \text{ mmHg} \tag{21}$$

from classical gas equations.

$$P_{A1} \cdot \dot{V}_A - P_{I1} \cdot \dot{V}_{IA} = \dot{Q} \cdot \lambda_1 (P_{\bar{V}1} - P_{A1}) \tag{22}$$

solving for P_{A1} :

$$P_{A1} = \frac{\dot{Q} \lambda_1 P_{\bar{V}1} + P_{I1} \cdot \dot{V}_{IA}}{\dot{V}_A + \dot{Q} \cdot \lambda_1} \tag{23}$$

dividing by $\dot{Q}$:

$$P_{A1} = \frac{\lambda_1 \cdot P_{\bar{V}1} + P_{I1} \cdot \dot{V}_{IA/Q}}{\dot{V}_{A/Q} + \lambda_1} \tag{24}$$

In order to express the alveolar tensions of the gas as a function of the variable $\frac{\dot{V}_{IA}}{\dot{Q}}$ substitute equations (24) into (21).

$$P_T = \frac{\dot{V}_{IA/Q} \cdot P_{I1} + \lambda_1 \cdot P_{\bar{V}1}}{\frac{\dot{V}_A}{\dot{Q}} + \lambda_1} \tag{25}$$

solving $\frac{\dot{V}_{IA}}{\dot{Q}}$ and simplifying we obtain:

$$\frac{\dot{V}_{IA}}{\dot{Q}} = \frac{P_T}{P_{I1}} \left(\frac{\dot{V}_A}{\dot{Q}} + \lambda_1 \right) - \lambda_1 \frac{P_{\bar{V}1}}{P_{I1}} \tag{26}$$

4.2.2 Exchange of Two Gases

Extending the model to two gases:

$$P_T = P_{A1} + P_{A2} = P_{BAR} \tag{27}$$

$$P_{A1} = \frac{\frac{\dot{V}_{IA}}{\dot{Q}} \cdot P_{I1} + \lambda_1 \cdot P_{\bar{V}1}}{\dot{V}_{A/Q} + \lambda_1} \tag{28}$$

$$P_{A2} = \frac{\frac{\dot{V}_{IA}}{\dot{Q}} \cdot P_{I2} + \lambda_2 \cdot P_{\bar{V}2}}{\frac{\dot{V}_A}{\dot{Q}} + \lambda_2} \tag{29}$$

Substituting equations (28) and (29) into (27):

$$P_T = \frac{\frac{\dot{V}_{IA}}{\dot{Q}} \cdot P_{I1} + \lambda_1 \cdot P_{\bar{V}1}}{\frac{\dot{V}_A}{\dot{Q}} + \lambda_1} + \frac{\frac{\dot{V}_{IA}}{\dot{Q}} \cdot P_{I2} + \lambda_2 \cdot P_{\bar{V}2}}{\frac{\dot{V}_A}{\dot{Q}} + \lambda_2} \tag{30}$$

solving for $\frac{\dot{V}_{IA}}{\dot{Q}}$ for two gases:

$$\frac{\dot{V}_{IA}}{\dot{Q}} = \frac{P_T - \left(\frac{\lambda_1 \cdot P_{\bar{V}1}}{\frac{\dot{V}_A}{\dot{Q}} + \lambda_1} + \frac{\lambda_2 \cdot P_{\bar{V}2}}{\frac{\dot{V}_A}{\dot{Q}} + \lambda_2} \right)}{\frac{P_{I1}}{\frac{\dot{V}_A}{\dot{Q}} + \lambda_1} + \frac{P_{I2}}{\frac{\dot{V}_A}{\dot{Q}} + \lambda_2}} \qquad (31)$$

4.2.3 Multigas Exchange In A Lung Model

Deriving a general equation for n gases:

$$\frac{\dot{V}_{IA}}{\dot{Q}} = \frac{P_T - \sum_{i=1}^{n} \frac{\lambda_i \cdot P_{\bar{V}i}}{\frac{\dot{V}_A}{\dot{Q}} + \lambda_i}}{\sum_{i=1}^{n} \frac{P_{Ii}}{\frac{\dot{V}_A}{\dot{Q}} + \lambda_i}} \qquad (32)$$

4.3 Elimination and Uptake In A Lung Model

In Figure (11) one of the gases is being eliminated while in Figure (12) two gases are being taken up.

4.3.1 Elimination Phase Figure (11)

Inspired gas tension (P_{IG}) = 0.00 mmHg

Venous gas tension ($P_{\bar{V}G}$) = 760 mmHg

4.3.2 Uptake Phase Figure (12)

Inspired gas tension (P_{IG}) = 380 mmHg(since there are two gases being taken up).

Venous gas tension ($P_{\bar{V}G}$) = 0.00 mmHg from equation (32).

For three gases:

$$\frac{\dot{V}_{IA}}{\dot{Q}} = \frac{P_T - \left(\frac{\lambda_1 \; P_{\bar{V}1}}{\frac{\dot{V}_{A/Q}}{\dot{Q}} + \lambda_1} + \frac{\lambda_2 \; P_{\bar{V}2}}{\frac{\dot{V}_A}{\dot{Q}} + \lambda_2} + \frac{\lambda_3 \; P_{\bar{V}3}}{\frac{\dot{V}_A}{\dot{Q}} + \lambda_3} \right)}{\frac{P_{I1}}{\frac{\dot{V}_{A/Q}}{\dot{Q}} + \lambda_1} + \frac{P_{I2}}{\frac{\dot{V}_A}{\dot{Q}} + \lambda_2} + \frac{P_{I3}}{\frac{\dot{V}_{A/Q}}{\dot{Q}} + \lambda_3}} \qquad (33)$$

first gas is being eliminated.

Therefore:

$$\frac{P_{I1}}{\frac{\dot{V}_{A/Q}}{\dot{Q}} + \lambda_1} = 0 \qquad (34)$$

second and third gases are being taken up

Therefore:

$$\frac{\lambda_2 \; P_{\bar{V}2}}{\frac{\dot{V}_{A/Q}}{\dot{Q}} + \lambda_2} + \frac{\lambda_2 \; P_{\bar{V}3}}{\frac{\dot{V}_{A/Q}}{\dot{Q}} + \lambda_3} = 0 \qquad (35)$$

Hence equation (33) becomes:

$$\frac{\dot{V}_{IA/Q}}{\dot{Q}} = \frac{P_T - \frac{\lambda_1 \; P_{\bar{V}1}}{\frac{\dot{V}_{A/Q}}{\dot{Q}} + \lambda_1}}{\frac{P_{I2}}{\frac{\dot{V}_{A/Q}}{\dot{Q}} + \lambda_2} + \frac{P_{I3}}{\frac{\dot{V}_{A/Q}}{\dot{Q}} + \lambda_3}} \qquad (36)$$

4.4 Model for Overall Gas Exchange

In this model the following factors are considered:

(a) Ten compartment model

(b) Three gases considered initially

(c) Various degrees of either ventilation or perfusion

4.4.1 Generation of Ventilation and Perfusion Data

Using a geometric progression of the form $A^{(R + (I - 1) B)}$ described elsewhere Scrimshire (11) and Scrimshire and Naqvi (71):

Value of I = 1 to 10 (ten compartment model)

B = 0 to 2.0 (degree of inequality)

R = 1 } G.P parameters

A = 2 }

4.4.2 Data Options

There are three options open to us which were described by Scrimshire (11):

(a) Unequal ventilation (constant perfusion)

(b) Unequal blood flow (constant ventilation)

(c) Homogeneous lung

4.5 $\dot{V}_{A/Q}$ Model

In this model, the value of the $\dot{V}_{A/Q}$ ratio is calculated using a quadratic equation for two gases and later by a cubic equation for three gases.

4.5.1 $\dot{V}_{A/Q}$ Model for A Homogeneous Lung

$$P_T = \frac{\frac{\dot{V}_{IA}}{\dot{Q}} \cdot P_{I1} + \lambda_1 \cdot P_{\bar{V}1}}{\frac{\dot{V}_A}{\dot{Q}} + \lambda_1} \qquad (37)$$

solving for $\dot{V}_{A/Q}$ ratio:

$$\frac{\dot{V}_A}{\dot{Q}} = \frac{\frac{\dot{V}_{IA}}{\dot{Q}} \cdot P_{I1} + \lambda_1 \cdot P_{\bar{V}1}}{P_T} - \lambda_1 \qquad (38)$$

4.5.2 $\dot{V}_{A/Q}$ Model For Two Gases

$$P_T = \frac{\frac{\dot{V}_{IA}}{\dot{Q}} \cdot P_{I1} + \lambda_1 \cdot P_{\bar{V}1}}{\frac{\dot{V}_A}{\dot{Q}} + \lambda_1} + \frac{\frac{\dot{V}_{IA}}{\dot{Q}} \cdot P_{I2} + \lambda_2 \cdot P_{\bar{V}2}}{\frac{\dot{V}_A}{\dot{Q}} + \lambda_2} \qquad (39)$$

solving for $\dot{V}_{A/Q}$ ratio using the quadratic form:-

$$x = \frac{-b \pm \sqrt{b^2 - 4ac}}{2a}$$

when $x = \dot{V}_{A/Q}$

$$a = P_T$$

$$b = (\lambda_1 + \lambda_2) P_T - (\frac{\dot{V}_{IA}}{\dot{Q}} \cdot P_{I1} + \lambda_1 \cdot P_{\bar{V}1}) -$$

$$(\frac{\dot{V}_{IA}}{\dot{Q}} \cdot P_{I2} + \lambda_2 \cdot P_{\bar{V}2})$$

$$c = P_T \cdot \lambda_1 \cdot \lambda_2 - \frac{\dot{V}_{IA}}{\dot{Q}} (\lambda_2 \cdot P_{I1} + P_{I2} \cdot \lambda_1) -$$

$$\lambda_1 \cdot \lambda_2 (P_{\bar{V}1} + P_{\bar{V}2})$$

$$\frac{\dot{V}_A}{\dot{Q}} = \frac{-b + \sqrt{b^2 - 4ac}}{2a}$$

taking the positive root only.

4.5.3 $\dot{V}_{A/Q}$ Model for Multigas Exchange

If we consider three gases, then:

$$= \frac{\frac{\dot{V}_{IA}}{\dot{Q}} \cdot P_{I1} + \lambda_1 \cdot P_{\bar{V}1}}{\frac{\dot{V}_A}{\dot{Q}} + \lambda_1} + \frac{\frac{\dot{V}_{IA}}{\dot{Q}} \cdot P_{I2} + \lambda_2 \cdot P_{\bar{V}2}}{\frac{\dot{V}_A}{\dot{Q}} + \lambda_2}$$

$$+ \frac{\frac{\dot{V}_{IA}}{\dot{Q}} \cdot P_{I3} + \lambda_3 \cdot P_{\bar{V}3}}{\frac{\dot{V}_A}{\dot{Q}} + \lambda_3} \qquad (40)$$

solving for the $\frac{\dot{V}_A}{\dot{Q}}$ ratio we use a cubic equation of the form

$$ax^3 + bx^2 + cx + d = 0$$

where $x = \frac{\dot{V}_A}{\dot{Q}}$

$$a = P_T$$

$$b = P_T (\lambda_1 + \lambda_2 + \lambda_3) - (\frac{\dot{V}_{IA}}{\dot{Q}} \cdot P_{I1} + \lambda_1 \cdot P_{\bar{V}1}) -$$

$$(\frac{\dot{V}_{IA}}{\dot{Q}} \cdot P_{I2} + \lambda_2 \cdot P_{\bar{V}2}) -$$

$$(\frac{\dot{V}_{IA}}{\dot{Q}} \cdot P_{I3} + \lambda_3 \cdot P_{\bar{V}3})$$

$$c = P_T (\lambda_1 \cdot \lambda_2 + \lambda_2 \cdot \lambda_3 + \lambda_1 \cdot \lambda_3) -$$

$$(\lambda_2 + \lambda_3) (\frac{\dot{V}_{IA}}{\dot{Q}} \cdot P_{I1} + \lambda_1 \cdot P_{\bar{V}1}) -$$

$$(\lambda_1 + \lambda_3) (\frac{\dot{V}_{IA}}{\dot{Q}} \cdot P_{I2} + \lambda_2 \cdot P_{\bar{V}2}) -$$

$$(\lambda_1 + \lambda_2) (\frac{\dot{V}_{IA}}{\dot{Q}} \cdot P_{I3} + \lambda_3 \cdot P_{\bar{V}3})$$

$$d = P_T (\lambda_1 \cdot \lambda_2 \cdot \lambda_3) - \lambda_2 \cdot \lambda_3$$

$$(\frac{\dot{V}_{IA}}{\dot{Q}} \cdot P_{I1} + \lambda_1 \cdot P_{\bar{V}1}) -$$

$$\lambda_1 \cdot \lambda_3 (\frac{\dot{V}_{IA}}{\dot{Q}} \cdot P_{I2} + \lambda_2 \cdot P_{\bar{V}2}) -$$

$$\lambda_2 \cdot \lambda_1 (\frac{\dot{V}_{IA}}{\dot{Q}} \cdot P_{I3} + \lambda_3 \cdot P_{\bar{V}3})$$

4.5.4 $\dot{V}_{A/Q}$ Model (Elimination Phase)

Inspired gas tension (P_{IG}) = 0.00 mmHg

Venous gas tension ($P_{\bar{V}G}$) = 760 mmHg

If we again use three gases for the elimination phase, and since we have chosen P_{IG} = 0.00 mmHg, we can eliminate all the products containing P_{IG} from equation (40).

i.e. $a = P_T$

$$b = P_T (\lambda_1 + \lambda_2 + \lambda_3) - (\lambda_1 \cdot P_{\bar{V}1}) - (\lambda_2 \cdot P_{\bar{V}2}) - (\lambda_3 \cdot P_{\bar{V}3})$$

$$c = P_T (\lambda_1 \cdot \lambda_2 + \lambda_2 \cdot \lambda_3 + \lambda_1 \cdot \lambda_3) - (\lambda_2 + \lambda_3)(\lambda_1 \cdot P_{\bar{V}1}) - (\lambda_1 + \lambda_3)(\lambda_2 \cdot P_{\bar{V}2}) - (\lambda_1 + \lambda_2)(\lambda_3 \cdot P_{\bar{V}3})$$

$$d = P_T (\lambda_1 \cdot \lambda_2 \cdot \lambda_3) - \lambda_2 \cdot \lambda_3 (\lambda_1 \cdot P_{\bar{V}1}) - \lambda_1 \cdot \lambda_3 (\lambda_2 \cdot P_{\bar{V}2}) - \lambda_2 \cdot \lambda_1 (\lambda_3 \cdot P_{\bar{V}3})$$

4.5.5 $\dot{V}_{A/Q}$ Model (Uptake Phase)

Inspired gas tension (P_{IG}) = 380 mmHg

Venous gas tension ($P_{\bar{V}G}$) = 0.00 mmHg

Using three gases for the uptake phase and by choosing the value of $P_{\bar{V}G}$ = 0.00 mmHg, then we can eliminate all of the products containing $P_{\bar{V}G}$ from equation (40).

i.e. $a = P_T$

$$b = P_T (\lambda_1 + \lambda_2 + \lambda_3) - (\frac{\dot{V}_{IA}}{\dot{Q}} \cdot P_{I1}) -$$

$$(\frac{\dot{V}_{IA}}{\dot{Q}} \cdot P_{I2}) - (\frac{\dot{V}_{IA}}{\dot{Q}} \cdot P_{I3})$$

$$c = P_T (\lambda_1 \cdot \lambda_2 + \lambda_2 \cdot \lambda_3 + \lambda_1 \cdot \lambda_3) -$$

$$(\lambda_2 + \lambda_3) (\frac{\dot{V}_{IA}}{\dot{Q}} \cdot P_{I1}) -$$

$$(\lambda_1 + \lambda_3) (\frac{\dot{V}_{IA}}{\dot{Q}} \cdot P_{I2}) -$$

$$(\lambda_1 + \lambda_2) (\frac{\dot{V}_{IA}}{\dot{Q}} \cdot P_{I3})$$

$$d = P_T (\lambda_1 \cdot \lambda_2 \cdot \lambda_3) - \lambda_2 \cdot \lambda_3 (\frac{\dot{V}_{IA}}{\dot{Q}} \cdot P_{I1}) -$$

$$\lambda_1 \cdot \lambda_3 (\frac{\dot{V}_{IA}}{\dot{Q}} \cdot P_{I2}) -$$

$$\lambda_2 \cdot \lambda_1 (\frac{\dot{V}_{IA}}{\dot{Q}} \cdot P_{I3})$$

4.6 Gas Exchange In A Two Compartment Model

from equation (24)

equation of the gas exchange in the first compartment:

$$P_{A1} = \frac{\frac{\dot{V}_{IA}}{\dot{Q}} \cdot P_{I1} + \lambda_1 \cdot P_{\bar{V}1}}{\frac{\dot{V}_A}{\dot{Q}} + \lambda_1} \qquad (41)$$

Extending to the gas exchange in the second compartment:

$$P_{A2} = \frac{\frac{\dot{V}_{IA}}{\dot{Q}} \cdot P_{I2} + \lambda_1 \cdot P_{\bar{V}2}}{\frac{\dot{V}_A}{\dot{Q}} + \lambda_1} \qquad (42)$$

since the gas being exchanged has the solubility λ_1, but different values for alveolar pressure (P_A), inspired pressure (P_I) and venous pressure ($P_{\bar{V}}$).

4.6.1 Gas Exchange In A Multicompartment Lung Model

from equation (41):

$$P_{A1} = \frac{\frac{\dot{V}_{IA}}{\dot{Q}} \cdot P_{I1}}{\frac{\dot{V}_A}{\dot{Q}} + \lambda_1} + \frac{\lambda_1 \cdot P_{\bar{V}1}}{\frac{\dot{V}_A}{\dot{Q}} + \lambda_1} \qquad (43)$$

Hence equation (42) becomes:

$$P_{A2} = \frac{\frac{\dot{V}_{IA}}{\dot{Q}} \cdot P_{I2}}{\frac{\dot{V}_A}{\dot{Q}} + \lambda_1} + \frac{\lambda_1 \cdot P_{\bar{V}2}}{\frac{\dot{V}_A}{\dot{Q}} + \lambda_1} \qquad (44)$$

$$P_{An} = \frac{\frac{\dot{V}_{IA}}{\dot{Q}} \cdot P_{In}}{\frac{\dot{V}_A}{\dot{Q}} + \lambda_1} + \frac{\lambda_1 \cdot P_{\bar{V}n}}{\frac{\dot{V}_A}{\dot{Q}} + \lambda_1} \qquad (45)$$

since

$$P_T = P_{A1} + P_{A2} + \ldots\ldots\ldots P_{An} \qquad (46)$$

$$P_{A1} + P_{A2} + \cdots + P_{An} = \frac{\frac{\dot{V}_{IA}}{\dot{Q}}}{\frac{\dot{V}_A}{\dot{Q}} + \lambda_1} \cdot P_{I1} + \frac{\frac{\dot{V}_{IA}}{\dot{Q}}}{\frac{\dot{V}_A}{\dot{Q}} + \lambda_1} \cdot P_{I2} + \cdots + \frac{\frac{\dot{V}_{IA}}{\dot{Q}}}{\frac{\dot{V}_A}{\dot{Q}} + \lambda_1} \cdot P_{In} + \frac{\lambda_1}{\frac{\dot{V}_A}{\dot{Q}} + \lambda_1} \cdot P_{\bar{V}1} + \frac{\lambda_1}{\frac{\dot{V}_A}{\dot{Q}} + \lambda_1} \cdot P_{\bar{V}2} + \cdots + \frac{\lambda_1}{\frac{\dot{V}_A}{\dot{Q}} + \lambda_1} \cdot P_{\bar{V}n} \quad (47)$$

Hence

$$\sum_{i=1}^{n} P_{Ai} = \frac{\frac{\dot{V}_{IA}}{\dot{Q}}}{\frac{\dot{V}_A}{\dot{Q}} + \lambda_1} \sum_{i=1}^{n} P_{Ii} + \frac{\lambda_1}{\frac{\dot{V}_A}{\dot{Q}} + \lambda_1} \sum_{i=1}^{n} P_{\bar{V}i} \quad (48)$$

extending the model to second gas:

from equation (48)

$$\sum_{j=1}^{n} P_{Aj} = \frac{\frac{\dot{V}_{IA}}{\dot{Q}}}{\frac{\dot{V}_A}{\dot{Q}} + \lambda_2} \sum_{j=1}^{n} P_{Ij} + \frac{\lambda_2}{\frac{\dot{V}_A}{\dot{Q}} + \lambda_2} \sum_{j=1}^{n} P_{\bar{V}j} \quad (49)$$

hence the third gas

$$\sum_{k=1}^{n} P_{Aj} = \frac{\frac{\dot{V}_{IA}}{\dot{Q}}}{\frac{\dot{V}_A}{\dot{Q}} + \lambda_3} \sum_{k=1}^{n} P_{Ik} + \frac{\lambda_3}{\frac{\dot{V}_A}{\dot{Q}} + \lambda_3} \sum_{k=1}^{n} P_{\bar{V}k} \quad (50)$$

4.6.2 Elimination In A Multicompartment Lung Model

Inspired gas tension (P_{IG}) = 0.00 mmHg

Venous gas tension ($P_{\bar{V}G}$) = 760 mmHg

for the first gas solubility $\lambda = \lambda_1$, from equation (48)

since $P_{IG} = 0.00$ mmHg

$$\frac{\frac{\dot{V}_{IA}}{\dot{Q}}}{\frac{\dot{V}_A}{\dot{Q}} + \lambda_1} \sum_{i=1}^{n} P_{Ii} = 0$$

Hence the equation (48) becomes:

$$\sum_{i=1}^{n} P_{Ai} = \frac{\lambda_1}{\frac{\dot{V}_A}{\dot{Q}} + \lambda_1} \sum_{i=1}^{n} P_{\bar{V}i} \qquad (51)$$

Solving for $\frac{\dot{V}_A}{\dot{Q}}$ from equation (51)

$$\frac{\lambda_1}{\frac{\dot{V}_A}{\dot{Q}} + \lambda_1} = \frac{\sum_{i=1}^{n} P_{Ai}}{\sum_{i=1}^{n} P_{\bar{V}i}} \qquad (52)$$

$$\frac{\lambda_1 + \frac{\dot{V}_A}{\dot{Q}}}{\lambda_1} = \frac{\sum_{i=1}^{n} P_{\bar{V}i}}{\sum_{i=1}^{n} P_{Ai}} \qquad (53)$$

$$\frac{\dot{V}_A}{\dot{Q}} = \lambda_1 \frac{\sum_{i=1}^{n} P_{\bar{V}i}}{\sum_{i=1}^{n} P_{Ai}} - \lambda_1 \qquad (54)$$

let

$$\frac{\sum_{i=1}^{10} P_{\bar{V}i}}{\sum_{i=1}^{10} P_{Ai}} = P'_i$$

Hence equation (54) becomes:

$$\frac{\dot{V}_A}{\dot{Q}} = \lambda_1 (P'_i - 1) \qquad (55)$$

4.6.3 Uptake In A Multicompartment Lung Model

Venous gas tension ($P_{\bar{V}G}$) = 0.00 mmHg

for the first gas solubility $\lambda = \lambda_1$

from equation (48)

since $P_{\bar{V}G}$ = 0.00 mmHg

$$\frac{\lambda_1}{\frac{\dot{V}_A}{\dot{Q}} + \lambda_1} \sum_{i=1}^{n} P_{\bar{V}i} = 0$$

Hence the equation (48) becomes

$$\sum_{i=1}^{n} P_{Ai} = \frac{\frac{\dot{V}_{IA}}{\dot{Q}}}{\frac{\dot{V}_A}{\dot{Q}} + \lambda_1} \sum_{i=1}^{n} P_{Ii} \qquad (56)$$

Solving for $\frac{\dot{V}_{IA}}{\dot{Q}}$:-

$$\frac{\dot{V}_{IA}}{\dot{Q}} = \frac{\sum_{i=1}^{n} P_{Ai}}{\sum_{i=1}^{n} P_{Ii}} \left(\frac{\dot{V}_A}{\dot{Q}} + \lambda_1 \right) \qquad (57)$$

Hence the value of $\frac{\dot{V}_{IA}}{\dot{Q}}$ for the gas with solubility $\lambda = \lambda_2$:-

$$\frac{\dot{V}_{IA}}{\dot{Q}} = \frac{\sum_{k=1}^{n} P_{Ak}}{\sum_{k=1}^{n} P_{Ik}} \left(\frac{\dot{V}_A}{\dot{Q}} + \lambda_2 \right) \qquad (58)$$

hence for any gas:

$$\frac{\dot{V}_{IA}}{\dot{Q}} = \frac{\sum_{t=1}^{t=n} P_{At}}{\sum_{t=1}^{n} P_{It}} \left(\frac{\dot{V}_A}{\dot{Q}} + \lambda_R \right) \qquad (59)$$

Assuming

$$\frac{\dot{V}_{IA}}{\dot{Q}} = \frac{\dot{V}_A}{\dot{Q}}$$

Let

$$\frac{\sum_{t=1}^{10} P_{At}}{\sum_{t=1}^{10} P_{It}} = P'_t \qquad (60)$$

Then equation (59) becomes:

$$\frac{\dot{V}_A}{\dot{Q}} = \frac{P'_t \cdot \lambda_R}{1 - P'_t} \qquad (61)$$

4.7 Analysis of Uptake and Elimination

Considering the introduction of three inert gases simultaneously. Keeping one gas ($\lambda = \lambda_1$) as a filler gas Stoetling (24), while the other two gases ($\lambda = \lambda_2$) and ($\lambda = \lambda_3$) are being taken up and eliminated respectively.

From equation (61) and (55):

$$\frac{\dot{V}_A}{\dot{Q}} = \frac{P'_j}{1 - P'_j} \lambda_2 \qquad (62)$$

$$\frac{\dot{V}_A}{\dot{Q}} = \lambda_3 (P'_k - \lambda_1) \qquad (63)$$

Combining these two equations:

$$\frac{P'_j}{1 - P'_j} \lambda_2 = \lambda_3 (P'_k - 1) \qquad (64)$$

let $$\frac{\lambda_3}{\lambda_2} = L$$

equation (64) becomes

$$P'_k = \frac{1}{L} \left(\frac{P'_j}{1 - P'_j} \right) + 1 \qquad (65)$$

from equation (65) it is apparent that the shape of the $\frac{\dot{V}_A}{\dot{Q}}$ curve is dictated only be the ratio of $\frac{\lambda_3}{\lambda_2}$ in this case regardless of the absolute value of λ_3 and λ_2. This analysis is very much similar to the Farhi and Yokoyama (37) and Farhi*.

* Personal communication Farhi, March 1984.

The value of this ratio is always less than 1, Farhi and Yokoyama (37), which is in accordance with the findings in this thesis.

4.8 The Newton-Raphson Method APPENDIX B

The Newton-Raphson method is a second order iterative method.

Let x_o be an approximation to the root (A) of the equation $f(x) = 0$

and let e_o be the error in this approximation so that:

$$A = x_o + e_o \tag{66}$$

then
$$0 = f(A) = f(x_o + e_o)$$
$$= f(x_o) + e_o f'(x_o) + \frac{1}{2} e_o^2 f''(x_o) + ... + \tag{67}$$

on expanding in a Taylor series.

Hence, provided e_o is "small"

$$f(x_o) + e f'(x_o) \simeq 0 \tag{68}$$

and so
$$e_o \simeq - \frac{f(x_o)}{f'(x_o)} \tag{69}$$

provided $f'(x_o) \neq 0$

Thus an improved approximation to the root (A) is:

$$x_1 = x_o - \frac{f(x_o)}{f'(x_o)} \tag{70}$$

and then a further improved approximation is

$$x_2 = x_1 - \frac{f(x_1)}{f'(x_1)} \tag{71}$$

provided $e_1 \simeq - \frac{f(X_1)}{f'(x_1)}$ is "small" (72)

Hence the iterative formulae given by

$$x_{n+1} = x_n - \frac{f(x_n)}{f'(x_n)} \tag{73}$$

$$x_{n+1} = F(x_n) \tag{74}$$

where

$$F(x) = x - \frac{f(x)}{f'(x)} \tag{75}$$

Using the Newton-Raphson technique to determine an approximation to the real root of the equation $x^3 - x^2 - x - 3$.

from equation (75)

$$x_{n+1} = x_n - \frac{x_n^3 - x_n^2 - x_n - 3}{3x_n^2 - 2x_n - 1} \tag{76}$$

Starting with $x_o = 2.5$ and rounding to three decimal places, the following results are obtained:

x	$f(x)$	$f'(x)$	$\frac{f(x)}{f'(x)}$
2.5	3.875	12.75	0.304
2.196	0.571	9.075	0.063
2.133	0.022	8.383	0.003
2.130	-0.003	8.351	0.000

Hence the root is 2.13 correct to two decimal places.

TABLE 1

GASES SUITABLE FOR USE IN SIMULATION

Gas	Formula	Mol wt.	Blood: gas partition coefficient ($37^{o}C$)
Sulphur hexafluoride	SF_6	146	0.0076 (1)
Methane	CH_4	16	0.038 (2)
Ethane	C_2H_6	30	0.092 (2)
Freon 12	$C\ Cl_2F_2$	121	0.26 (2)
Cyclopropane	C_3H_6	42	0.414 (3)
Acetylene	C_2H_2	26	0.842 (4)
Fluroxene	$C_4F_3H_5O$	126	1.37 (5)

FIGURE 11

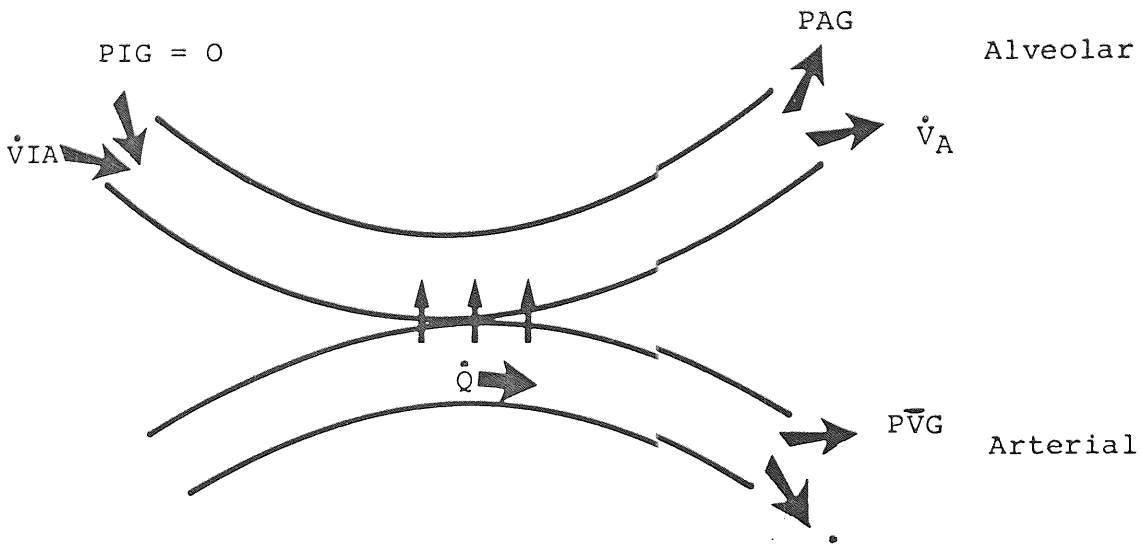

Elimination - gas is being eliminated via the alveolars inspired gas concentration (P_{IG})=O

FIGURE 12

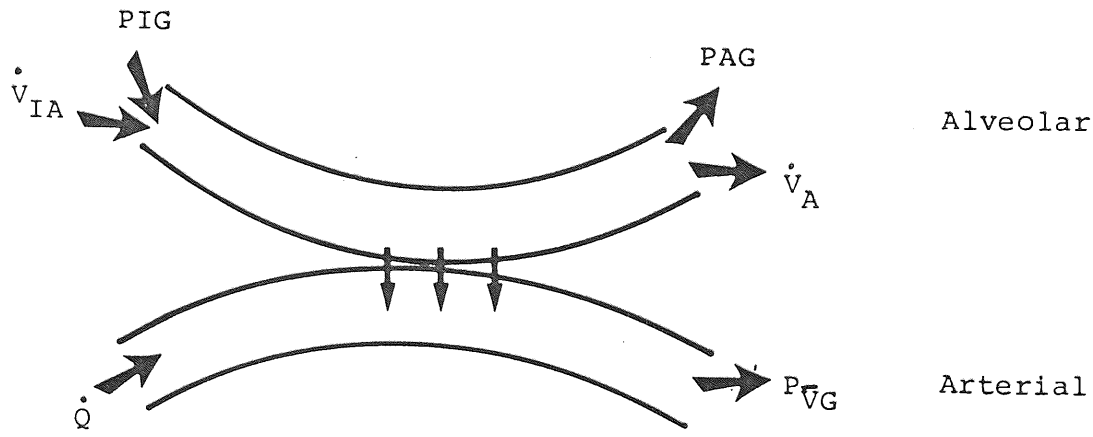

Uptake - gas is being taken up by the arteries.

CHAPTER 5

RESULTS OF SIMULATION

The model was simulated using a P.E.T Commodore 32K microcomputer using the basic language. West (16) pointed out that 1000 compartments were probably near to the number of true gas exchange compartments in the human lung, but he considered that ten compartments was a reasonable compromise for the purpose of calculation. A ten compartment model was used for this simulation.

5.1 Independent $\dot{V}_A$ and $\dot{Q}$ Distributions

In order to assess the effects of independent regional inequalities, a mathematical formula was used to generate values for both ventilation and blood flow, to each of the alveolar compartments of the model. This function enabled particular degrees of either, ventilation or blood flow inequality to be defined by means of a single parameter.

The assumptions made were those described by Scrimshire (11), Scrimshire and Naqvi (71), i.e. that the respiratory parameter under consideration, be it ventilation or blood flow, varied in the form of a geometric progression from compartment to compartment.

i.e $$\dot{V}'_A(n) \text{ or } \dot{Q}'(n) = 2^{(n-1)B} \qquad (77)$$

where $\dot{V}'_A$ and $\dot{Q}'$ are the magnitude of ventilation or blood flow to any compartment, n.

The generated values are scaled so that they sum to the given minute, volume and cardiac output, respectively, thus:

$$\dot{V}_A(n) = \dot{V}'_A(n) \cdot \dot{V}_{M/} \sum \dot{V}'_A(n) \qquad (78)$$

$$\dot{Q}(n) = \dot{Q}'(n) \cdot \dot{Q}c / \sum \dot{Q}'(n) \qquad (79)$$

A set of results were generated using the values of parameter B from 0.0 to 2.0. The small values of the parameter B naturally gave rise to a mild degree of inequality and higher values produced correspondingly more marked inequalities. With parameter B set to zero a perfectly even distribution was produced. A further set of results were generated for the solubilities Having the values (λ_1, λ_2, λ_3). APPENDIX A.

Simultaneously, two gases were taken up while the third was being eliminated Figure 13. A set of curves for P_{aG} against the $\dot{V}_{IA/\dot{Q}}$ ratio were plotted.

5.2 Effect of Increasing The Solubility of Uptake

The gas which was being eliminated was kept at a solubility of 0.001, while the solubility of one of the gases being taken up was increased gradually from 0.001 (almost insoluble) to 10.0 (highly soluble). Even though the gas which was being eliminated was kept at a constant solubility, its partial pressure P_{aG} varied between 100 mmHg to 150 mmHg.

5.2.1 Solubility of Uptake $\lambda_1 = 0.001$

It was noted that the gas with constant solubility ($\lambda_1 = 0.001$) started with a high value of P_{aG} (760 mmHg), but gradually decreased to almost half of its value P_{aG} (370 mmHg) as the $\frac{\dot{V}_{IA}}{\dot{Q}}$ ratio decreased. Figure 14.

The second gas, however, started with low pressure P_{aG} of almost (0.00 mmHg) and increased to P_{aG} (370 mmHg). It was also found that both uptake curves for the constant solubility $\lambda_1 = 0.001$, with λ_2 varying from 0.001 to 10.0 were almost mirror images of each other. There was a slight rise in the value of P_{aG} for the gas with low solubility ($\lambda_1 = 0.001$) when the values of the solubility (λ_2) of the second gas of uptake were

varied from (10.0 to 1.0) respectively, curves 1 and 2 in Figure (14). A rise of P_{aG} of 45 mmHg was observed between the $\frac{\dot{V}_{IA}}{\dot{Q}}$ ratios of 0.02 to 0.2.

5.2.2 Solubility of Uptake $\lambda_1 = 0.01$

Increasing the value for the solubility of the gas by a factor of 10 produced a similar set of results. The curves were shifted slightly to the right. This time a rise of 45 mmHg for alveolar pressure P_{aG} was observed between the values of the $\frac{\dot{V}_{IA}}{\dot{Q}}$ ratio of 0.03 and 0.3. Figure (15).

for $\lambda_2 < \lambda_1$ $P_{aG_2} > P_{aG_1}$ (80)

$\lambda_1 = \lambda_2$ $P_{aG_2} = P_{aG_1}$ (81)

$\lambda_2 > \lambda_1$ $P_{aG_2} < P_{aG_1}$ (82)

5.2.3 Solubility of Uptake $\lambda_1 = 0.1$

It was observed that as the value of solubility of the gas being taken up (λ_1) was increased, the shape of the curve started to show a definite peak for the $\frac{\dot{V}_{IA}}{\dot{Q}}$ ratio of approximately 0.125 mmHg. Uptake gas pressure (P_{aG}) reached a definite peak at the $\dot{V}_{IA/\dot{Q}}$ ratio minimum at 500 mmHg. The uptake of the second gas started from a minimum of almost zero pressure ($P_{aG} = 0$) to a maximum of 250 or 350 mmHg. Figure (16).

5.2.4 Solubility of Uptake $\lambda_1 = 1.0$

As the solubility of the first gas of uptake was increased by a factor of ten to $\lambda_1 = 1.0$, the curves for various solubilities were clustered together. The gas with a constant solubility started with $P_{aG} = 675$ mmHg at the $\dot{V}_{IA/\dot{Q}}$ ratio of 0.02 rising to a maximum value of 710 mmHg, and afterwards gradually decreasing to a value of $P_{aG} = 400$ mmHg. When a value was set so that $\lambda_1 = \lambda_2 = 1.0$, then it was observed that for the $\dot{V}_{IA/\dot{Q}}$ ratio of 1.0 to 40.0 the value of P_{aG} stayed constant at 375 mmHg,

which is consistent with the fact that the gases of equal solubilities were taken up by equal amounts. Figure (17).

5.2.5 Solubilities of Uptake $\lambda_1 = 10.0$

In this case the curves for uptake were clustered more closely together. The value of the P_{aG} started from 675 mmHg and rose to a maximum of 750 mmHg at the $\dot{V}_{IA/\dot{Q}}$ ratio of 0.2 and then gently fell to 525 mmHg at the $\dot{V}_{IA/\dot{Q}}$ ratio of 10.0, when the value of uptake became $\lambda_1 = \lambda_2 = 10.0$ (highly soluble) the value of P_{aG} stayed constant at 375 mmHg for $\dot{V}_{IA/\dot{Q}}$ ratio of 10.0 to 70.0. Figure (18).

5.3 Effect of Increasing The Solubility of Elimination By A Factor of Ten

Another set of results were obtained by increasing the solubility of the gas being eliminated by a factor of 10 each time. Figures (19 - 21).

5.3.1 Solubility of Uptake $\lambda_1 = 0.001$

It was noted that the partial pressure of the gas being eliminated started from 475 mmHg for the $\frac{\dot{V}_{IA}}{\dot{Q}}$ ratio of 0.01 and that it decreased to almost 0.00 mmHg for the $\frac{\dot{V}_{IA}}{\dot{Q}}$ ratio of 2.0 to 10.0. The curves were spread out, showing definite peaks at partial pressure of 710 mmHg at the $\frac{\dot{V}_{IA}}{\dot{Q}}$ ratio of 0.6, and then gently dropping to 500 mmHg at the $\frac{\dot{V}_{IA}}{\dot{Q}}$ ratio of 15.0. Figure (19).

5.3.2 Solubility of Uptake $\lambda_1 = 0.01$

The Partial pressure of the gas being taken up, rose to a maximum value of 720 mmHg at the $\dot{V}_{IA/\dot{Q}}$ ratio of 0.15 then fell steeply to 500 mmHg at the $\frac{\dot{V}_{IA}}{\dot{Q}}$ ratio of 13. When the values of the solubilities were set to $\lambda_2 = \lambda_1 = 0.01$, the curves were superimposed upon each other, i.e. both gases were taken up by the same amount. The P_{aG} value of the uptake started

from a minimum value of 250 mmHg at the $\frac{\dot{V}_{IA}}{\dot{Q}}$ ratio of 0.01 and rose to a steady value of 375 mmHg at the $\frac{\dot{V}_{IA}}{\dot{Q}}$ ratio of 0.4. This value of P_{aG} stayed constant up to the $\frac{\dot{V}_{IA}}{\dot{Q}}$ ratio of 14.0. Figure (20).

5.3.3 Solubility of Uptake $\lambda_1 = 0.1$

The elimination curves were spread out, starting from 475 mmHg, falling steeply to almost 0.00 mmHg for the $\frac{\dot{V}_{IA}}{\dot{Q}}$ ratio of 3 onwards. There were definite peaks in the uptake curves at the $\frac{\dot{V}_{IA}}{\dot{Q}}$ ratio of 1.0, and the maximum value of P_{aG} was observed to be 675 mmHg. Figure (21).

5.3.4 Solubility of Uptake $\lambda_1 = 1.0$ and $\lambda_1 = 10.0$

The value of P_{aG} for uptake curves was decreased for higher values of solubilities. P_{aG} was decreased by 500 mmHg to 650 mmHg with peaks observed at $\frac{\dot{V}_{IA}}{\dot{Q}}$ ratios of 0.15, 0.4 and 2.5 . The elimination pressure P_{aG} fell sharply at the $\frac{\dot{V}_{IA}}{\dot{Q}}$ ratios between 0.01 to 2.0. Figures (22) and (23).

5.4 Effect of Increasing The Solubility of Elimination from 0.001 to 10.0

Looking at the Figures (14 - 38) it is observed that as the solubility of the gas being eliminated is increased from 0.001 to 10.0, then the partial pressure P_{aG} starts with a high value of 700 mmHg for the low value of the $\frac{\dot{V}_{IA}}{\dot{Q}}$ ratio of 0.01, then falls to almost zero for the $\frac{\dot{V}_{IA}}{\dot{Q}}$ ratio of 10.0, with a value for λ_3 (gas of elimination) equal to 1.0 and 10.0. There are no peaks observed as the solubility of eliminating gas is increased. In Figure (34) the P_{aG} value of uptake starts from 750 mmHg and gently drops to 400 mmHg at the $\frac{\dot{V}_{IA}}{\dot{Q}}$ ratio of 10.0. The uptake of the second gas starts from almost 0.00 mmHg, rising to 400 mmHg for the $\frac{\dot{V}_{IA}}{\dot{Q}}$ ratio of 10.0. As the value of elimination is increased, the curve

becomes less steep and the plateau moves to the right, i.e. for a higher value of the $\frac{\dot{V}_{IA}}{\dot{Q}}$ ratio, the curve for uptake gases moves as the solubility of elimination is increased. P_{aG} starts with a high value and stays at that value until the curve gradually moves down to a pressure P_aG of 380 mmHg. There is a definite maximum for the $\frac{\dot{V}_{IA}}{\dot{Q}}$ ratio of 10.0. As the elimination is increased, uptake of the gases is increased by P_{aG} = o.6 mmHg at high ratios of the $\frac{\dot{V}_{IA}}{\dot{Q}}$.

5.5 Effect of Changing The Degree of Inequality B

The model was simulated for various degrees of inequality (B = 0.0 to B = 2.0). A series of curves were plotted for uptake against degrees of inequality for various degrees of solubility.

5.6 Overall Gas Exchange

Overall gas exchange was observed and sets of curves for various degrees of inequality and solubilities were compared to give a complete picture of the situation.

5.6.1 Effect of Changing The Solubility of Uptake From 0.001 to 10.0

For this set of curves it was observed that the uptake was enhanced for λ_2 = 0.01, 0.1, 1.0 and 10.0. There was no enhancement in uptake at the value of λ_2 = 0.001. Figure (39).

5.6.2 Effect of Increasing The Solubility of Elimination (λ) by a Factor of 10

Another set of uptake curves were plotted for various degrees of inequality by increasing the value of elimination by a factor of 10, i.e. from 0.001 to 0.01. It was found that the enhancement of uptake occurred at the values of λ_2 = 0.1 and 1.0. There was no enhancement in uptake for the uptake values of λ_2 = 0.001, 0.01 and 10.0. A general equation

was derived and is described in the next chapter giving the conditions for enhancement in the values of solubility of uptake. There was no enhancement in uptake for the rest of the results. Figure (40)

5.7 Individual Uptake

A set of curves were plotted for individual uptake using a different scale so that the enhancement could be observed. The curves for constant ventilation and constant perfusion were drawn.

5.7.1 Constant Ventilation λ_2 = 0.01,0.1

In curve 1 the value of uptake was 2.5 mmHg for a degree of inequality B = 0.0. This pressure was maintained until the value of B reached 0.5. The value of uptake pressure gently rose to a maximum value for a degree of inequality B = 1.1. Uptake pressure dropped to 2.0 mmHg as the value for degree of inequality reached the maximum value of 2.0.. Looking at curve 2, the value of uptake rose sharply to 3.05 mmHg at the value of B 1.2, falling steeply to 2.4 mmHg for the degree of inequality of 2.0. These curves showed definite enhancement in the value of uptake pressure. Figure (41).

5.7.2 Constant Perfusion λ_2 = 0.01,0.1

The first graph shows a gentle rise in the uptake from 2.5 mmHg, to 2.54 mmHg at degrees of inequality of 1.5. For the second graph the rise in uptake pressure was rapid, rising to a maximum of 3.02 mmHg at the degree of inequality of 2.0. However, there was no drop in uptake pressure for constant perfusion curves. Figure (42).

5.7.3 Constant Ventilation λ_2 = 1, 10

For this pair of curves, a definite enhancement in uptake was observed, the uptake pressure at degree of inequality B = 0 was 3.33 mmHg rising to

a maximum value of 3.9 mmHg at the value of B = 1.0, then falling sharply to 2.83 mmHg for B = 2.0. The second graph had an initial uptake value of 4.58 mmHg rising gently to 4.63 at degree of inequality of 0.6, then falling very sharply at the value of B = 1.0, dropping to 3.2 mmHg at B = 2.0. Figure (43).

5.7.4 Constant Perfusion λ_2 = 1, 10

Looking at the first curve, the value of uptake started at 3.32 mmHg rising to 4.20 mmHg at the degree of inequality of 2.0. In the second curve, the uptake value started from 4.58 mmHg rising to a maximum value of 4.9 mmHg at the degree of inequality B = 2.0.

It was noted that uptake enhancement and the uptake pressure did not fall below the original value at B = 0.0. Figure (44).

5.7.5 Constant Ventilation λ_2 = 1.00, 0.1 for λ_3 = 0.01

The value of P_{aG} was 2.5 mmHg for the degree of inequality B = 0.0 rising to a maximum of 2.71 mmHg for the degree of inequality of B = 0.838, then sharply falling to 1.6 mmHg for B = 2.0. For the two curve λ_2 = 1.0 and λ_2 = 0.1, the value of P_{aG} started from 3.3 mmHg rising to 3.52 mmHg, then falling sharply to a minimum value of 2.0 mmHg for the $\dot{V}_{IA}/\dot{Q}$ ratio of 2.0. The maximum value was shifted to the left and it was noted that the rise in uptake was 0.21 mmHg in both cases. Figure (45).

5.7.6 Constant Perfusion λ_2 = 1.0, 0.1 for λ_3 = 0.01

In these curves, the value of uptake carried on increasing and showed a definite enhancement. Looking at the first curve, the uptake started from the P_{aG} value of 2.59 mmHg, rising to a maximum of 2.87 mmHg for the $\dot{V}_{IA}/\dot{Q}$ ratio of 2.0. In the second instance the minimum value at P_{aG} was 3.3 mmHg,

LIBRARY

rising to a maximum of 4.0 mmHg, i.e. an increase of 0.3 mmHg in the pressure of uptake, compared with the previous gas and 0.7 mmHg in the latter. Figure (46).

5.8 Comparison of All The Uptake Curves

A set of curves for all the uptakes against degrees of inequality B = 0 (mild) to B = 2.0 (severe) were drawn for constant ventilation and constant perfusion, and compared.

5.8.1 Constant Ventilation

For this set of curves, it was noticed, that as the value of λ_2 was increased, starting from λ_2 = 0.01 and raised by a multiple of 10 until λ_2 was = 10.0 (highly soluble), the value of uptake was increased from 2.5 mmHg to 2.55 mmHg. The maximum rise in uptake pressure was small, i.e. 0.05 mmHg. Figure (47).

5.8.2 Constant Perfusion

It was noticed that the uptake was enhanced for λ_2 = 1.0. It was found that the uptake was enhanced by an amount of 0.9 mmHg, i.e. exactly the same factor as it was for the constant ventilation. There were similarities in these curves and in Figure (46) such enhancement was maximum for the same degrees of inequalities and values of λ uptake. Figure (48).

5.9 Uptake Curves for $\dot{V}_{A/Q}$ Model

Solving a cubic equation for these gases produced a set of results, and graphs of uptake against degrees of inequality were plotted. It was found that there was an enhancement in uptake, a maximum being by a factor of 0.6 mmHg for curve 6. The uptake for curve 5 was 1.31 mmHg for B = 0, gently rising to 1.32 mmHg. For B = 0.2, in curve 10, the uptake rose from 1.33 to 1.8 mmHg. For B = 1.5 in curve 5, there was a slight fall

LIBRARY

in uptake and the enhancement by 0.2 mmHg,, similar patterns were observed for all the curves. Figure (49).

FIGURE 13

Uptake - Elimination

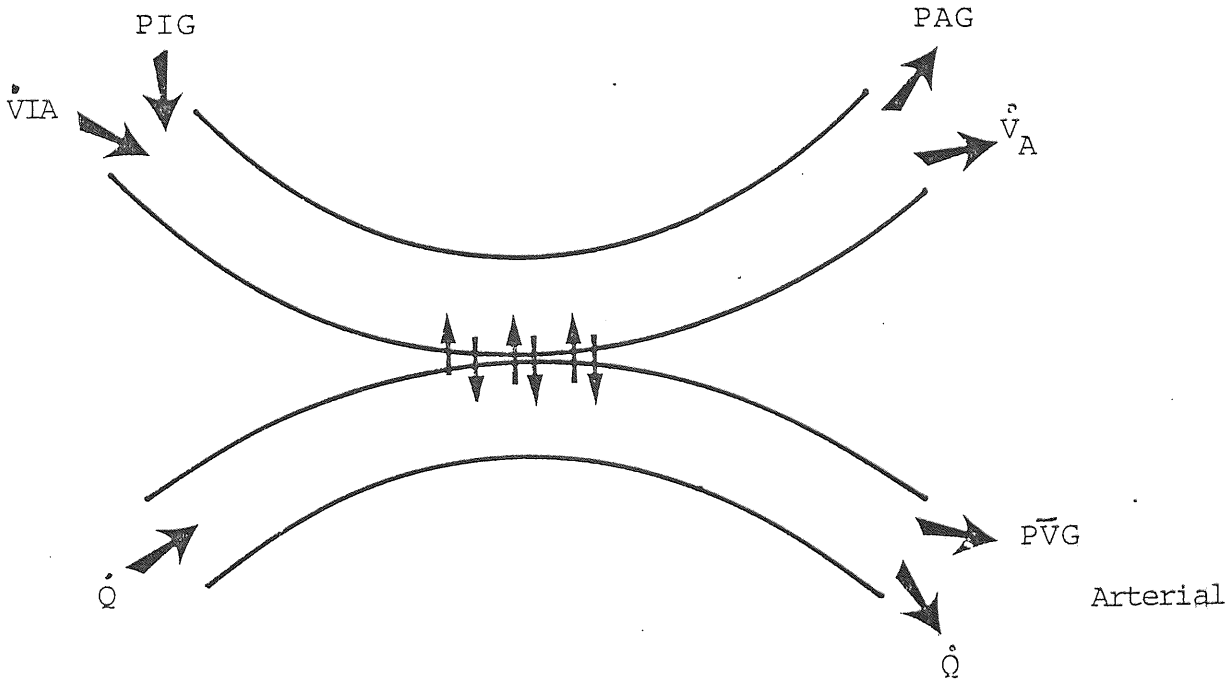

UPTAKE - ELIMINATION some gas is being taken up while rest is being eliminated.

FIGURE 14

Uptake Elimination Curves

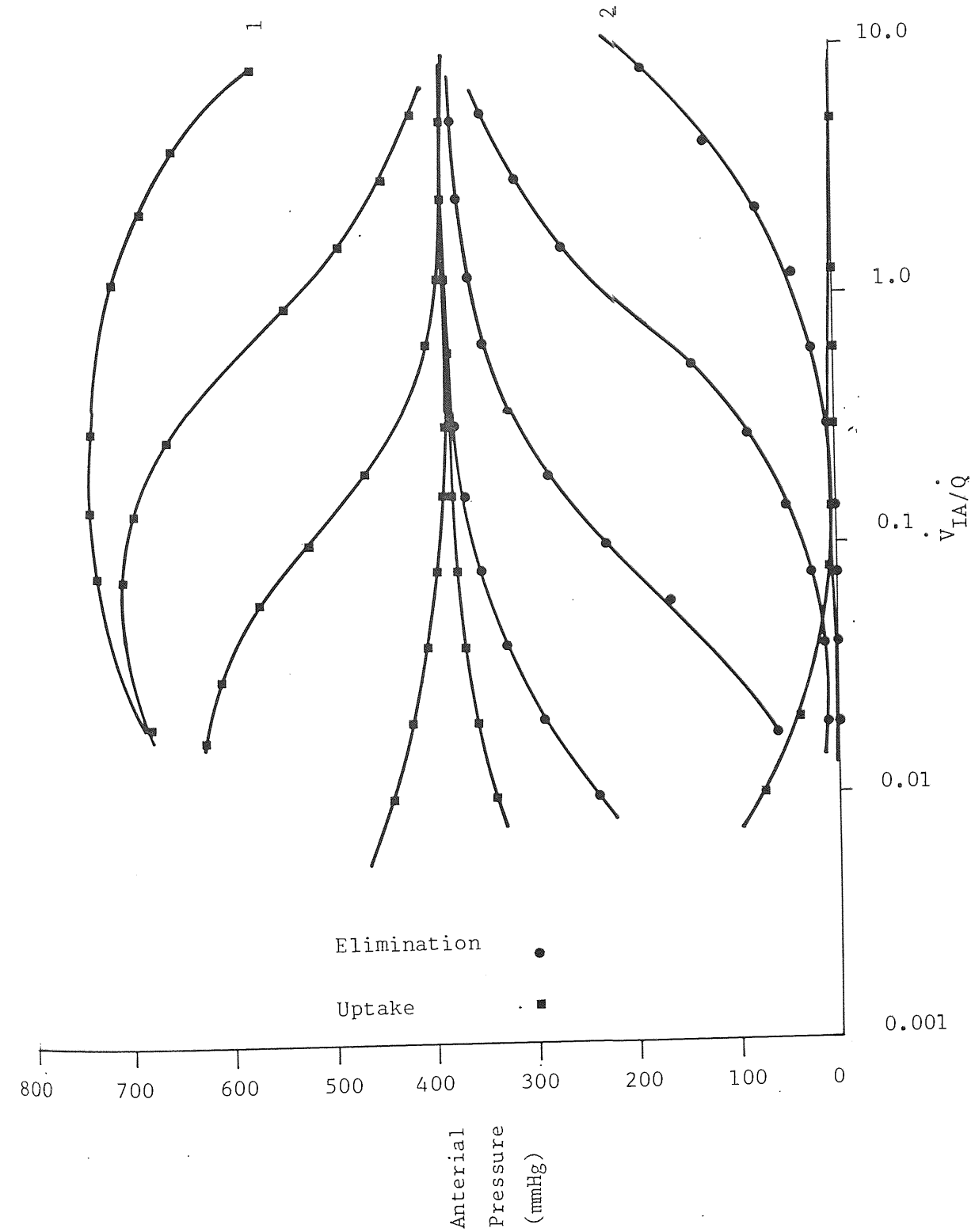

LIBRARY

FIGURE 15

Uptake Elimination Curves

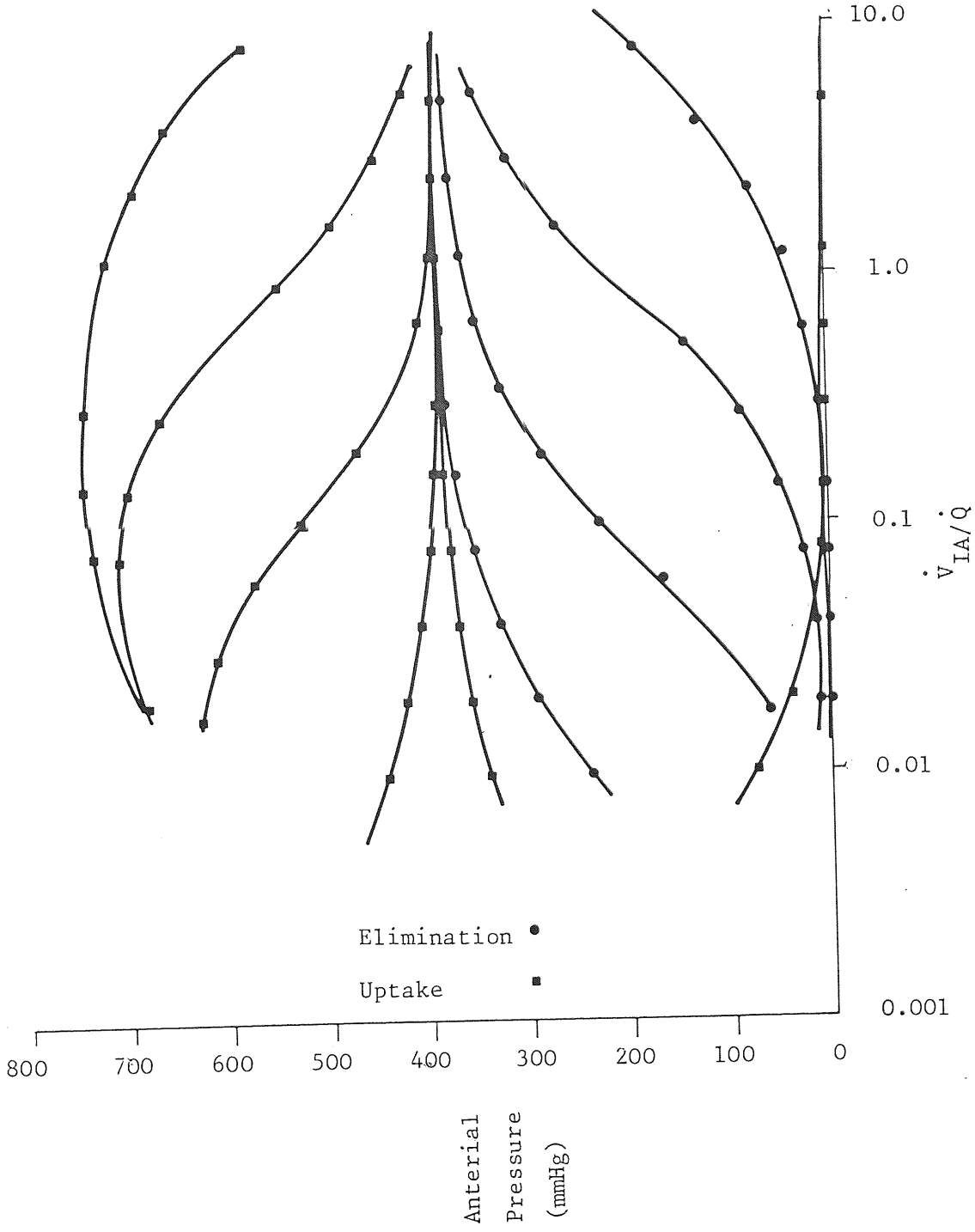

FIGURE 16

Uptake Elimination Curves

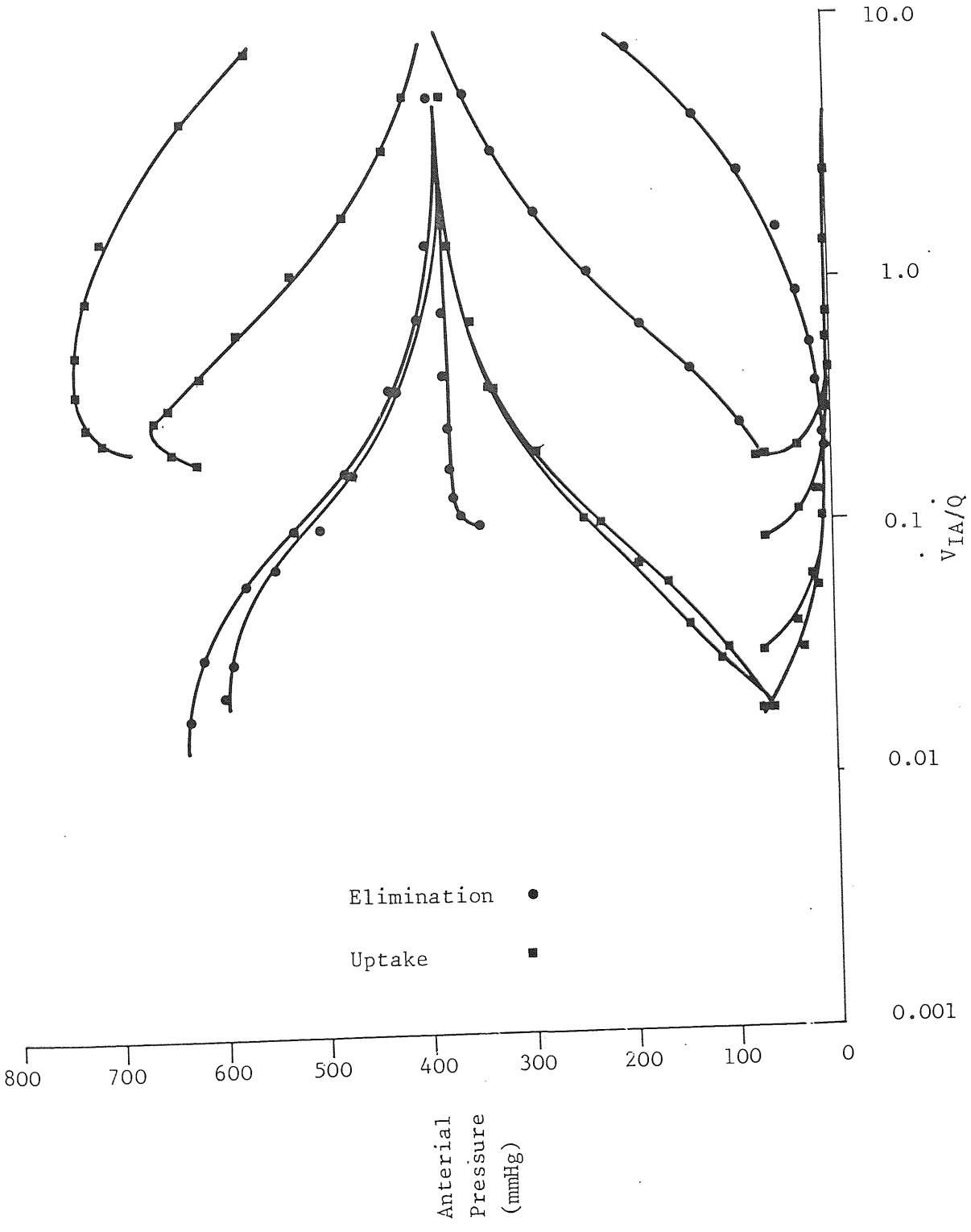

LIBRARY

FIGURE 17

Uptake Elimination Curves

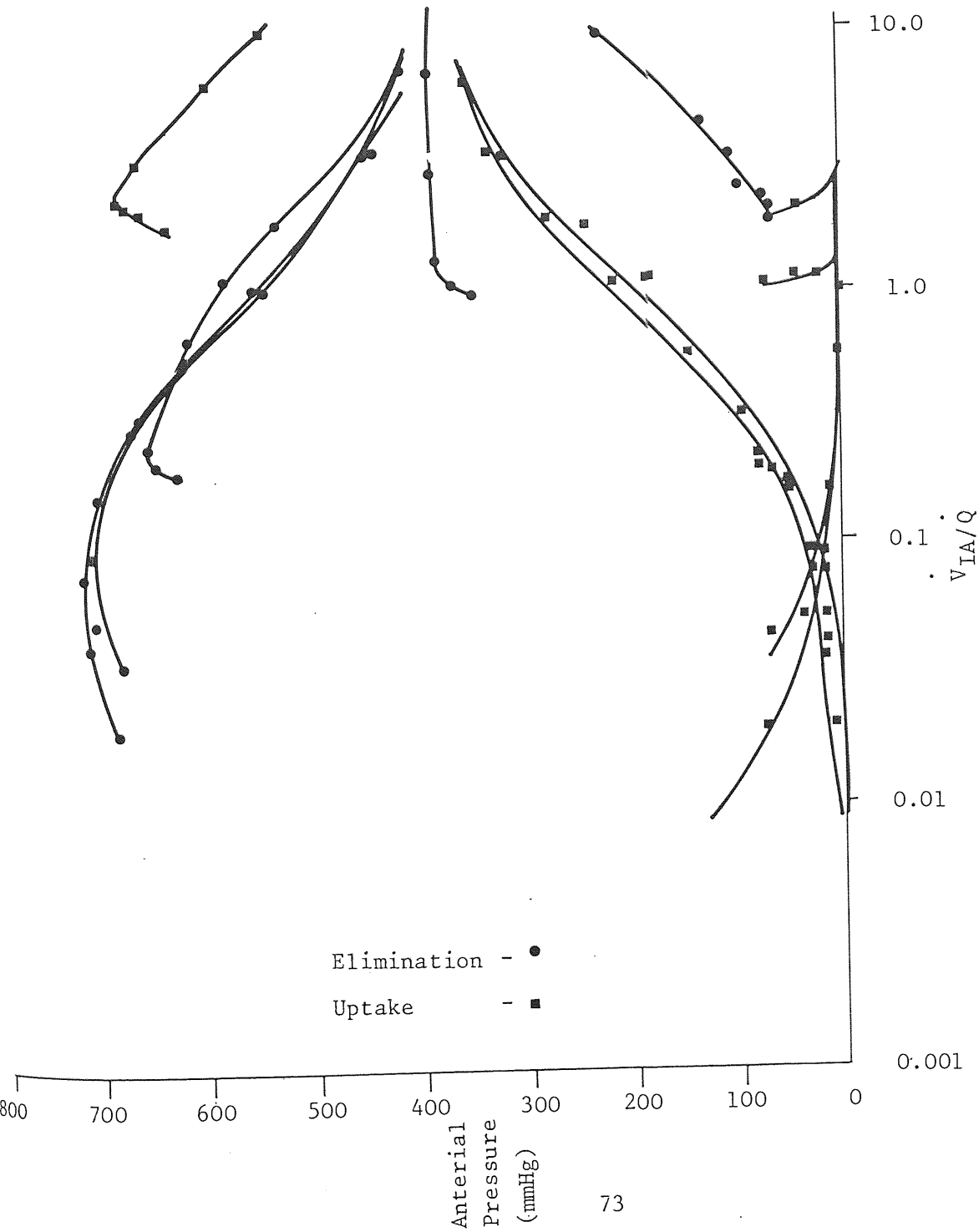

FIGURE 18

Elimination/Uptake Curves

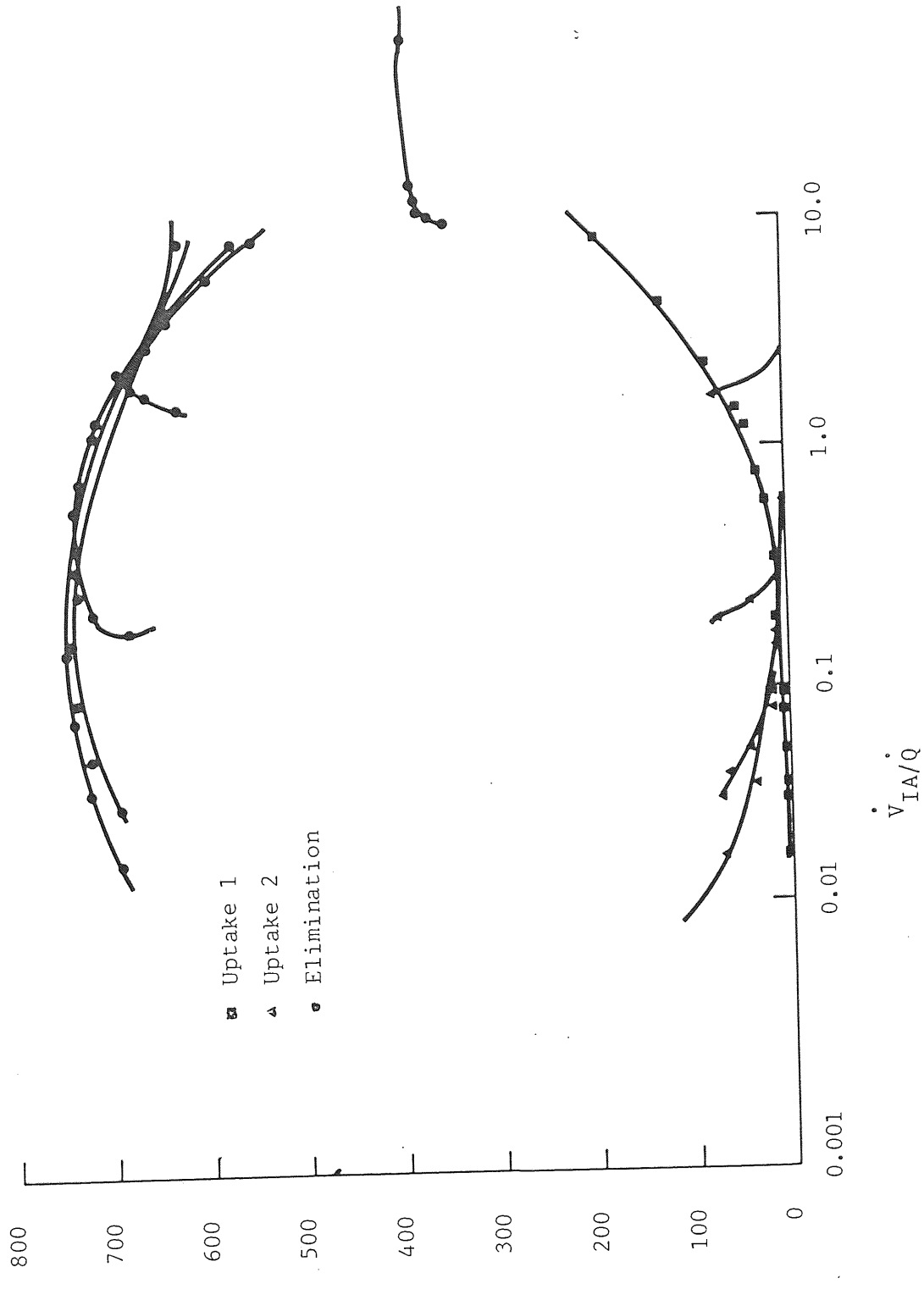

FIGURE 19

Elimination/Uptake Curves

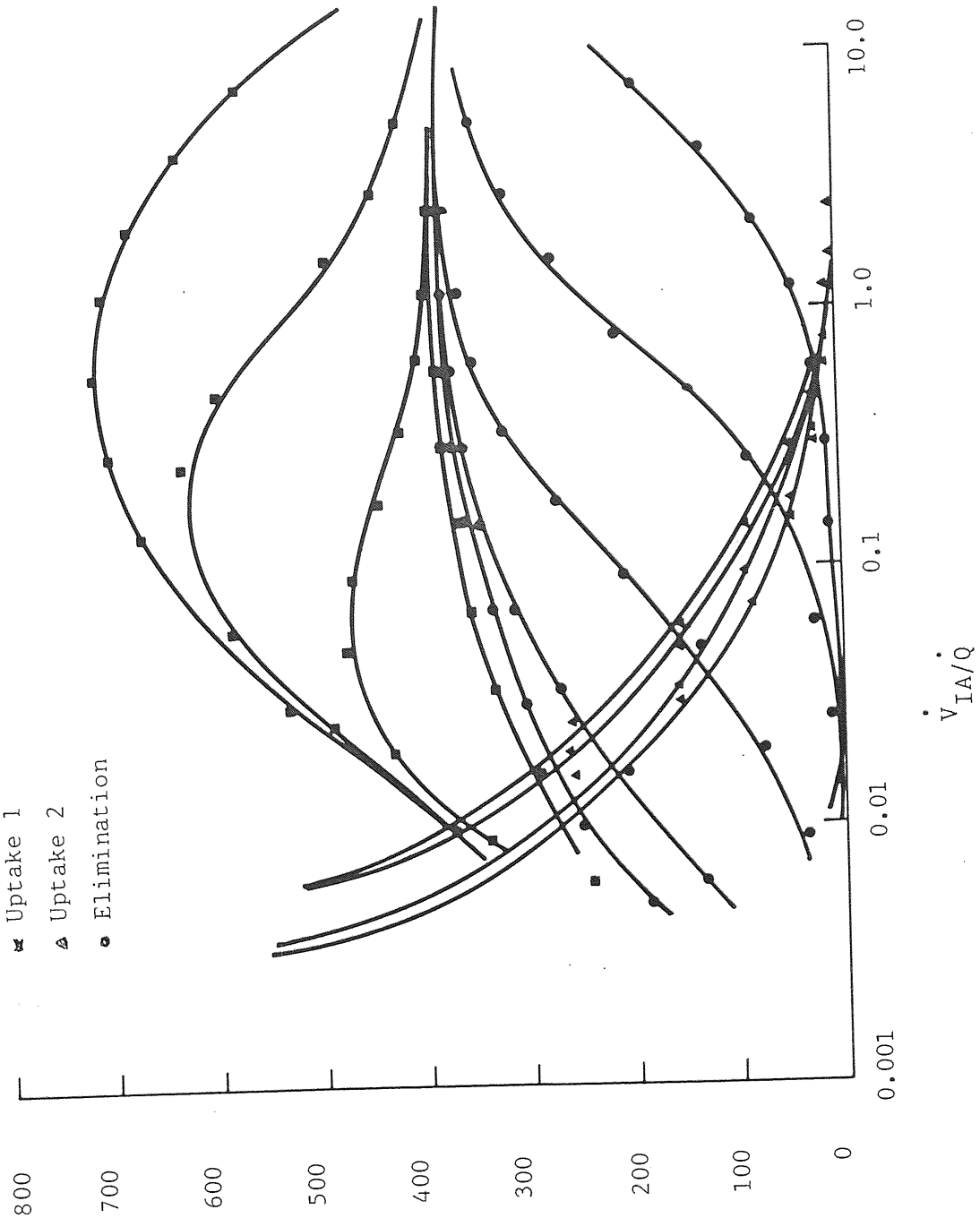

FIGURE 20

Elimination/Uptake Curves

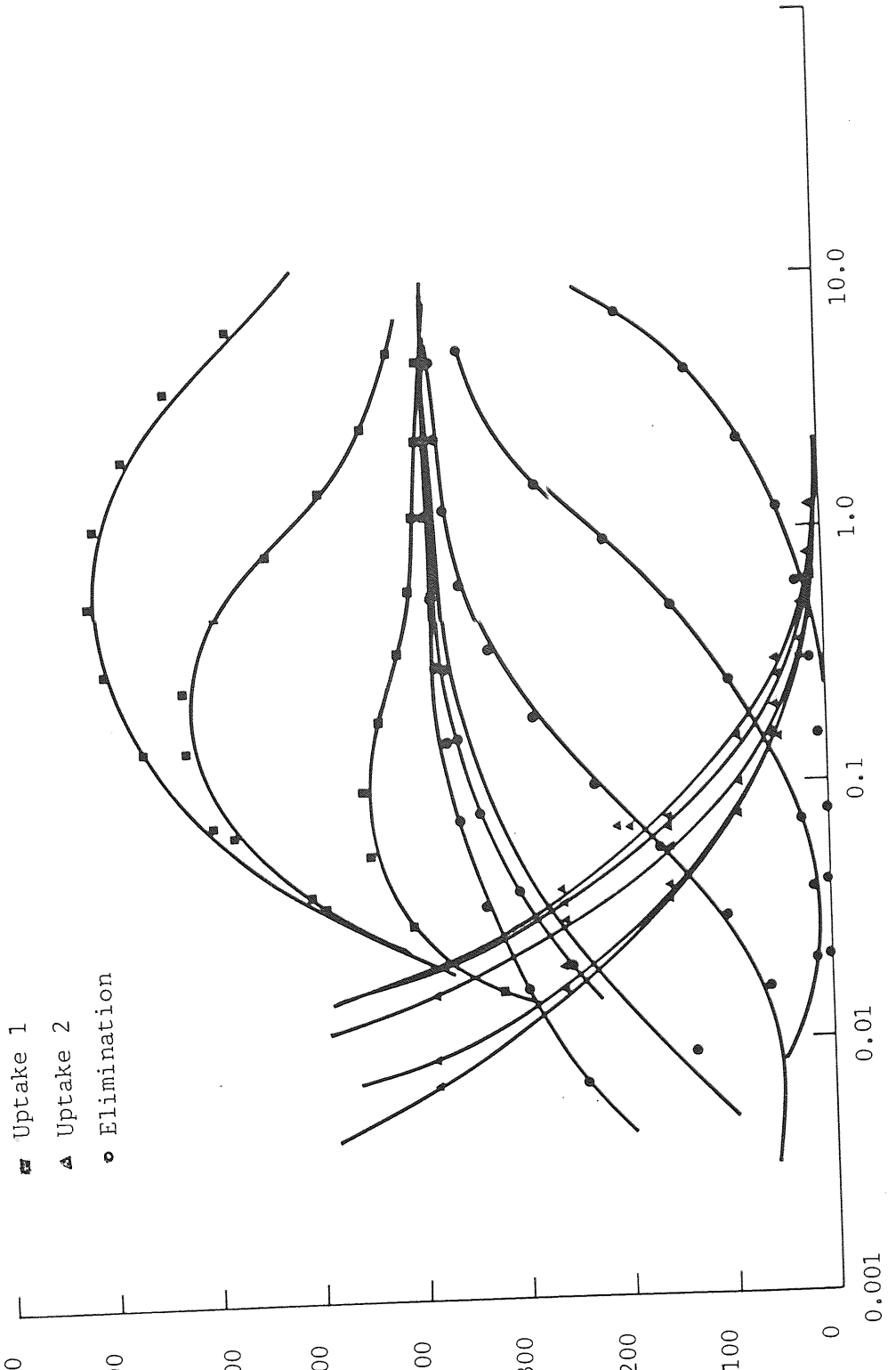

FIGURE 21

Elimination/Uptake Curves

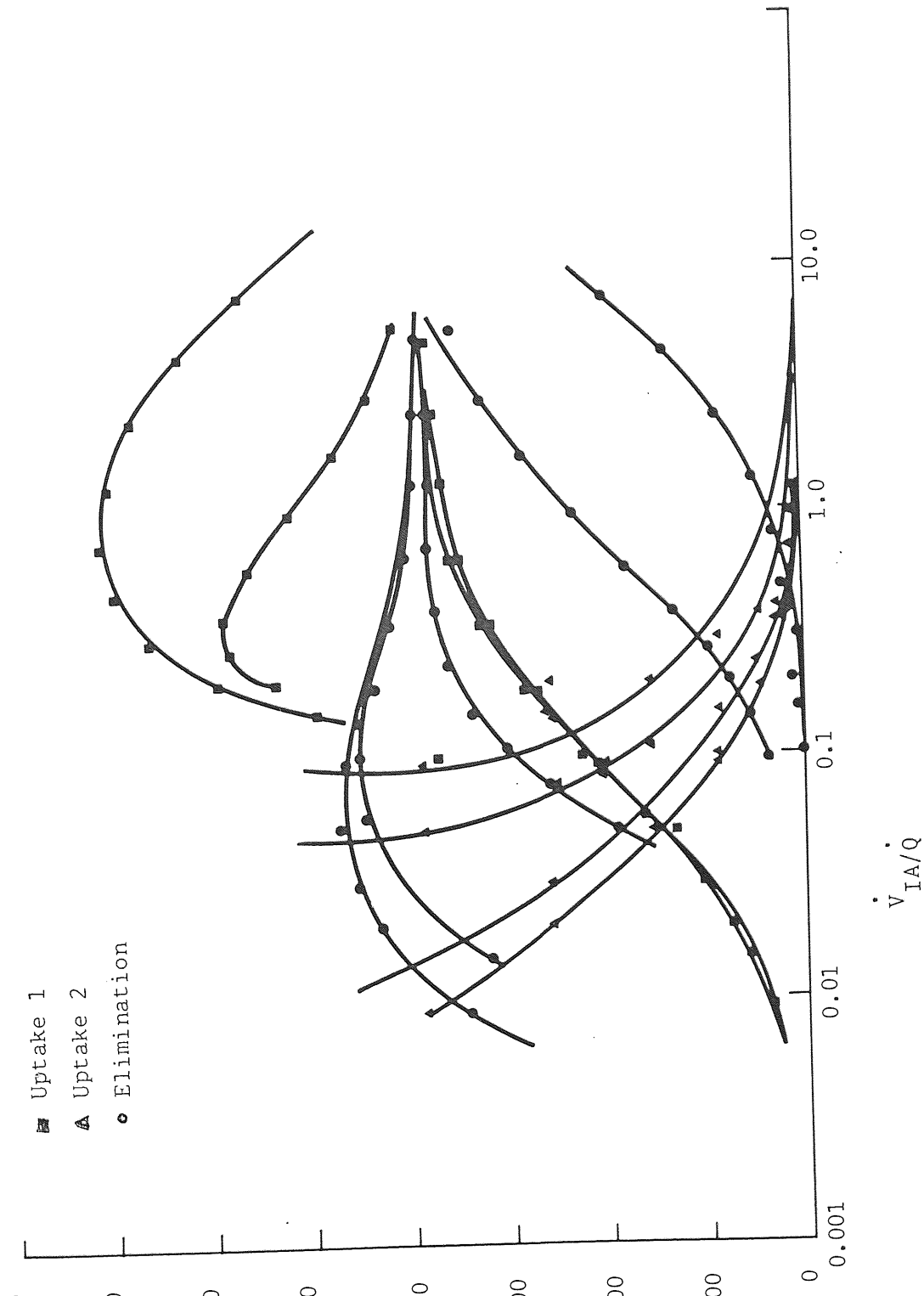

FIGURE 22

Elimination/Uptake Curves

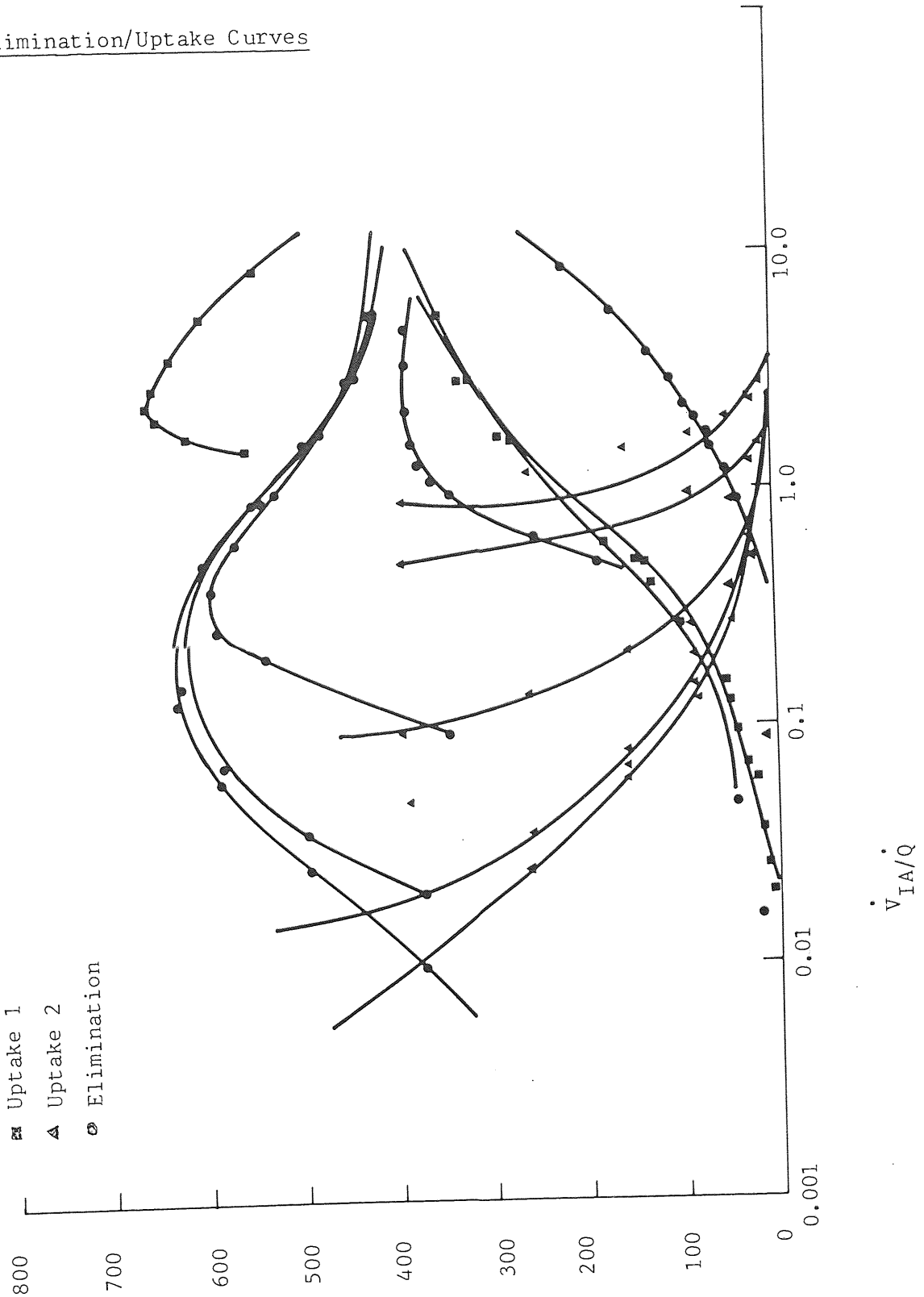

FIGURE 23

Elimination/Uptake Curves

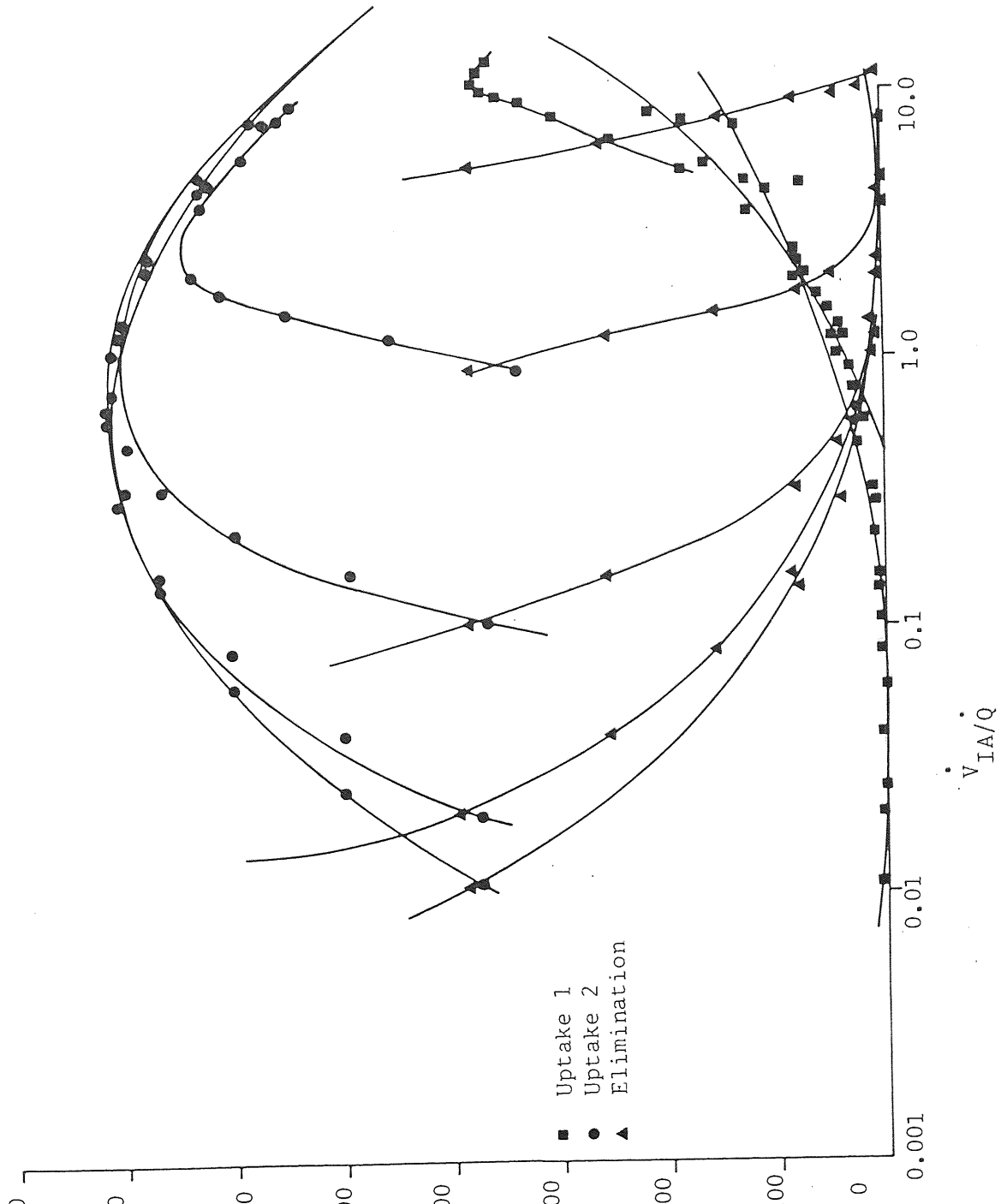

FIGURE 24

Elimination/Uptake Curves

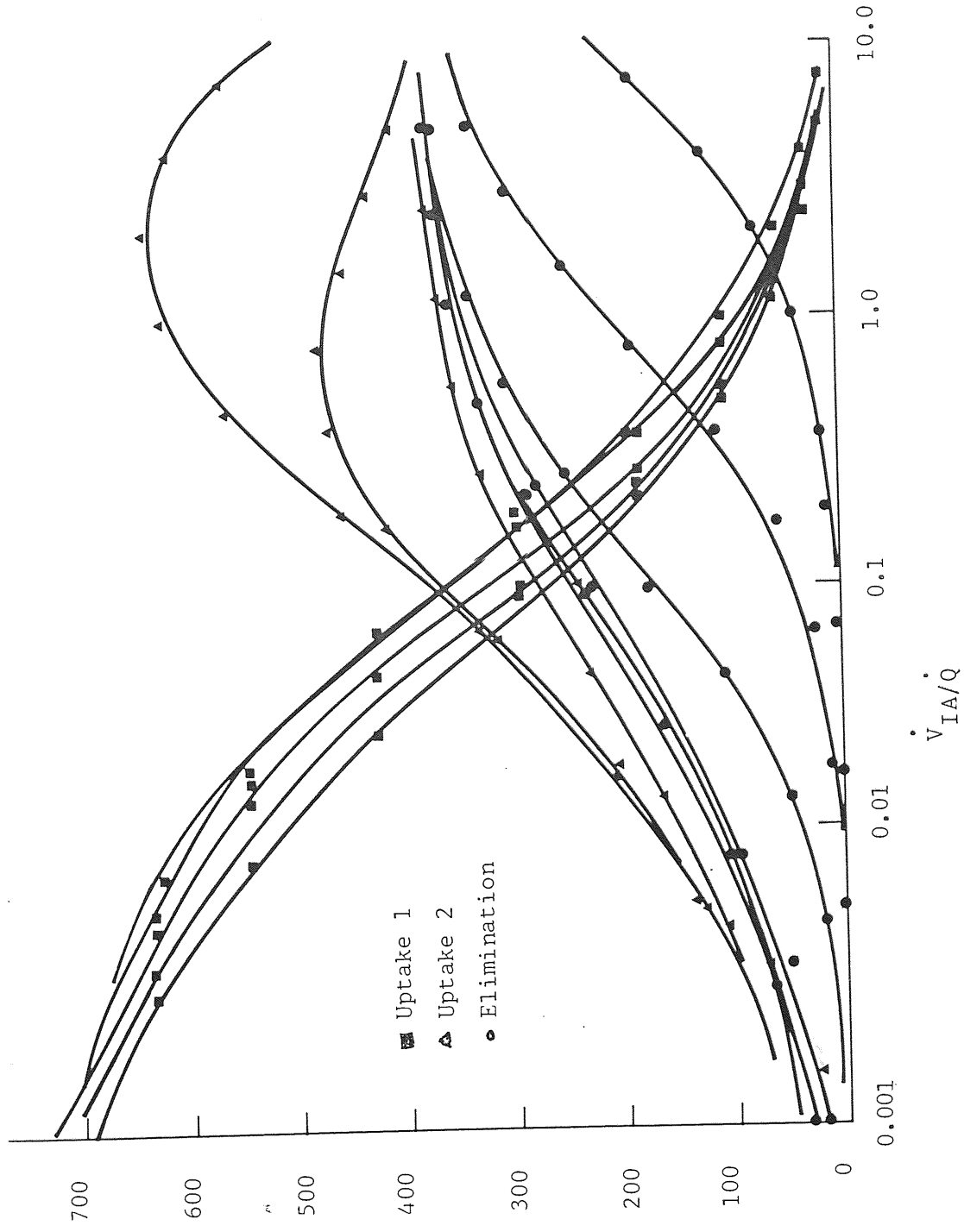

FIGURE 25

Elimination/Uptake Curves

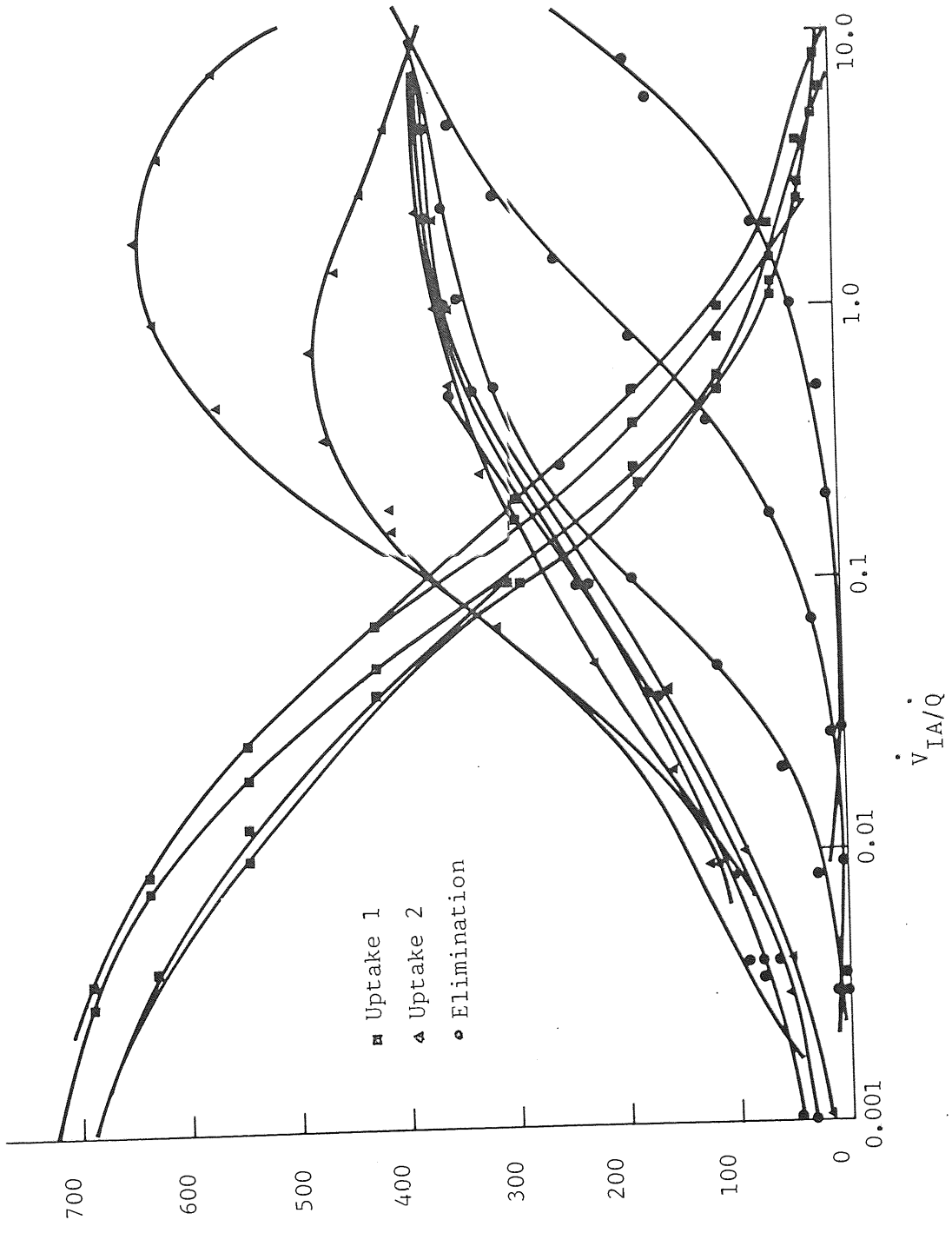

FIGURE 26

Elimination/Uptake Curves

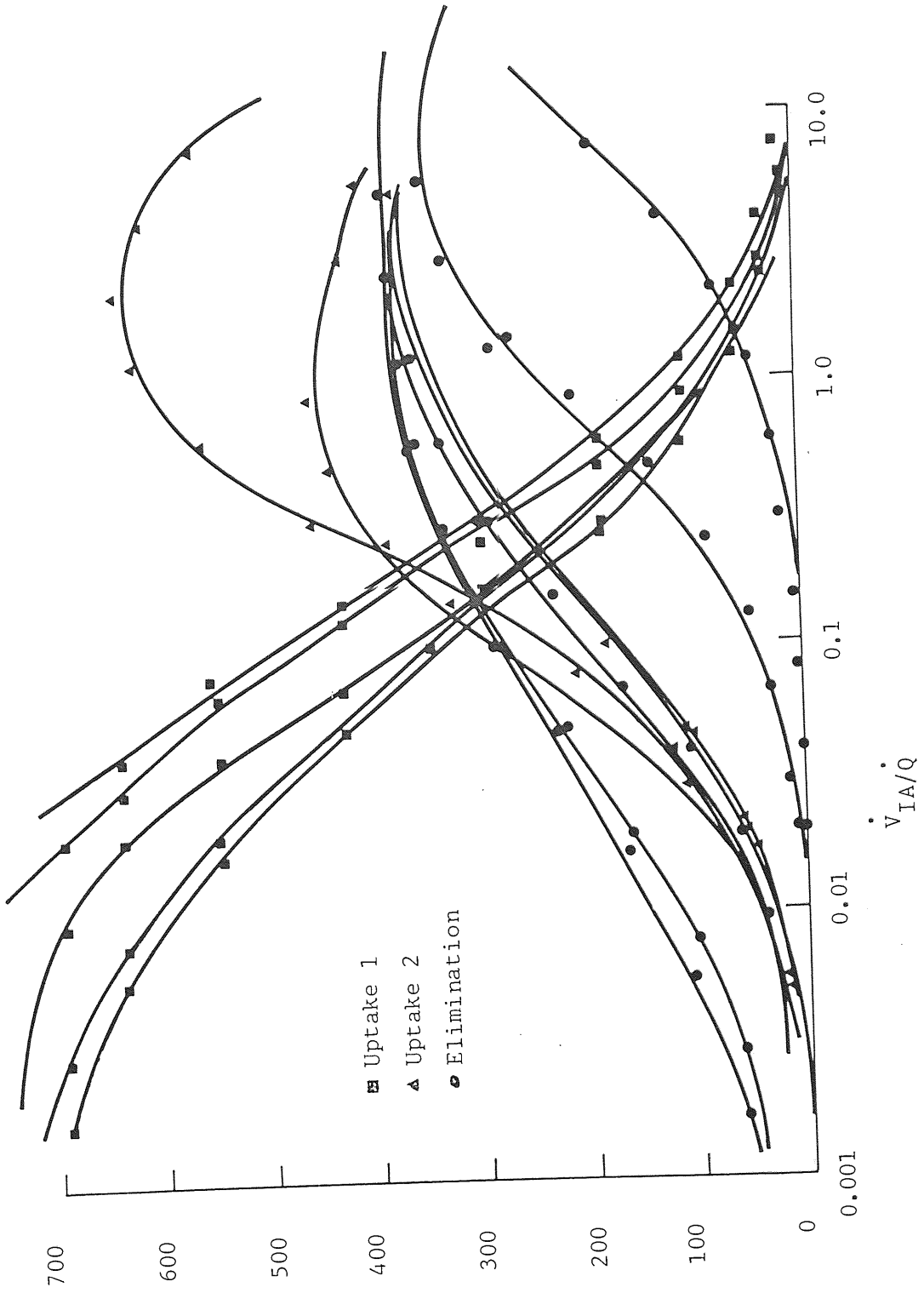

FIGURE 27

Elimination/Uptake Curves

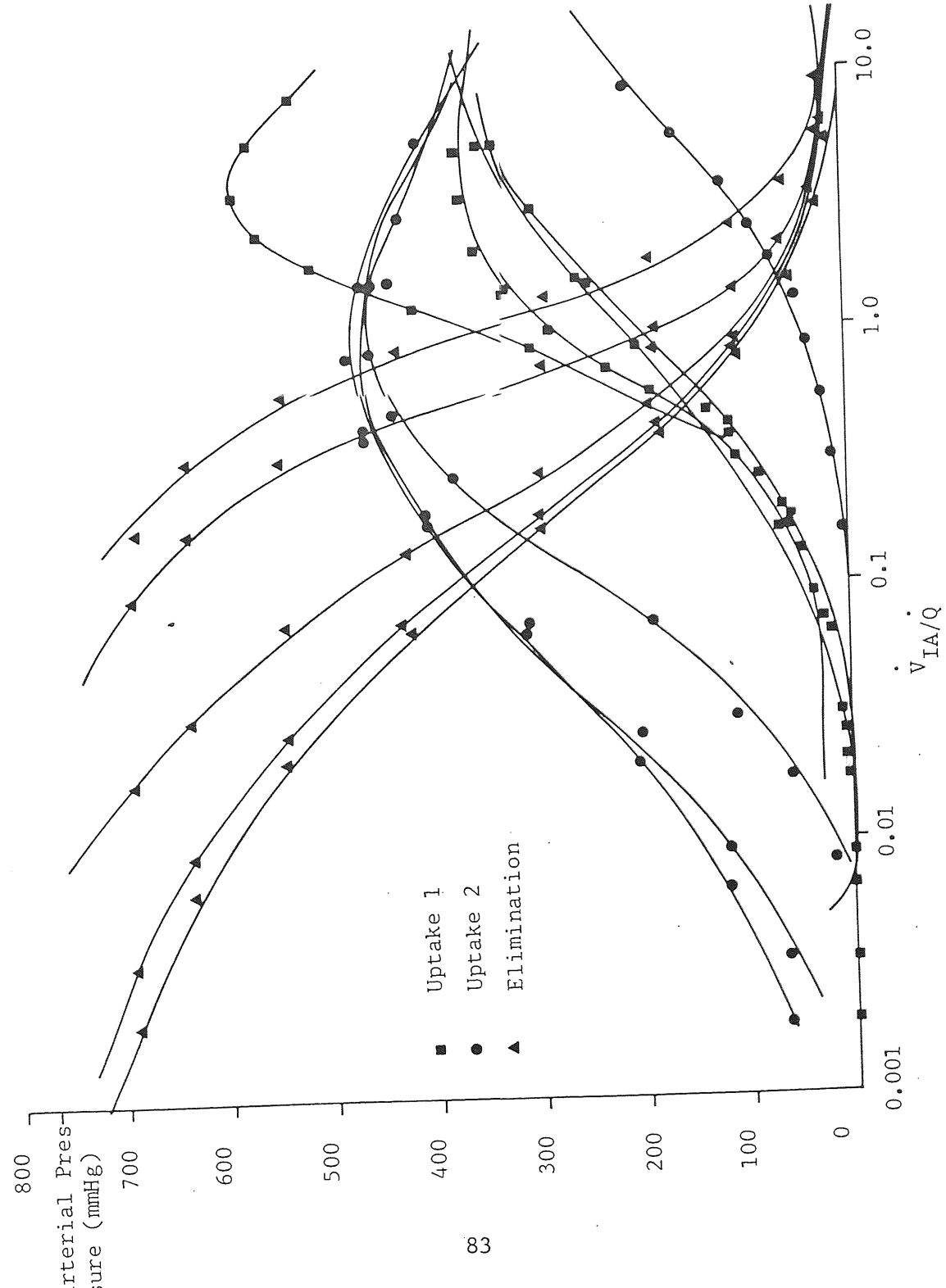

FIGURE 28

Elimination/Uptake Curves

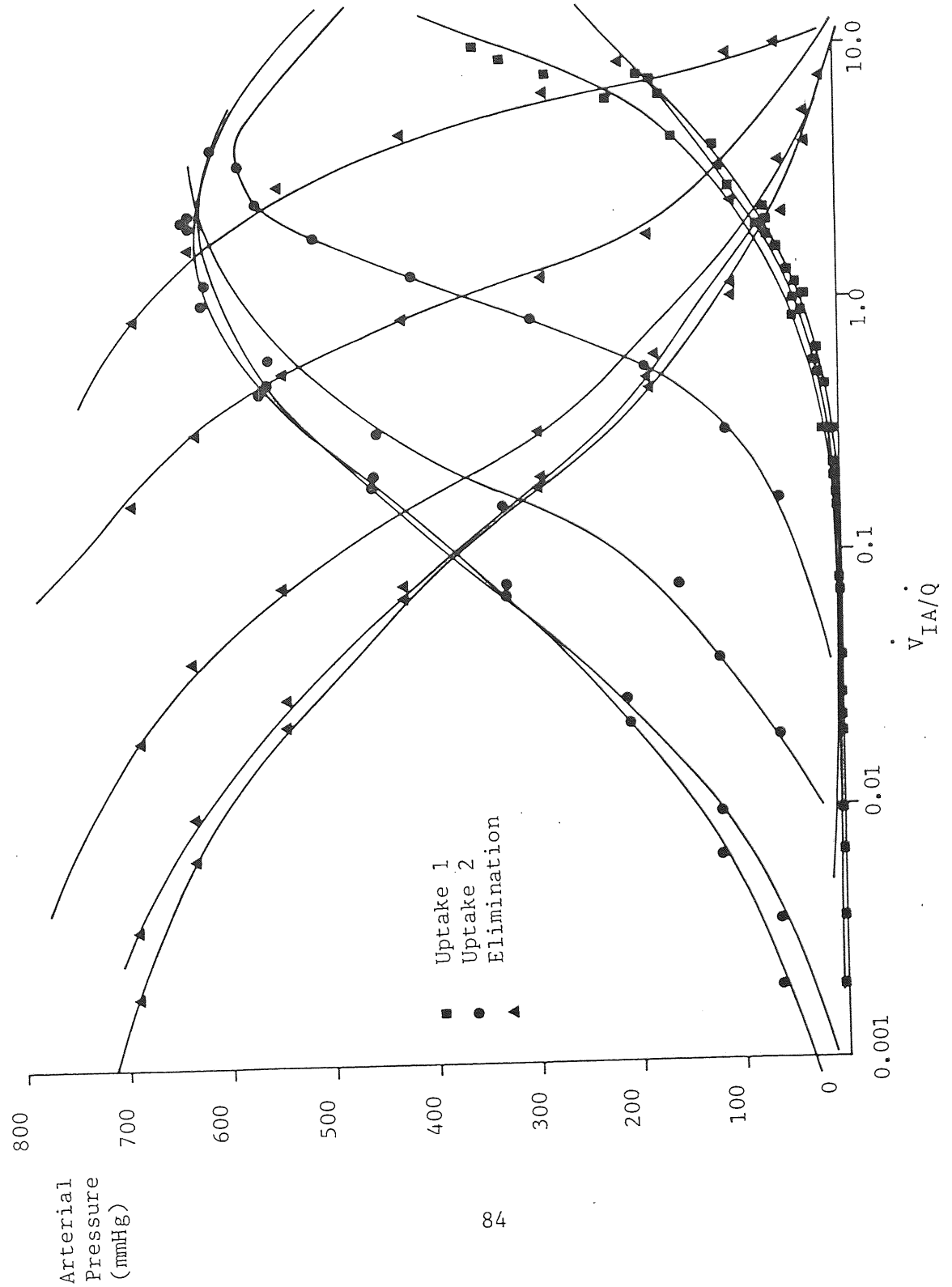

FIGURE 29

Elimination/Uptake Curves

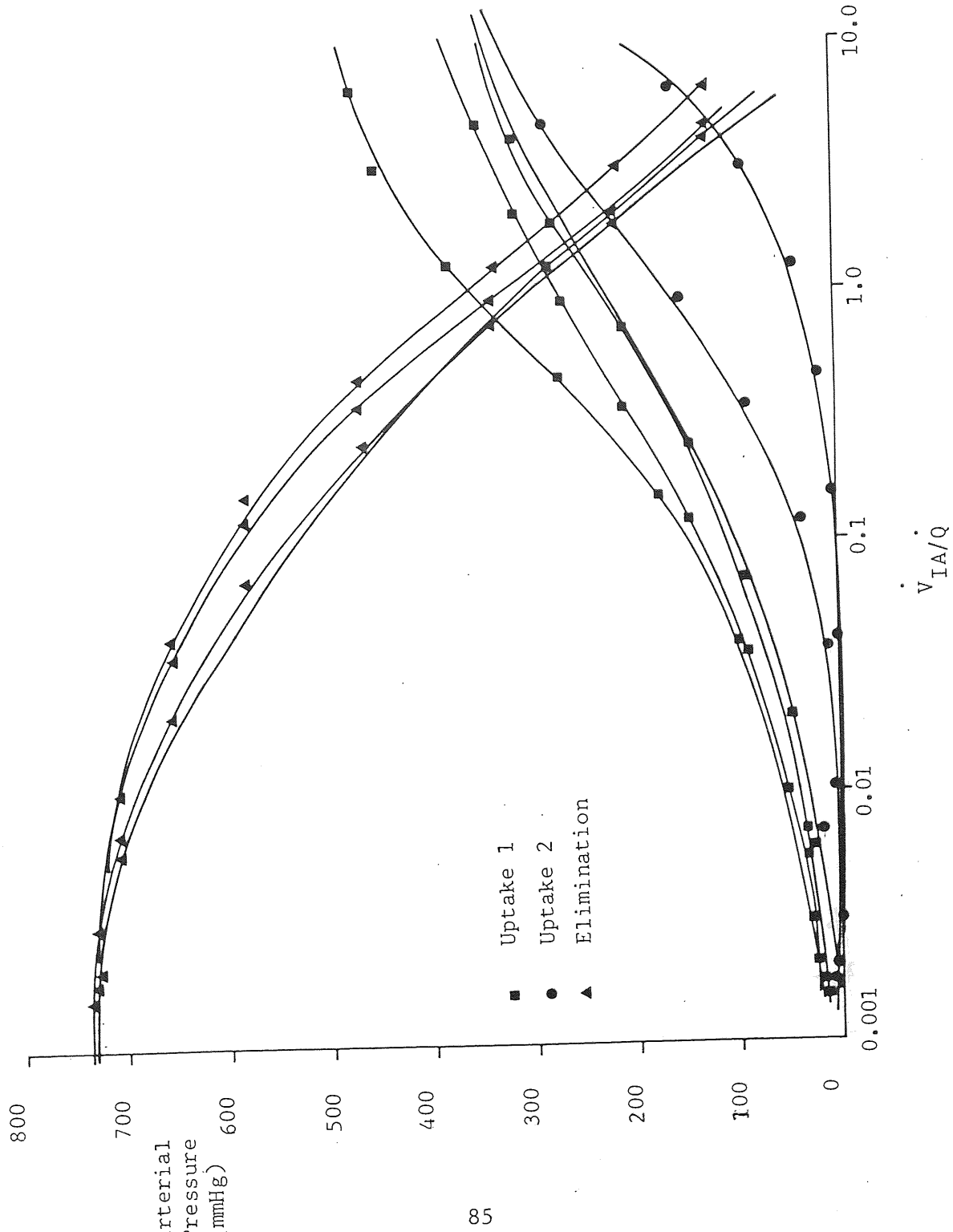

FIGURE 30

Elimination/Uptake Curves

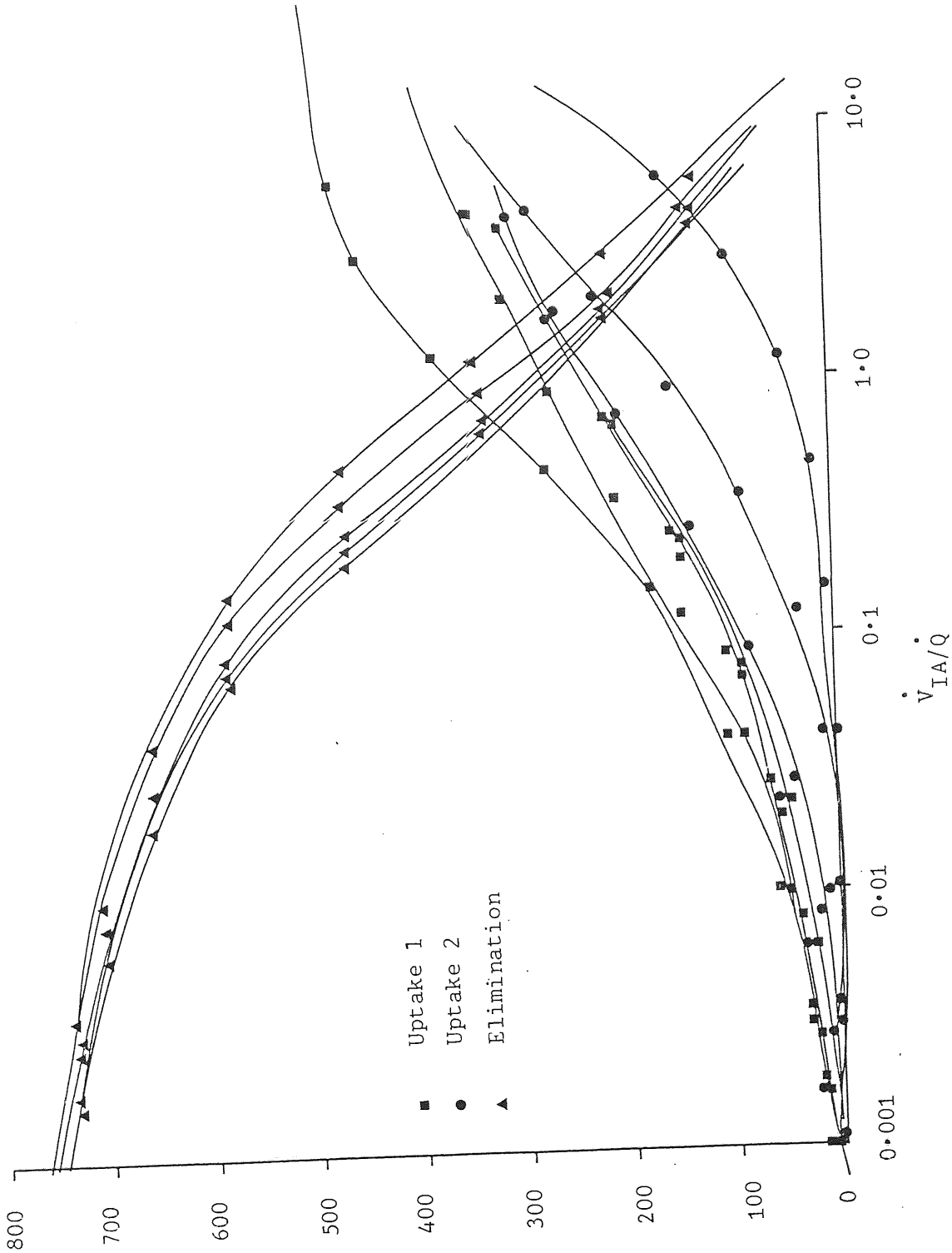

FIGURE 31

Elimination/Uptake Curves

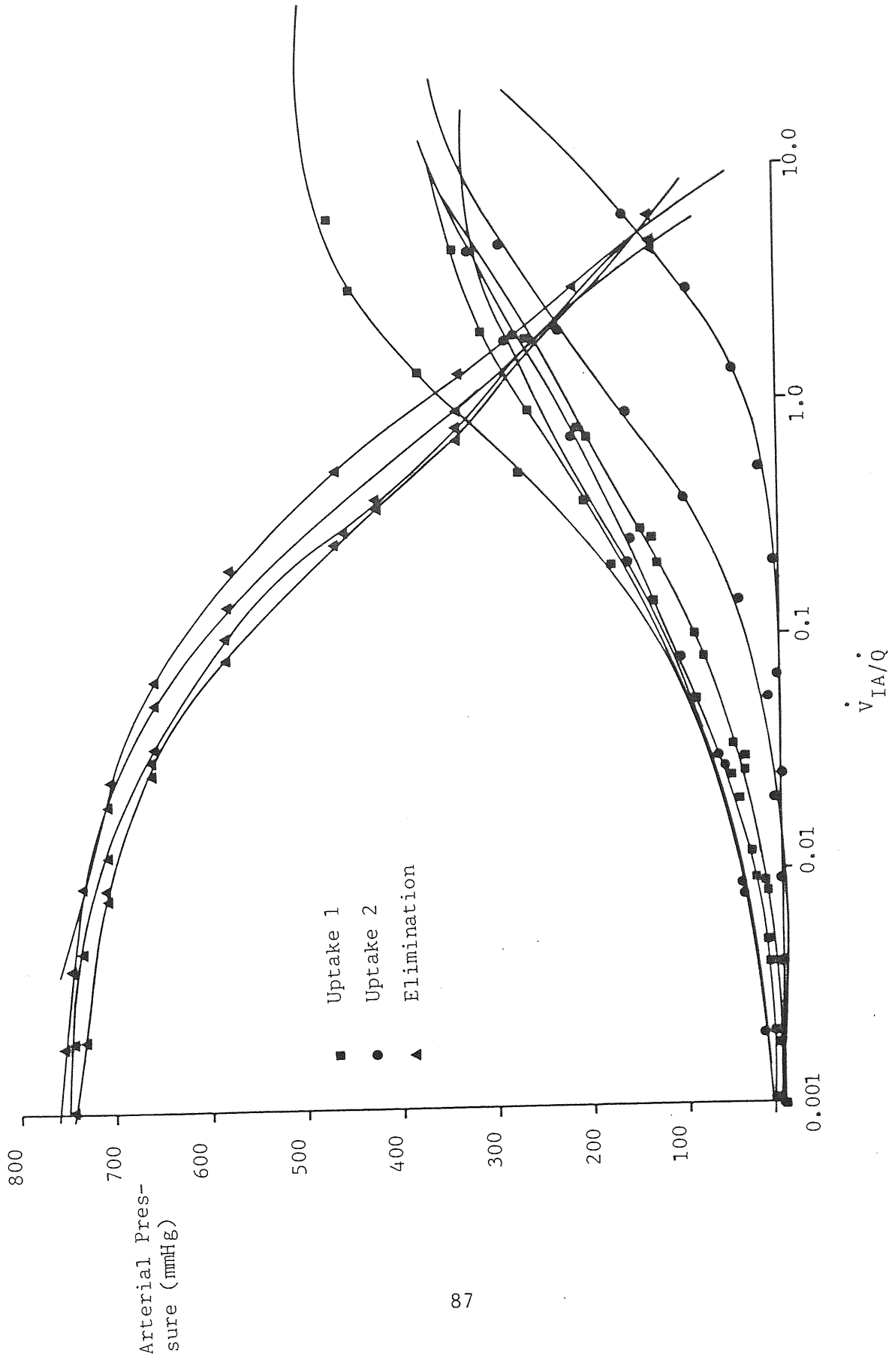

FIGURE 32

Elimination/Uptake Curves

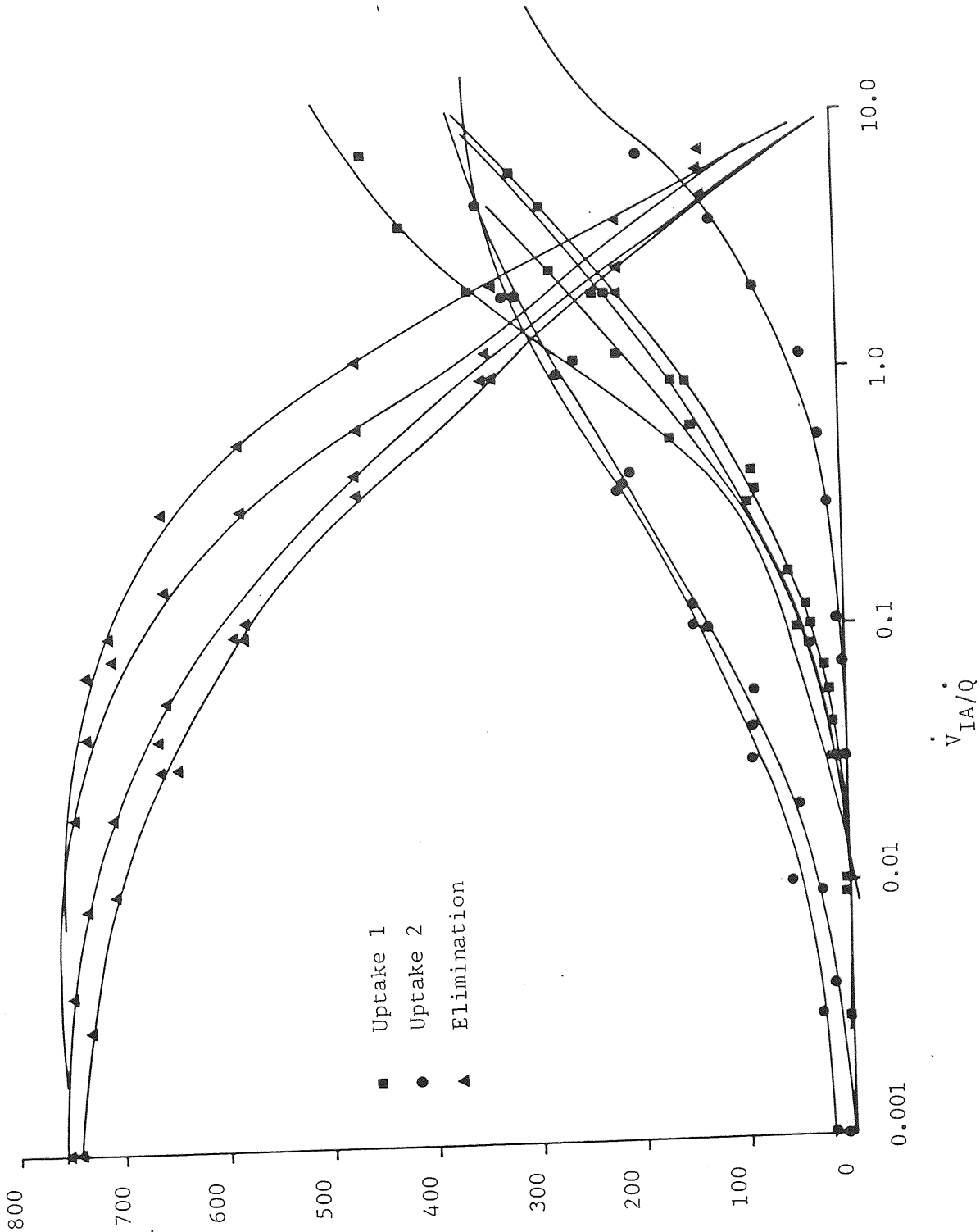

FIGURE 33

Elimination/Uptake Curves

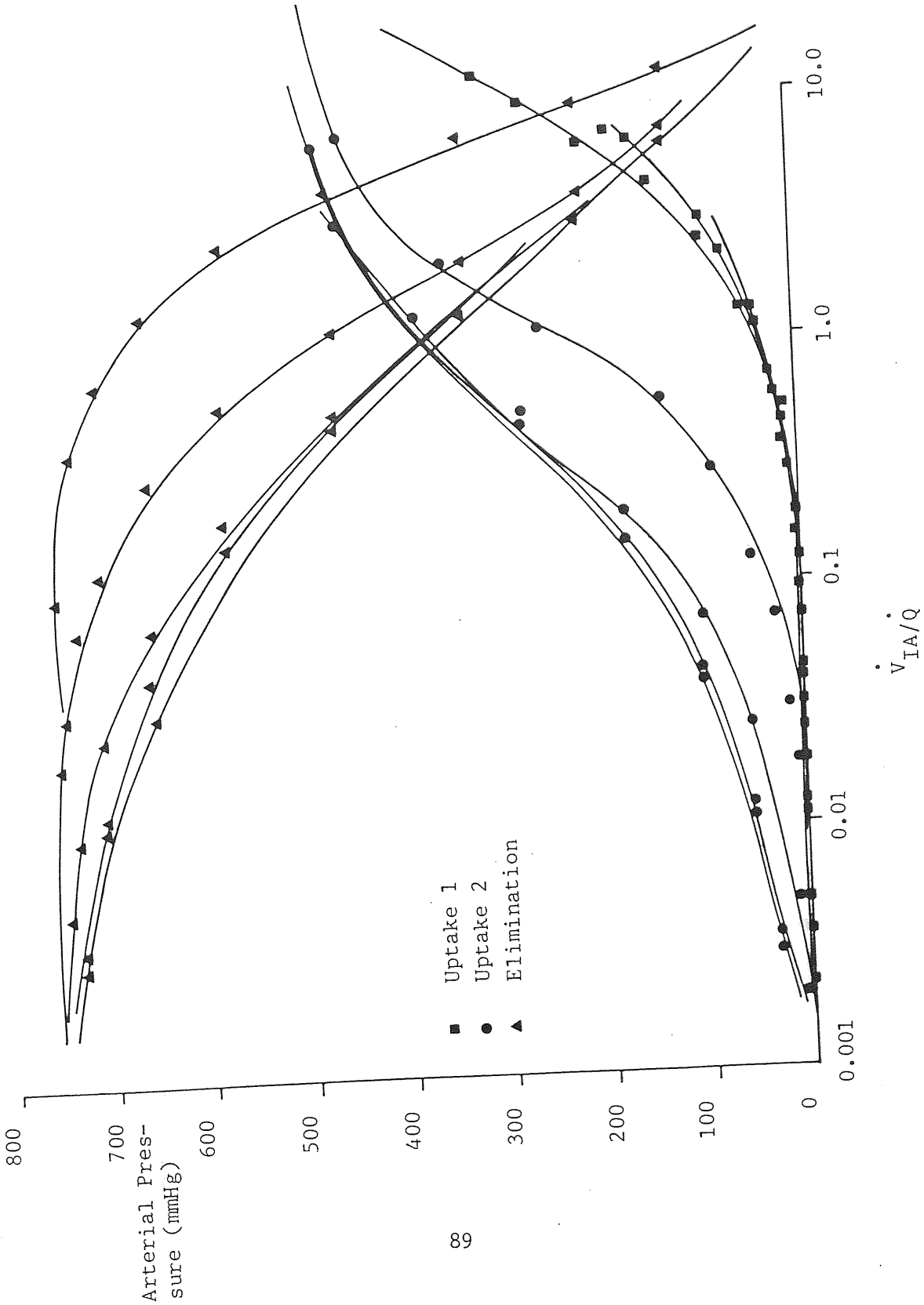

FIGURE 34

Elimination/Uptake Curves

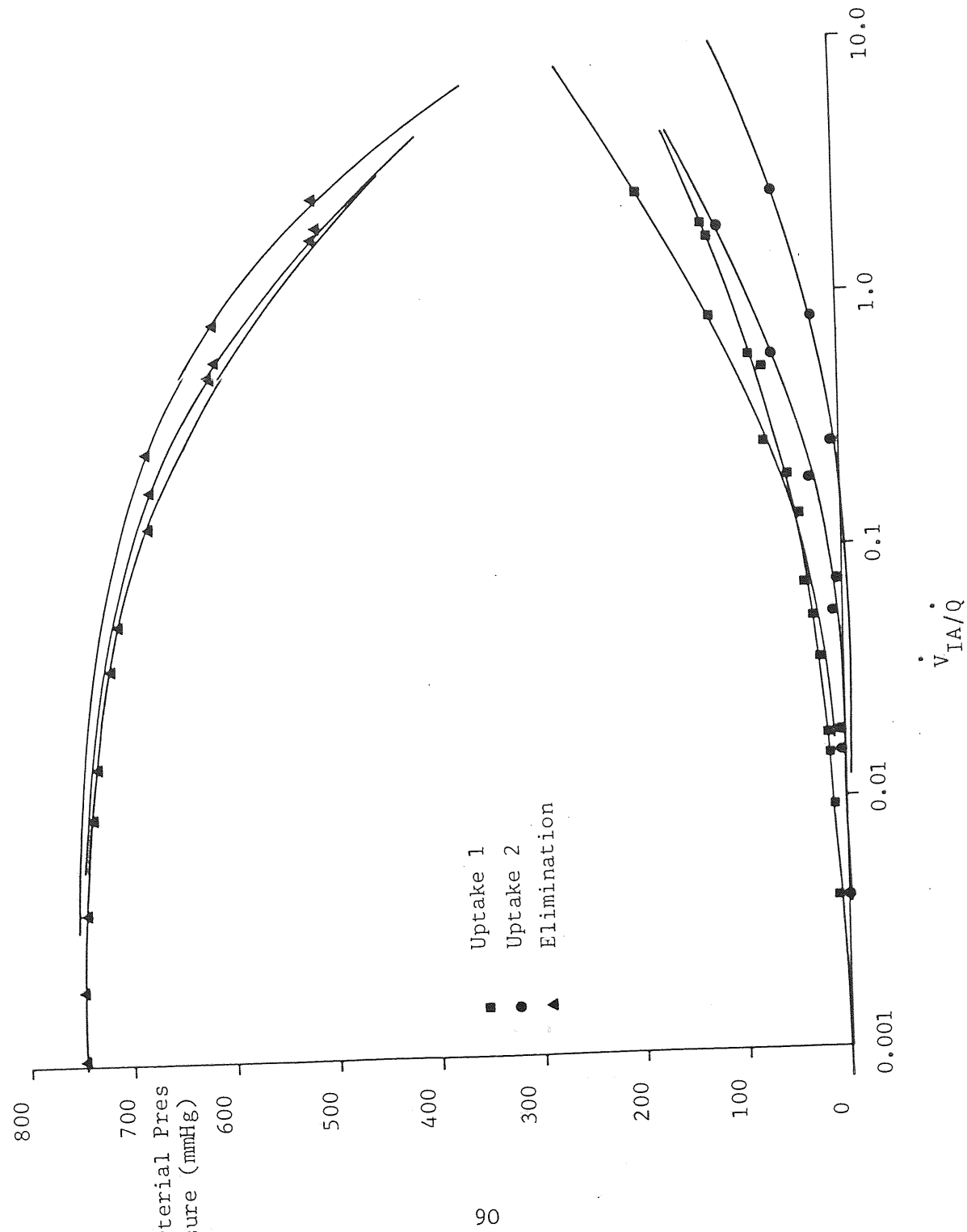

FIGURE 35

Elimination/Uptake Curves

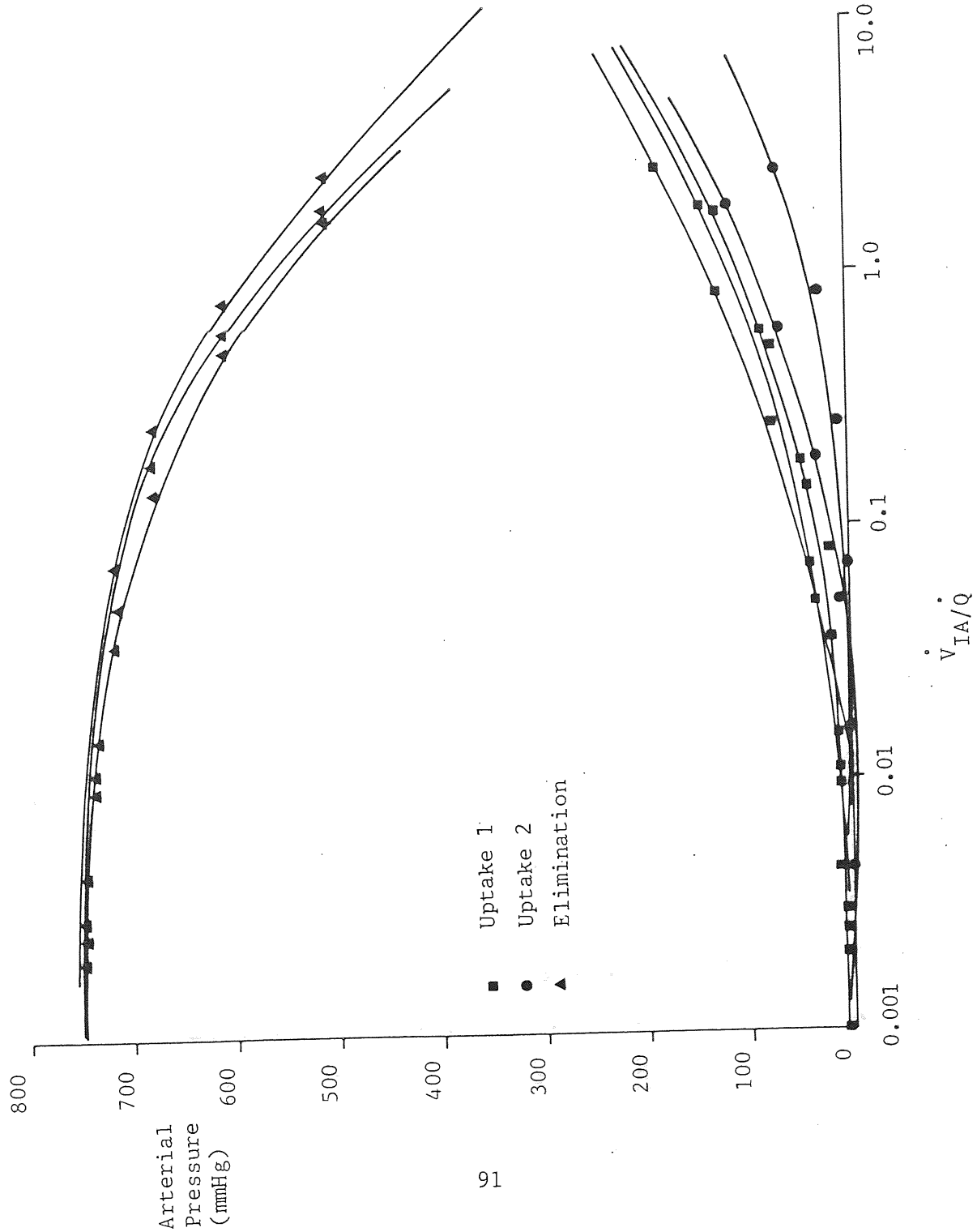

FIGURE 36

Elimination/Uptake Curves

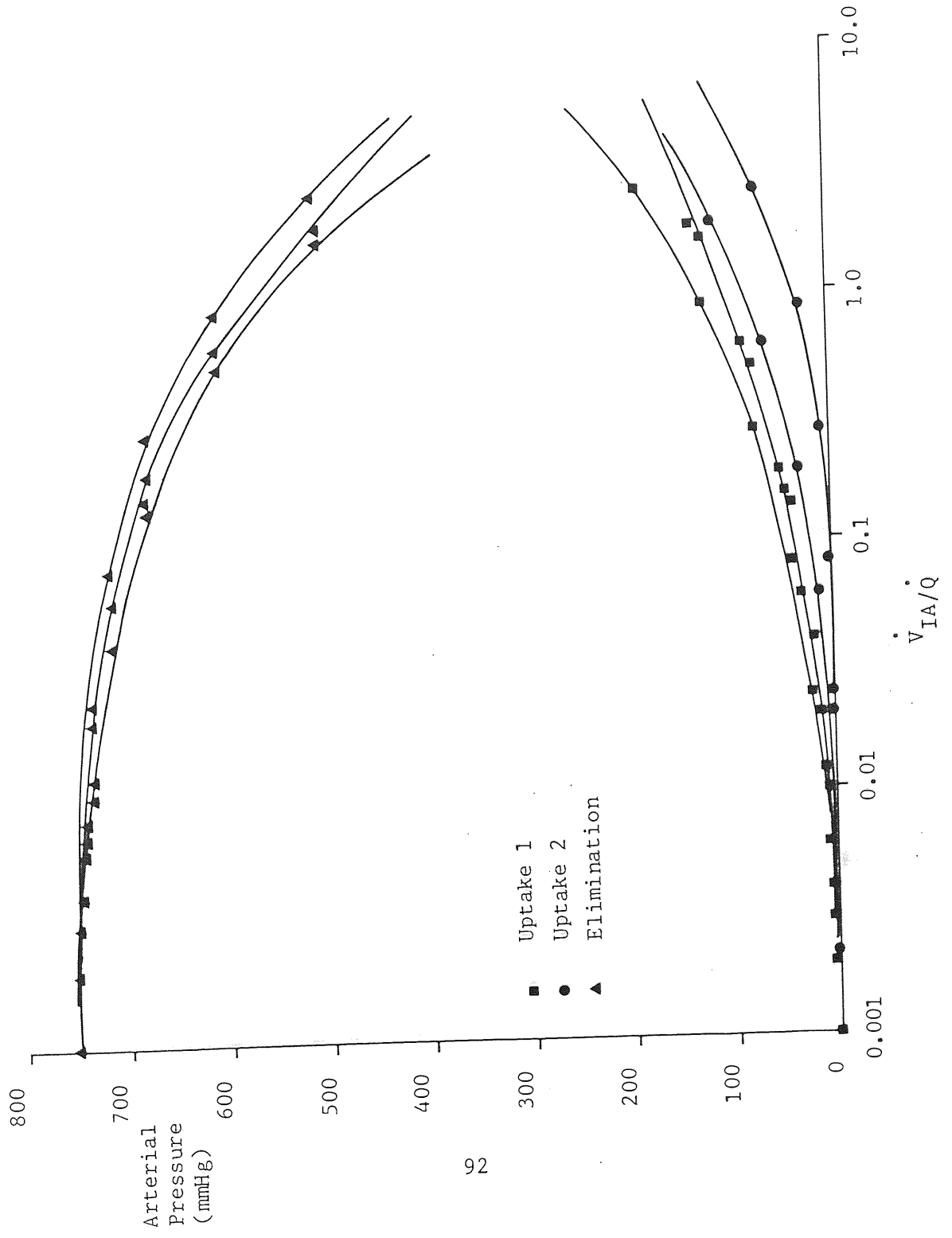

FIGURE 37

Elimination/Uptake Curves

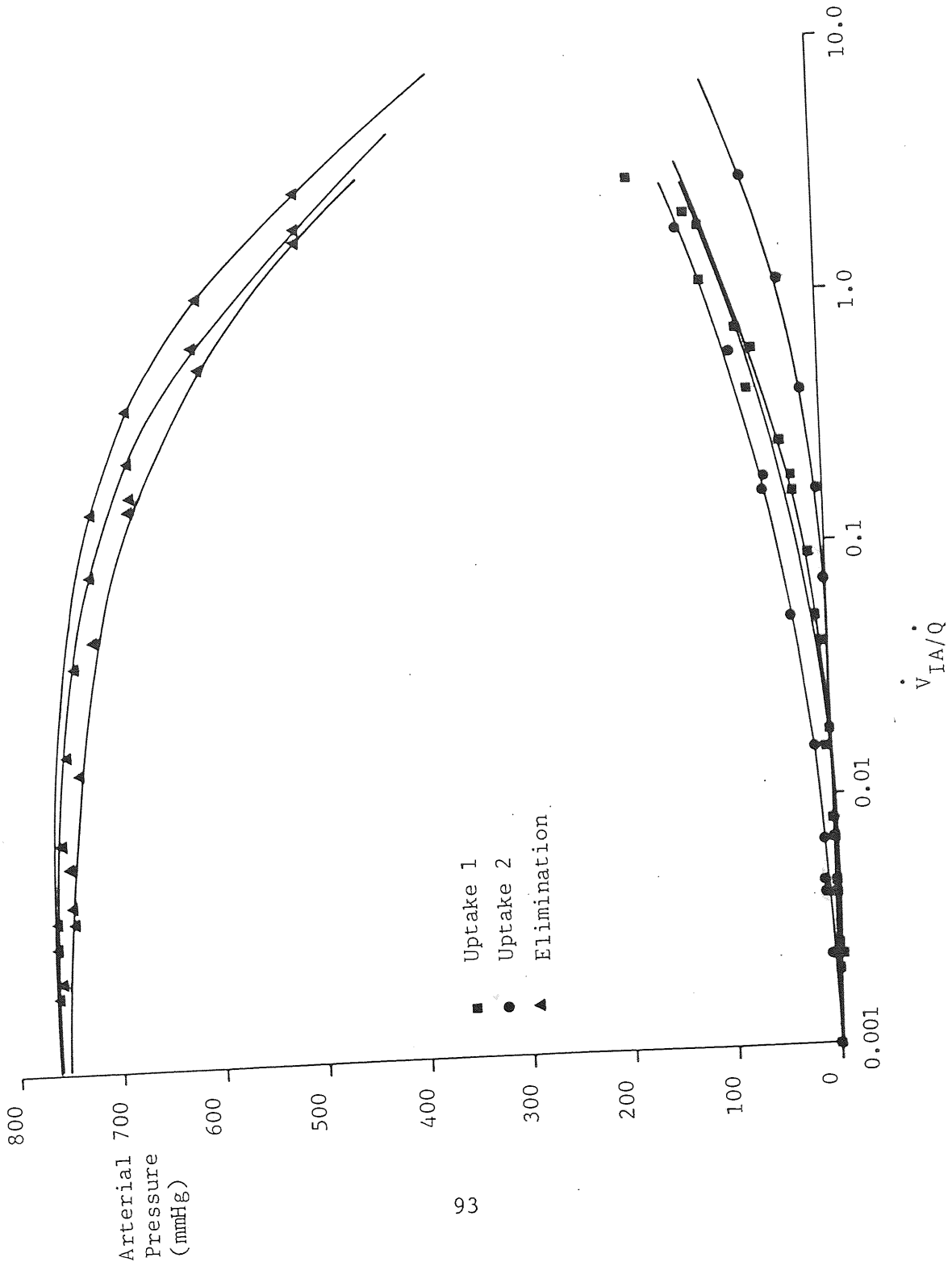

FIGURE 38

Elimination/Uptake Curves

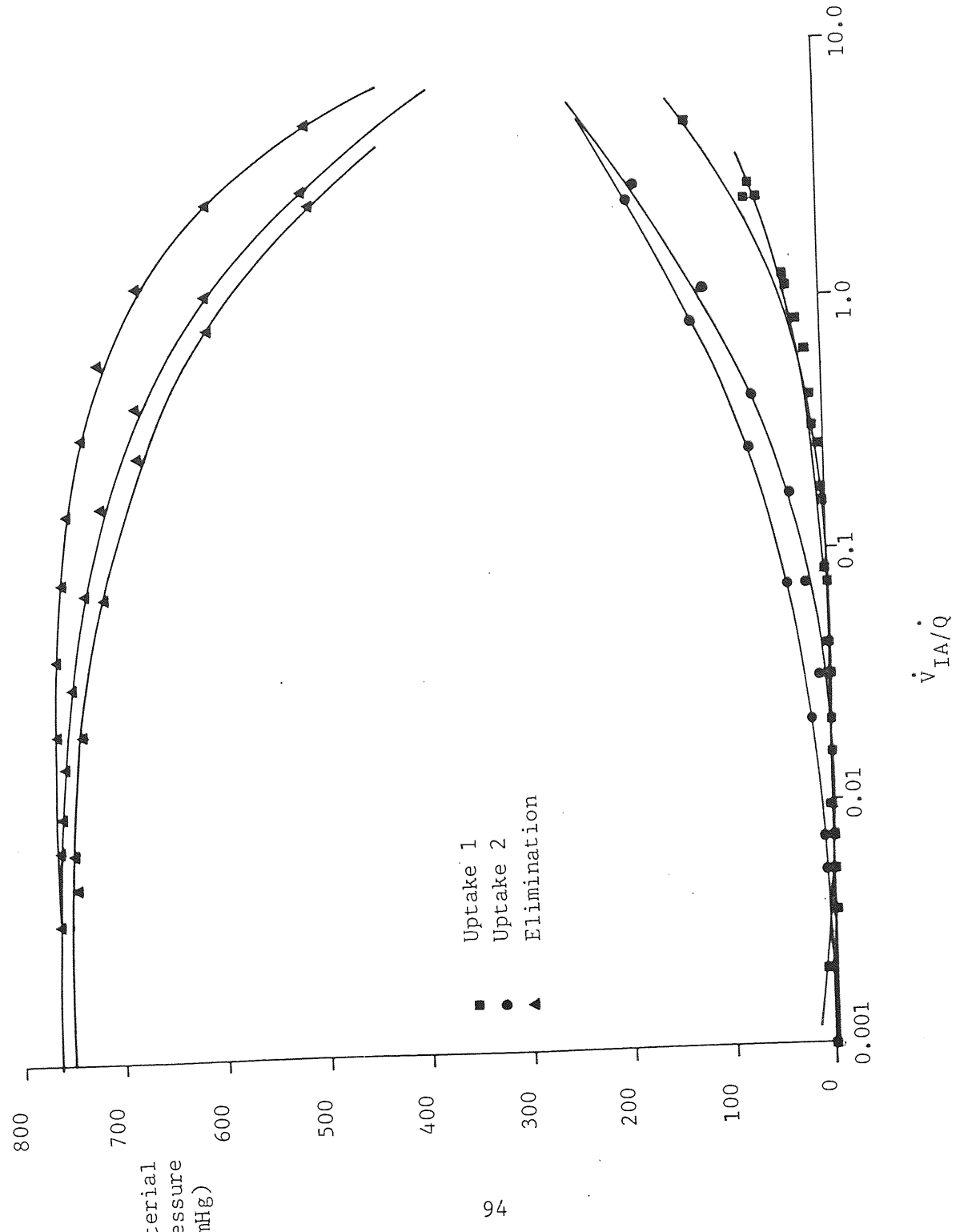

FIGURE 39

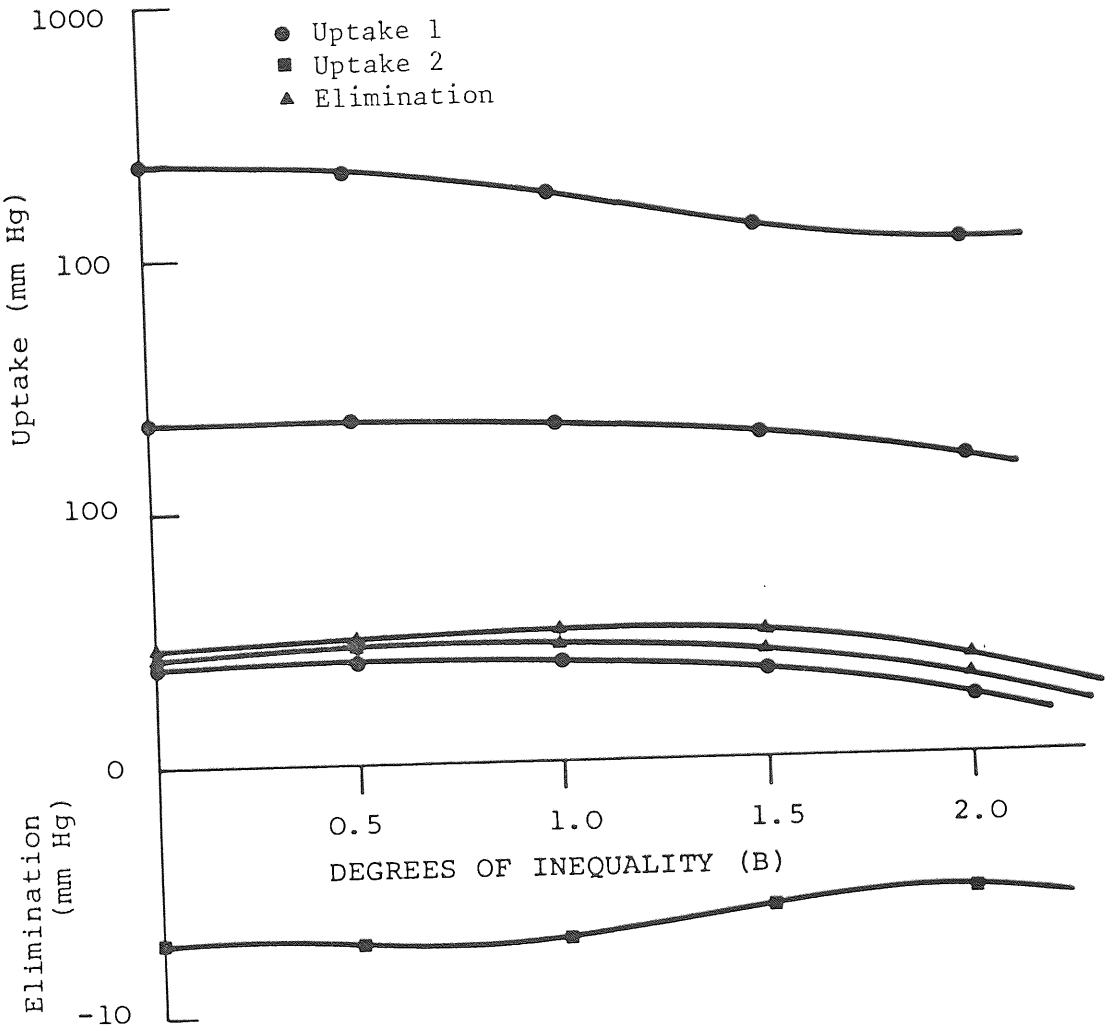

Uptake - Elimination curve for various degrees of inequality using a log linear scale

FIGURE 40.

Uptake/Elimination Curve For Various Degrees of Inequality Using A Log Linear Scale

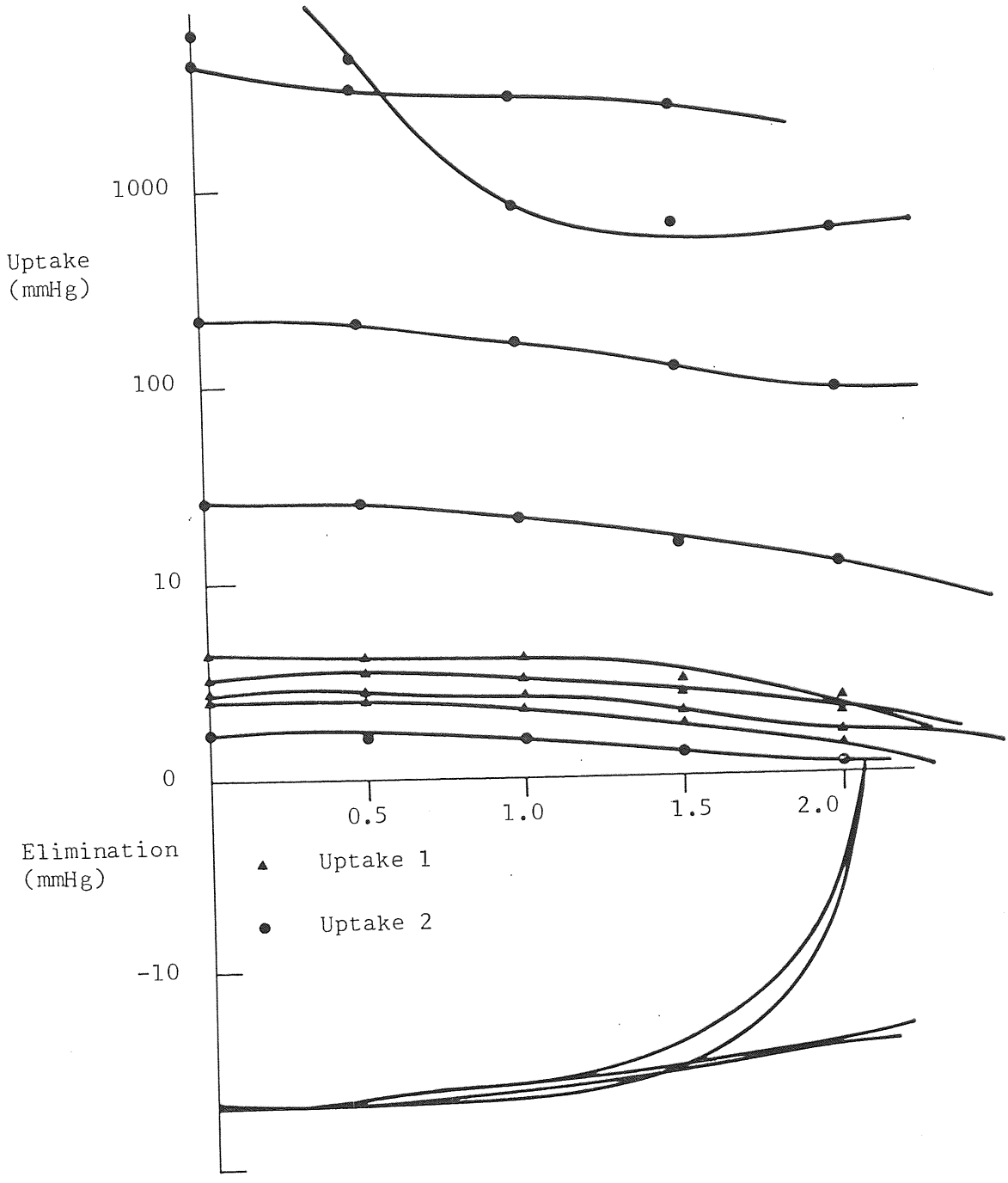

FIGURE 41

Enhancement in Uptake

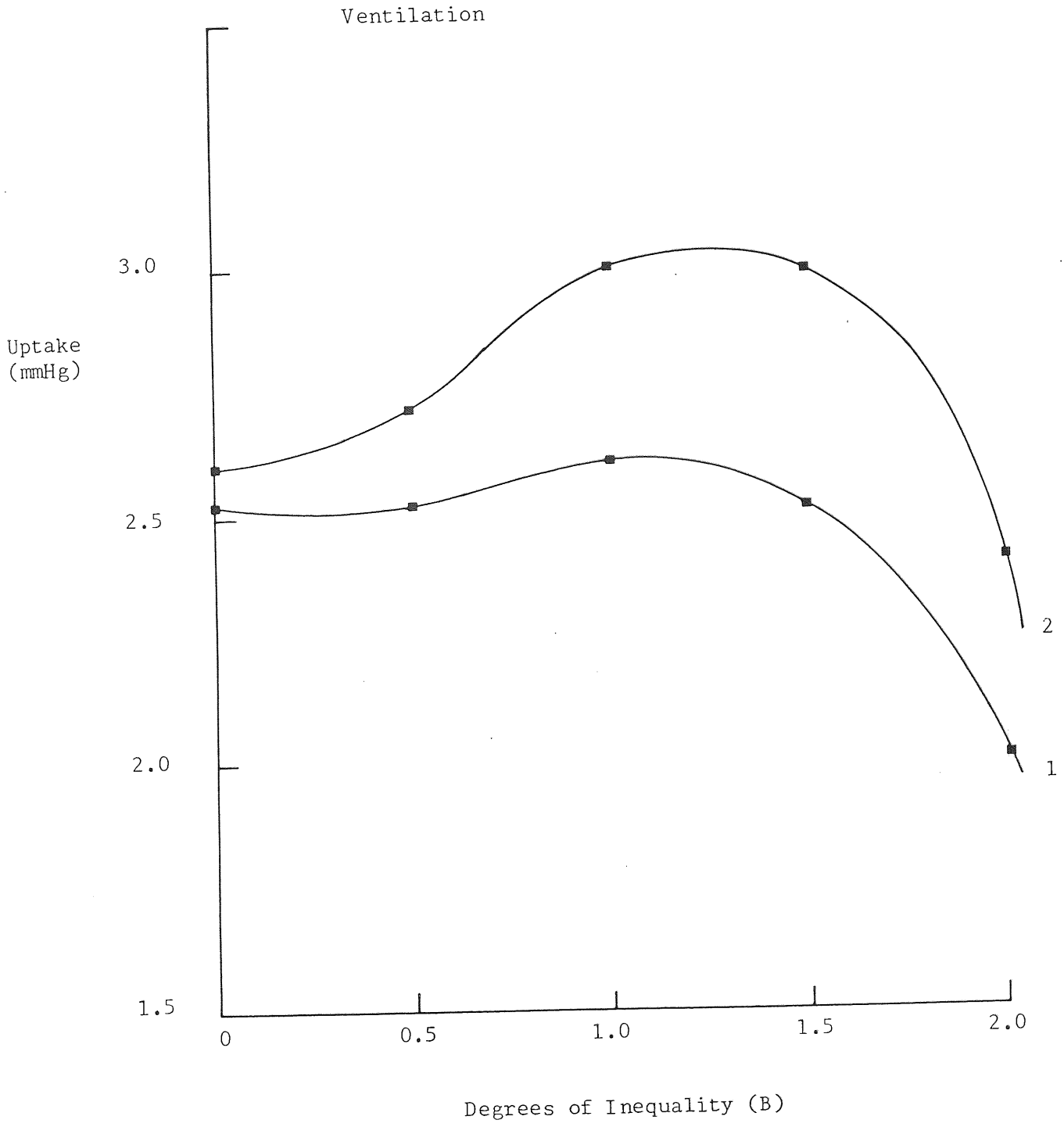

FIGURE 42

Enhancement in Uptake

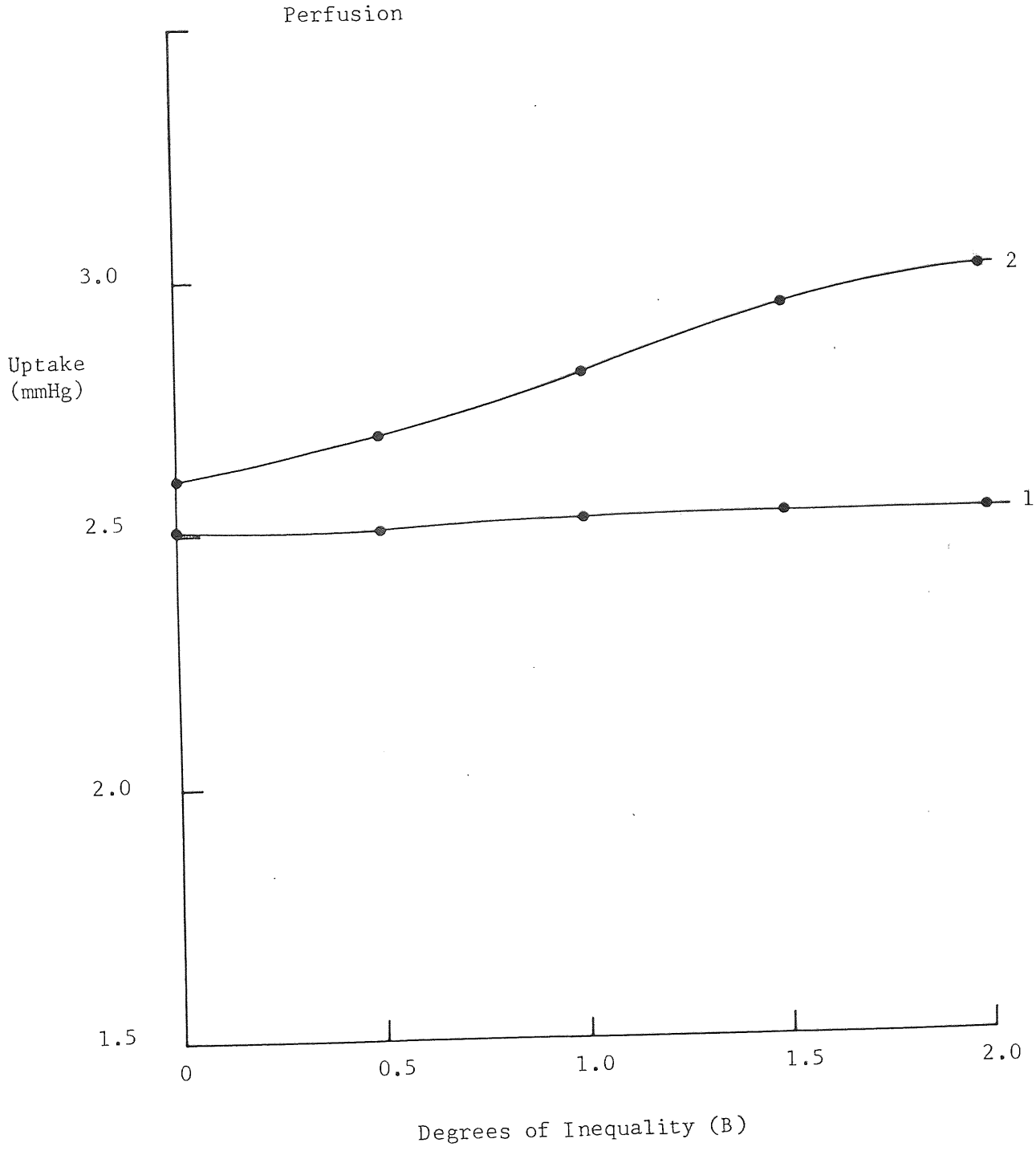

FIGURE 43

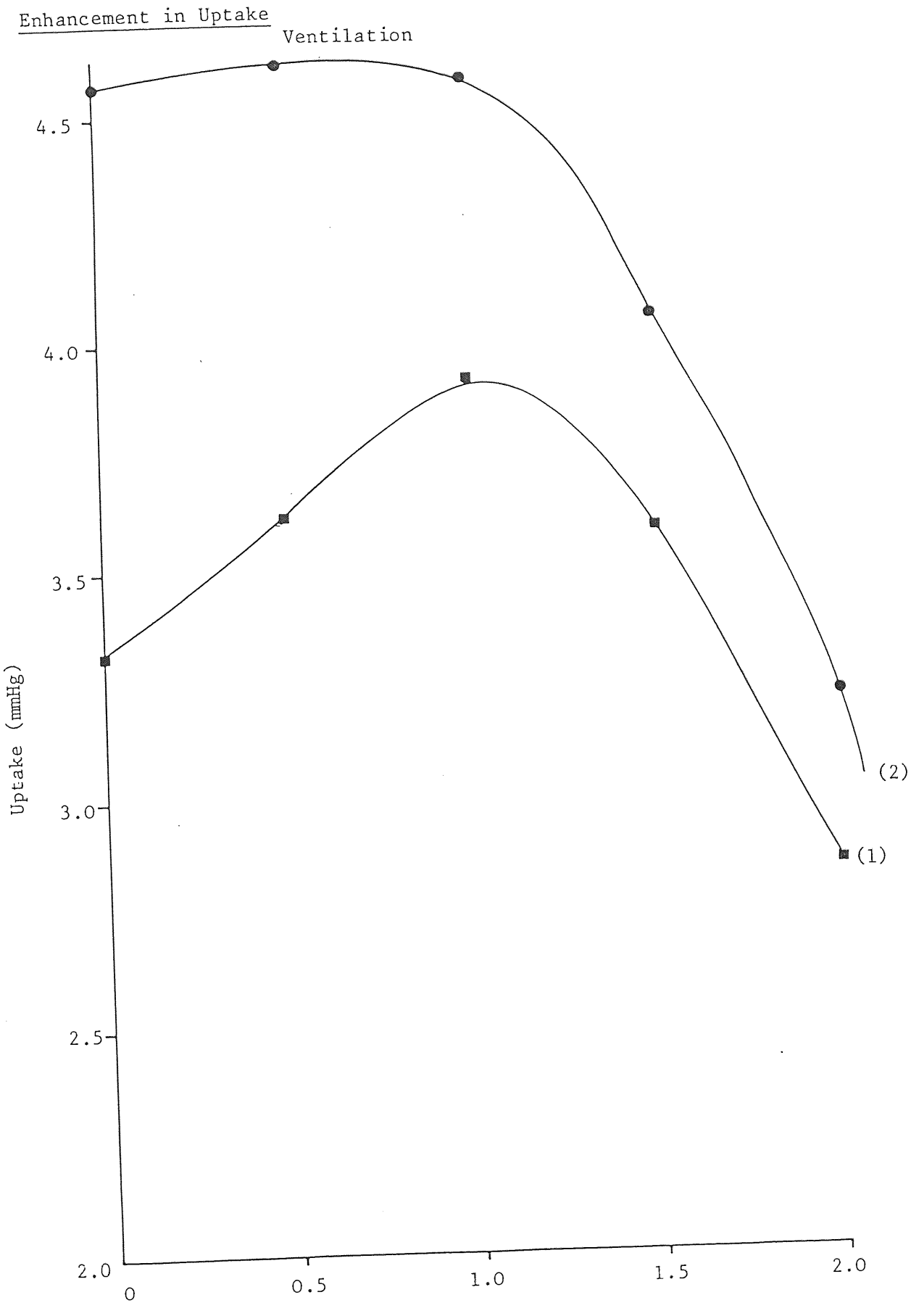
Enhancement in Uptake
Ventilation
4.5
4.0
3.5
3.0
2.5
2.0
Uptake (mmHg)
0
0.5
1.0
1.5
2.0
(2)
(1)

FIGURE 44

Enhancement in Uptake

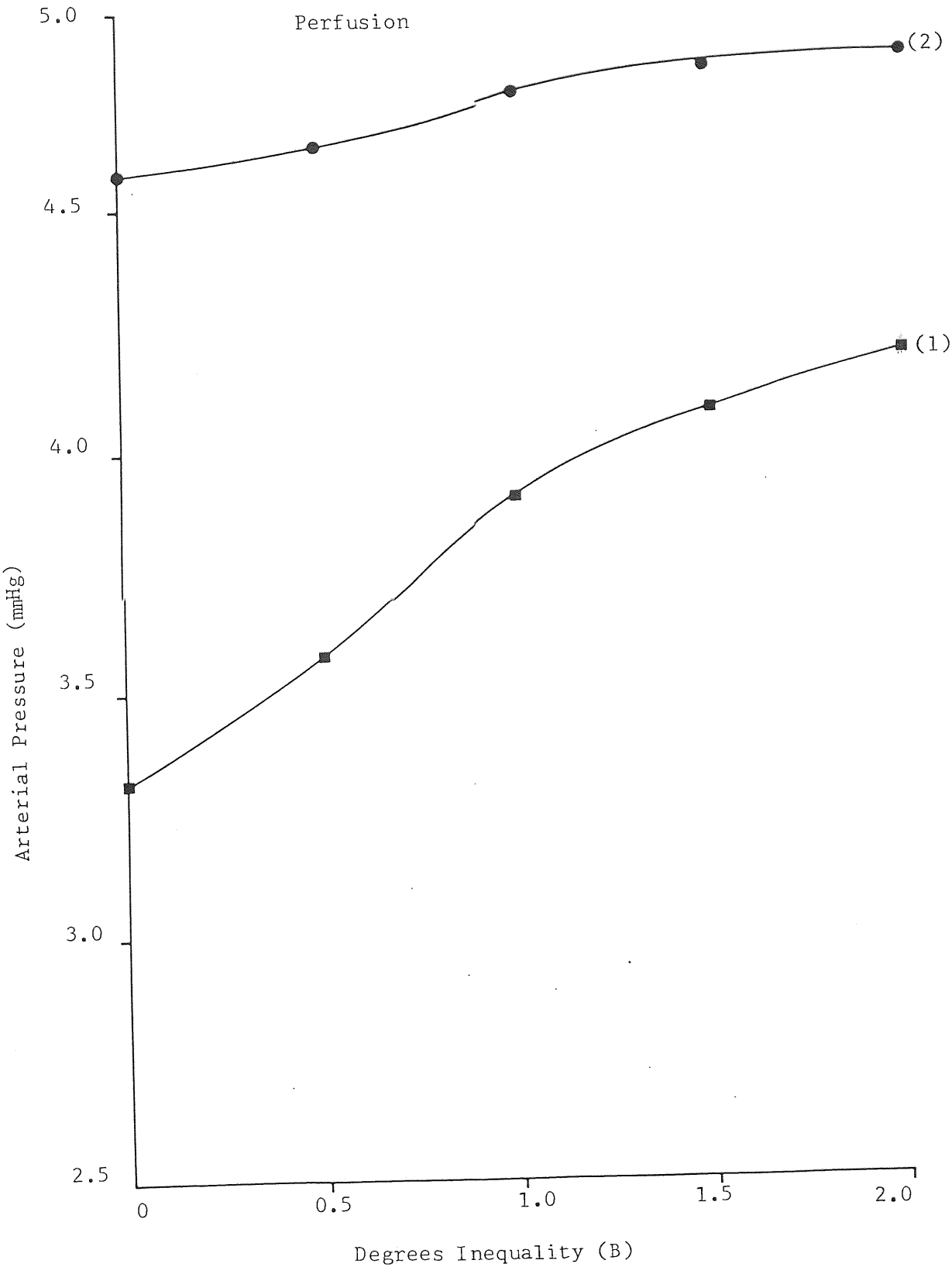

FIGURE 45

Enhancement in Uptake

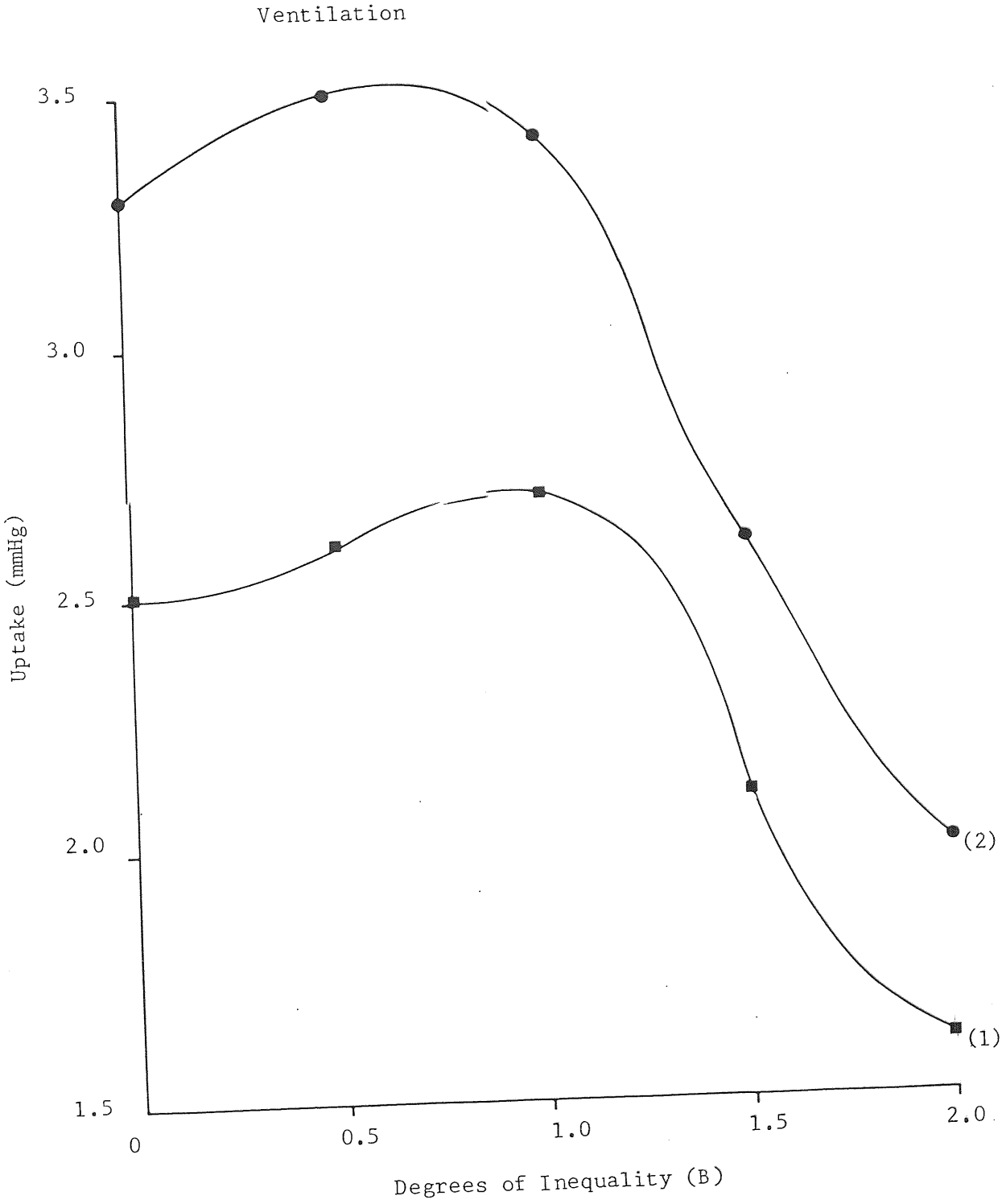

FIGURE 46

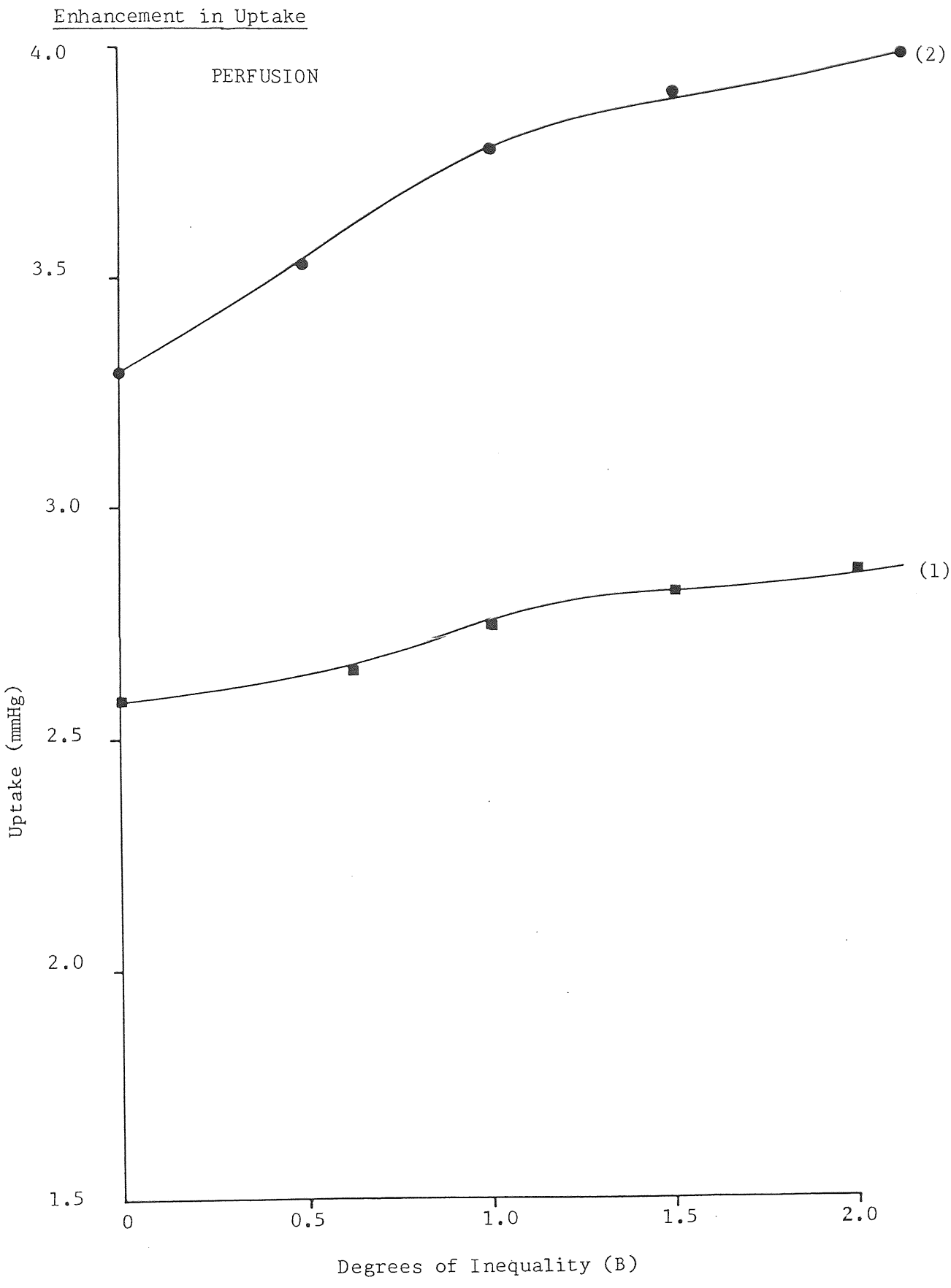
Enhancement in Uptake
PERFUSION
(2)
(1)
4.0
3.5
3.0
2.5
2.0
1.5
Uptake (mmHg)
0
0.5
1.0
1.5
2.0
Degrees of Inequality (B)

FIGURE 47

Enhancement in Uptake

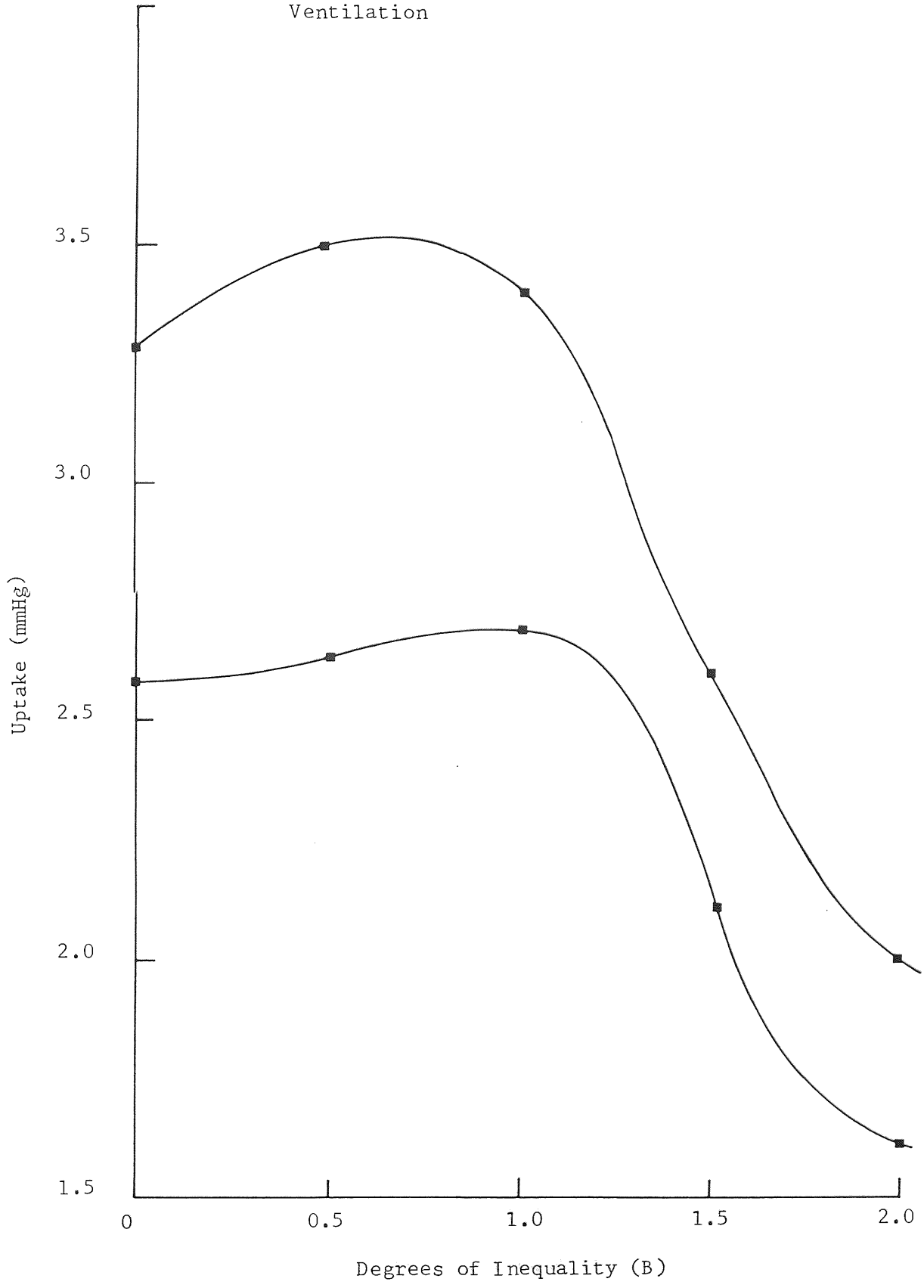

FIGURE 48

Enhancement in Uptake

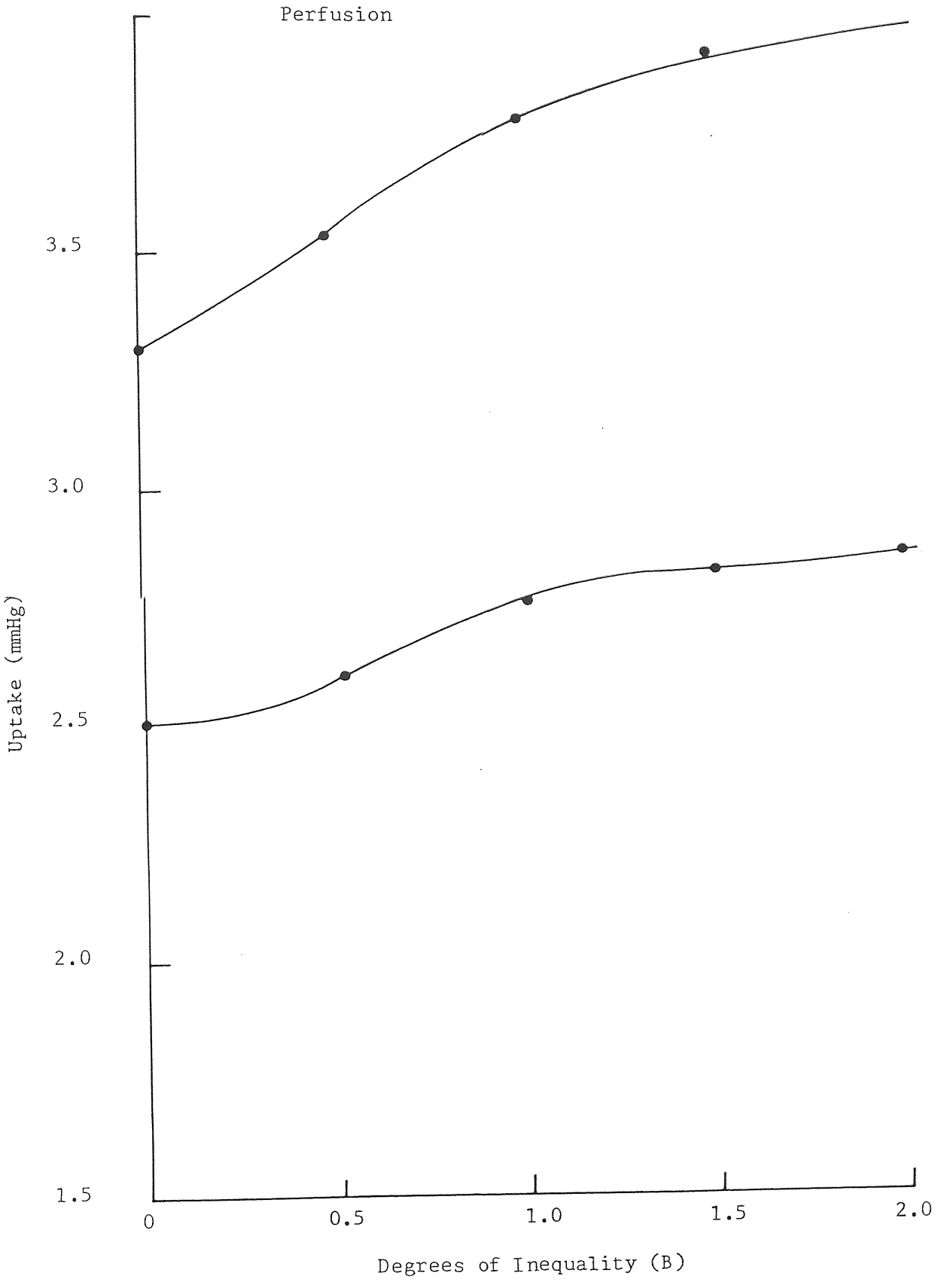

FIGURE 49

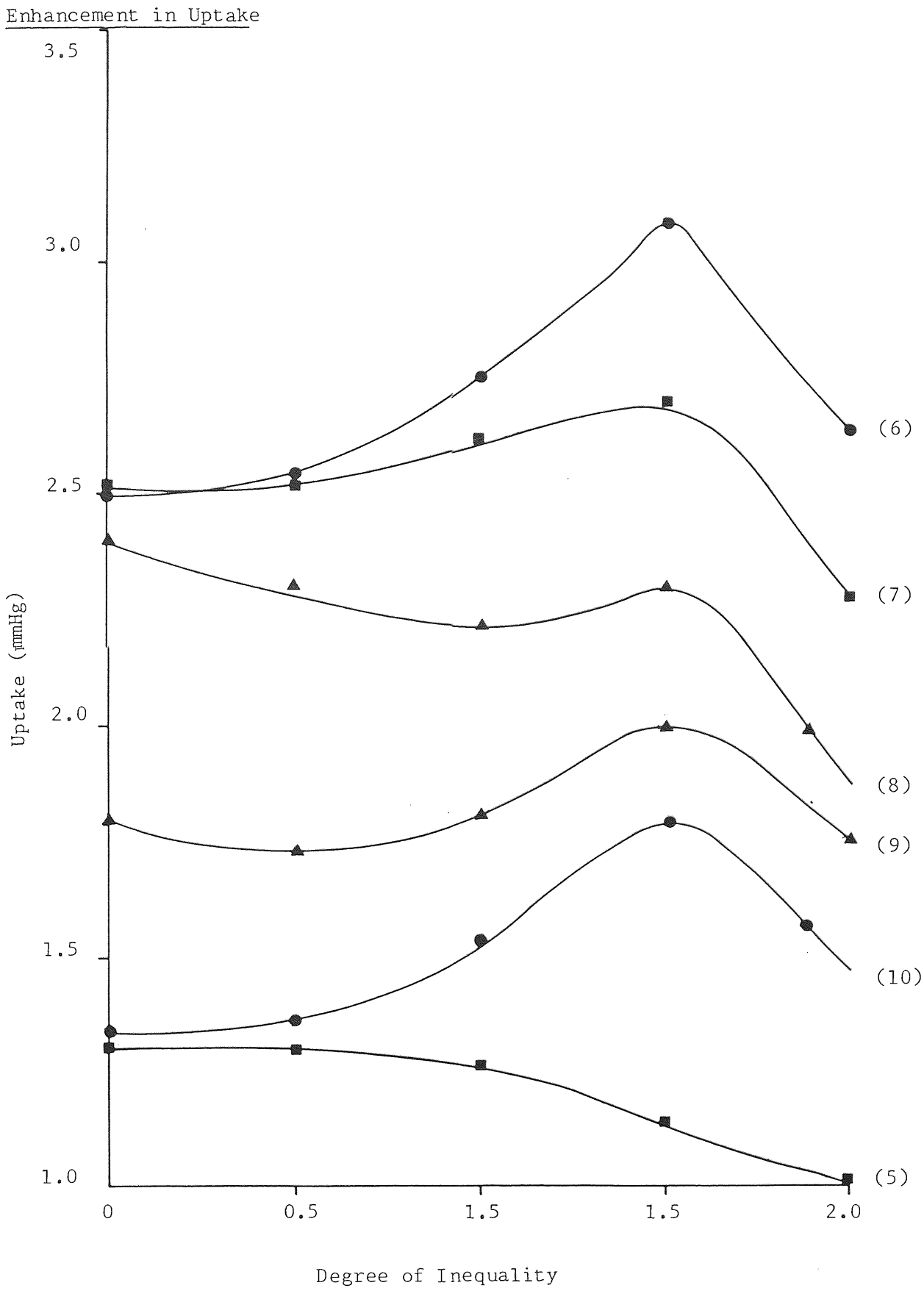
Enhancement in Uptake
3.5
3.0
2.5
2.0
1.5
1.0
Uptake (mmHg)
(6)
(7)
(8)
(9)
(10)
(5)
0
0.5
1.5
1.5
2.0
Degree of Inequality

CHAPTER 6

DISCUSSION

The statement that the presence of regional $\dot{V}_{A/\dot{Q}}$ inequalities always reduces the efficiency of pulmonary gas exchange, has perpetuated for two main reasons; first, multicompartment models based on the classical analysis of Riley and Cournand (6) and Rahn (7) invariably give rise to hypoxia and hypercarbia when subjected to unequal distribution of the respiratory parameters, irrespective of the particular form assumed, i.e. Farhi and Rahn (8), West (9), West (72), Kelman (10) and Scrimshire (11).

Secondly, by considering the exchange of a single physiologically inert gas, Farhi (12) has demonstrated that both elimination and uptake will be impaired when $\dot{V}_{A/\dot{Q}}$ ratios within the lung become unequal. Moreover, the recent work of Wagner et al (67) has substantiated this a priori observation by means of an elegant, mathematical model.

The models of Farhi (12) and Evans (49) were developed by calculating alveolar tension of one inert, tracer gas and the assumption that $\frac{\dot{V}_A}{\dot{Q}} = \frac{\dot{V}_{IA}}{\dot{Q}}$ and the model postulated and developed in Chapter 4 was based largely on this work.

In extending this work to the exchange of two inert gases and then to three inert gases, the $\dot{V}_{A/\dot{Q}}$ ratio was equated to alveolar pressure for uptake and elimination in each case.

6.1 Calculation of Alveolar Tension of One Inert Tracer Gas

6.1.1 Farhis Equations

Assuming no venous return, then the alveolar pressure is:

$$P_{AG} = \frac{\dot{V}_{IA/\dot{Q}}}{\dot{V}_{A/\dot{Q}} + \lambda_G} \cdot P_{IG}$$

i.e. $$\frac{P_{AG}}{P_{IG}} = \frac{\dot{V}_{IA/\dot{Q}}}{\dot{V}_{A/\dot{Q}} + \lambda_G} \qquad (83)$$

further, assuming that $\dot{V}_{IA/\dot{Q}}$ is supplied as data, we must either calculate or assume a value for $\dot{V}_{A/\dot{Q}}$

Using Farhi's equations and assuming

$$\dot{V}_{A/\dot{Q}} = \dot{V}_{IA/\dot{Q}}$$

we have, by substituting into (83):

$$\frac{P_{AG}}{P_{IG}} = \frac{\lambda_1}{1 + \frac{\lambda_G}{\dot{V}_{IA/\dot{Q}}}} \qquad (84)$$

6.1.2 Evans' Equations

Using the approach of Evans et al, with $\dot{V}_{IA/\dot{Q}}$ as the independant variable and by further assuming that no other gas is being exchanged, then

$$\dot{V}_A (P_{BAR} - P_{AG}) = \dot{V}_{IA} (P_{BAR} - P_{IG}) \qquad (85)$$

thus $$\frac{\dot{V}_A}{\dot{Q}} = \frac{\dot{V}_{IA}}{\dot{Q}} \frac{P_{BAR} - P_{IG}}{P_{BAR} - P_{AG}} \qquad (86)$$

now $$P_{AG} = P_{IG} \frac{\dot{V}_{IA/\dot{Q}}}{\dot{V}_{A/Q} + \lambda_G} \qquad (87)$$

Substituting for $\dot{V}_{A/\dot{Q}}$ in (87) from (86) yields the quadratic equation as follows:-

$$- \lambda P_{AG}^2 + \left[\frac{\dot{V}_{IA}}{\dot{Q}} \cdot P_{BAR} + \lambda_G \cdot P_{BAR} \right] P_{AG} - P_{BAR} P_{IG} \frac{\dot{V}_{IA}}{\dot{Q}} = 0 \qquad (88)$$

or on rearrangement,

$$P_{AG} = - P_{BAR} \left[\frac{\dot{V}_{IA}}{\dot{Q}} + \lambda_G \right] + \sqrt{P_{BAR}^2 \left[\frac{\dot{V}_{IA}}{\dot{Q}} + \lambda_G \right]^2 - \frac{4 \lambda_G P_{BAR} P_{IG} \frac{\dot{V}_{IA}}{\dot{Q}}}{-2 \lambda_G}} \qquad (89)$$

6.2 Gas Exchange of Two Inert Gases, Expressed in Term of $\dot{V}_{A/\dot{Q}}$ Ratio

Consider an alveolous or homogenous lung region containing two gases, each having a finite solubility and assume that one gas has a high solubility (suffix H) while the other has a low solubility (suffix L).

The total pressure of the two gases must always be atmospheric, hence it follows that

$$P_T = P_{AL} + P_{AH} = P_{BAR} \qquad (90)$$

from 'classical' gas exchange analysis (Farhi and others) then:

$$P_{AH} = \frac{\dot{V}_{IA/\dot{Q}} \cdot P_{IH} + \lambda_H \cdot P_{\bar{V}H}}{\dot{V}_{A/\dot{Q}} + \lambda_H} \qquad (91)$$

and

$$P_{AL} = \frac{\dot{V}_{IA/Q} \cdot P_{IL} + \lambda_L \cdot P_{\bar{V}L}}{\dot{V}_{A/\dot{Q}} + \lambda_L} \qquad (92)$$

In order to express the alveolar tension of the gases as a function of the variable $\dot{V}_{A/\dot{Q}}$ only, it is first necessary to derive an expression for the related variable $\dot{V}_{IA/\dot{Q}}$

Substituting equation (91) and (92) for P_{AL} and P_{AH} into equation (90) then:

$$P_T = \frac{\dot{V}_{IA/Q} \cdot P_{IH} + \lambda_H \cdot P_{\bar{V}H}}{\dot{V}_{A/\dot{Q}} + \lambda_H} + \frac{\dot{V}_{IA/Q} \cdot P_{IL} + \lambda_L \cdot P_{\bar{V}L}}{\dot{V}_{A/\dot{Q}} + \lambda_L} \qquad (93)$$

by solving for $\dot{V}_{IA/\dot{Q}}$ and simplifying, we obtain:

$$\frac{\dot{V}_{IA}}{\dot{Q}} = \frac{P_T - \frac{\lambda_H P_{\bar{V}H}}{\frac{\dot{V}_A}{\dot{Q}} + H} + \frac{\lambda_L P_{\bar{V}L}}{\frac{\dot{V}_A}{\dot{Q}} + \lambda_L}}{\frac{P_{\bar{V}L}}{\dot{V}_{A/Q} + \lambda_L} + \frac{P_{IH}}{\frac{\dot{V}_A}{\dot{Q}} + \lambda_H}} \qquad (94)$$

Assuming $P_{\bar{V}L} = P_{\bar{V}H} = 0$ in equation (94) then

$$\dot{V}_{IA/\dot{Q}} = \frac{P_T}{\frac{P_{IL}}{\dot{V}_{A/\dot{Q}} + \lambda_L} + \frac{P_{IH}}{\dot{V}_{A/\dot{Q}} + \lambda_H}} \qquad (95)$$

Looking at the literature, it is apparent that the previous researchers considered only one gas at a time during uptake or elimination. Evans et al (36) showed that mismatching of ventilation must reduce the pulmonary elimination or uptake of any gas which had a linear dissociation curve, irrespective of the pattern of ventilation perfusion ratios, and that uptake by a homogenous lung exceeds that of a non-homogenous lung.

This was demonstrated using the convexity and concavity properties of a mathematical function. It might have been simpler to provide an experimental proof. Colburn et al (35) used an (n) compartment lung model very similar to the ten compartment model used in this thesis and would have found it equally efficient to use such a ten compartment model for the reasons already explained. He used two gases; one was classified as the vehicle gas, the other as the main gas, but his mathematical analysis was tedious and unnecessary.

West (16) showed progressive falls in Oxygen uptake and Carbon Dioxide output which occurred with increasing ventilation perfusion ratio inequality. The inequality was either produced by unevenly distributing ventilation per unit volume and keeping blood flow constant, or the reverse. It was shown,that while Oxygen uptake was not severely affected, Carbon Dioxide (CO_2) output was impaired nearly as much. He concluded that Oxygen (O_2) uptake was reduced by 45% of its original value, while the corresponding figure for Carbon Dioxide output was about 55%. He obtained similar results with a mixed inequality of ventilation and blood flow.

Another approach used by West et al (73) was partial pressure solubility diagrams. Using such a technique, he assumed that gas is supplied in a diluent state which in itself undergoes no net,gas exchange in any lung unit. It is difficult to agree with this statement because blood always contains some tracers. Dantzker et al (15) used a third gas as a tracer with solubility ($\lambda_3 \cong 0$) and thus obtained a cubic equation for the uptake, which in turn provides at least one positive solution, although the other two could be negative thus giving a positive value of $\dot{V}_A$ (i.e.

no collapse of the alveoli). However, all three solutions could be positive giving three valid answers.

In the model proposed here where the critical $\dot{V}_{A/\dot{Q}}$ ratio is high, then an increasing number of lung units will become vulnerable to collapse, due to Oxygen (O_2) enrichment. If Nitrogen (N_2) is replaced by other gases (relatively insoluble $\lambda_3 = 0$) it will help to retard the collapse of the alveoli. The gases used in the model were SF_6 and N_2O Table (I). The conclusion drawn, was that if the third gas is entirely insoluble ($\lambda_3 = 0$) then there is no flow of this gas from the alveolous into the blood. Therefore, no matter how low $\dot{V}_{A/\dot{Q}}$ is, or how high the Oxygen (O_2) concentration is, there will not be a collapse of the unit. Thus, there is no critical value of $\dot{V}_{A/\dot{Q}}$. The results in this thesis are in agreement with this statement. It is also shown that there is a definite reduction in uptake of gas.

Farhi and Yokoyama (37) considered the simultaneous elimination of two inert gases in isolation and produced $\dot{V}_{A/\dot{Q}}$ curves similar to the ones in this work. They proved that as the $\dot{V}_{A/\dot{Q}}$ ratio increases, the partial pressure of gas being eliminated is reduced, thus ventilatory efficiency of the alveolous is reduced. Similarly, during gas uptake, alveoli with a high ventilation, perfusion ratio are very effective in transferring gases of high solubility. Farhi and Olszowka (14) also showed that as $\dot{V}_{A/\dot{Q}}$ increases from zero to infinity, the concentrating effect passes through a definite maximum, thus as $\dot{V}_{A/\dot{Q}}$ rises, the Nitrous Oxide (N_2O) uptake (which is closely related to perfusion), begins to drop while the Carbon Dioxide (CO_2) elimination, which is mainly ventilation dependant, is enhanced. (Suskind and Rahn (74), Farhi (12)). At a later stage, four

gases are used, Nitrogen (N_2), Oxygen (O_2), Carbon Dioxide (CO_2) and Nitrous Oxide (N_2O), as a filler gas due to its low solubility (Table II). Rahn (75), Farhi (76), and Wagner (18) confirm the work of Scrimshire (11), that a maldistribution of ventilation has a more pronounced effect on Oxygen (O_2), who also concluded that there is very little difference between the reduction in Oxygen (O_2) as opposed to Carbon Dioxide (CO_2) transfer, as noted by West (16).

Scrimshire (11) showed that an impairment in breathing efficiency is substantially influenced by the manner in which ventilation or blood flow is altered in disease. He demonstrated, that disruptions in ventilations always give rise to a greater degree of hypoxema than cases in which blood flow is affected, and that these differences became more marked when breathing is increased. He also showed that any imbalance in the normal relationship between blood flow and ventilation must impair overall gas exchange.

6.3 Acute Effects of Ventilation - Perfusion Inequality on Gas Exchange

If a derangement of the ventilation perfusion ratio ($\dot{V}_{A/Q}$) occurs due to the exposure of some physiological insult to the lung having uniform ventilation and bloow flow, such as a sudden acceleration; then assuming that the composition of mixed venous blood is to remain constant, one must look at the effects of ventilation - perfusion ratio inequality.

Figure (14) shows the graphs of Arterial Pressure (P_{aG}) against inspired ventilation to perfusion ratio inequality for the gases with solubilities of $\lambda_1 = 0.001$ (uptake 1), $\lambda_3 = 0.001$ (elimination) and $\lambda_1 = 0.001$ to 10.0 (uptake 1). The inequality was produced, either by an unevenly distributed ventilation per unit volume (perfusion limited), or an unevenly distributed perfusion per unit volume (ventilation limited).

It was seen that for the degree of inequality B = 1.0 the (P_{aG}) of the first gas with a low solubility was affected quite severely compared with the second gas. The arterial pressure of (P_{aG}) of the first gas was reduced from 625 mmHg to 400 mmHg thus showing a drop in (P_{aG}) of 225 mmHg, i.e. almost 35% of its original value. This explains the findings of West (16) who showed that the fall in arterial pressure of Oxygen (O_2) by a factor of 50% of its original value, was due to the difference in solubility of Oxygen (O_2). This is comparable with the gases used in this research.

Looking at the uptake curves Figure (41),it was found that for the values of λ_2 = 0.01 there was an increase in uptake by o.1 mmHg, i.e. from 2.5 to 2.61 mmHg which is only a small rise in uptake, namely a factor of 5%,thus contradicting West (16), while enhancement in uptake of the gas with λ_2 = 0.1 was by a 0.45 mmHg, i.e. by 20% which is a relatively large enhancement in uptake. The solubilities used in the model could be compared with real gases such as Argon (λ = 0.92) and Nitrous Oxide (N_2O) with a solubility (λ = .013). According to West (16) the impairment of Oxygen (O_2) was as much as 45% of its original value. Looking at Figure (42) with constant perfusions, the enhancement in uptake was found to be very similar to the graph with constant ventilation, i.e. by 0.04 mmHg for λ_2 = 0.01 and 0.43 mmHg for λ_2 = 0.1. The enhancement in uptake was from 2% to 20%. If the value of solubility is increased by a factor of 10 (from 0.01 to 0.1) in agreement with West's (16) findings, the impairment is the same whether the distribution is ventilation limited or perfusion limited. It was found that enhancement in uptake was by an identical factor, irrespective of distribution being ventilation limited or perfusion limited.

6.4 Effect of Increasing Ventilation

If the ventilation is increased, then it is apparent that the $\dot{V}_{IA/\dot{Q}}$ ratio is progressively increased in a similar manner. According to West (16), the rise in arterial pressure of Carbon Dioxide (CO_2) which always accompanies ventilation perfusion inequality can be reduced rapidly by an increase in ventilation. Looking at Figure (47) it is apparent that, as the ventilation is increased, the ventilation perfusion inequality is increased and the P_{aG} of the second gas is increased to a value of P_{aG} = 700 mmHg. If the ventilation of 5.21 used by West (16) is assumed here, then the $\dot{V}_{IA/\dot{Q}}$ inequality is $\frac{5.2}{0.05}$ = 1.04 and the value of P_{aG} is approximately 25 mmHg, Figure (43) with a value of λ = 10.0 (highly soluble), then the value of $\dot{V}_{IA/\dot{Q}}$ inequality is doubled to 2.08 and the value of P_{aG} rises to 500 mmHg which is in agreement with West (16).

6.5 Effect of Increasing Blood Flow

If the blood flow is increased then the ratio $\dot{V}_{IA/\dot{Q}}$ is reduced. If the blood flow is doubled whilst keeping the ventilation constant, then the value of P_{aG} either increases or decreases according to the solubility of uptake, Figure (47). If the $\dot{V}_{IA/\dot{Q}}$ ratio is reduced from 1.0 to 0.5, then the value of P_{aG} drops from 700 mmHg to 680 mmHg for λ uptake = 0.10. For λ uptake = 10.0 the value of P_{aG} rises from 25 mmHg to 50 mmHg and is observed to be in agreement with West (16). This reaffirms the findings of West-that increases in total blood flow cause relatively small changes in blood gas tensions compared with increases in ventilation.

Farhi and Yokoyama (37) showed that alveoli with a high ventilation perfusion ratio are very effective in eliminating gases of high solubility,

while alveoli with a low ventilation perfusion ratio are particularly efficient at clearing the blood of gases. This is because, in lungs with a normal ventilation - perfusion ratio, alveoli eliminating gases of high solubility waste much of their blood flow, while for gases of low solubility ($\lambda \cong 0.001$), much of their ventilation is useless. In the same way, during gas uptake, alveoli with a high ventilation - perfusion ratio are very effective in transferring gases of high solubility, and vice versa. According to Farhi and Yokoyama (37) in a lung with a wide spectrum of ventilation - perfusion ratioes, e.g. 0.001 to 10, as is the case for this study, the gases with very high and very low solubilities are still effectively catered for, but the gases of medium solubility are transferred inefficiently. West (77) used a similar argument. A parallel with West's argument can be drawn referring to the curves in Figure (16). For the value of $\lambda_1 = 1.0$, alveoli with low ventilation - perfusion inequality in the order of 0.01 to 0.1 are efficient in clearing the gas with low solubility from the blood. The gas which is eliminated and having a value of $\lambda_3 = 0.001$, shows that the drop in pressure is from 100 mmHg to 5 mmHg. Similarly, looking at Figure (22) the gas of elimination has a solubility of 0.01 while the eliminating pressure drops from 375 mmHg to 100 mmHg. Using Figure (37), for the gas with value of solubility $\lambda_3 = 10.0$, it is seen that the elimination is more efficient at a higher $\dot{V}_{IA/Q}$ ratio, i.e. for a $\dot{V}_{IA/Q}$ ratio greater than 1.0 but less efficient at a $\dot{V}_{IA/Q}$ value of 0.01. The fall in pressure at a low $\dot{V}_{IA/Q}$ ratio is only 5 mmHg, while at higher values of the $\dot{V}_{IA/Q}$ ratio it is almost 250 mmHg which is in agreement with Farhi and Yokoyama (37) and West (77). Looking at the uptake curves, alveoli with a high ventilation - perfusion ratio are very effective at transferring gases of high solubility, e.g. $\lambda_1 = 10.0$.

Figure (38), and conversely, gases with a low ventilation-perfusion ratio are very effective at transferring gases of low solubility in the order of $\lambda_1 = 0.001$, Figure (14). Surprisingly, it was found that the gas uptake in the blood is enhanced by up to 20% of its value for this latter condition.

Looking at moderately soluble gas ($\lambda = 1.0$), it is apparent that the fractional elimination is very sensitive to a change in the ventilation-perfusion ratio Figure (17) when this is near 1.0 (normal value), which is again in agreement with West (77).

West et al (73) confirm the earlier findings of Colburn et al (35) and West (77), namely that there is one solubility for which the fractional fall is maximum and that all gases which have a fractional fall higher or lower than this, have smaller fractional falls. There is only one minimum when the partition coefficient of the gas is equal to the overall ventilation - perfusion ratio. Looking at the gas of elimination Figures (24) to (28) and $\lambda_3 = 0.1$, it is seen that for the $\dot{V}_{IA/Q}$ ratio of 0.1, maximum proportional fall is observed. The P_{aG} fell from 760 mmHg to 350 mmHg, almost 50% of its value, for the range of $\dot{V}_{IA/Q}$ values of 0.1 and 10.0 it only fell by 200 mmHg, which is only 30% of the total value, and this is in agreement with the above findings.

6.6 Critical Inspired Ventilation-Perfusion Ratio

Looking at Figure (14) it is found that as the $\dot{V}_{IA/Q}$ was increased, the value of elimination reached a figure approaching zero. This occurred, when the rate of delivery of gas into the unit by inspired ventilation equalled the net rate of transfer of gas from the unit into the blood. This particular value of the $\dot{V}_{IA/Q}$ ratio was termed the critical value by Dantzker et al (15). He found that at the critical value the magnitude

of the $\dot{V}_{IA/\dot{Q}}$ ratio was 0.044. In this curve, the value of elimination pressure started from 75 mmHg for the $\dot{V}_{IA/\dot{Q}}$ ratio of 0.01, and gradually reduced to zero at the $\dot{V}_{IA/\dot{Q}}$ ratio of 0.048, which was in agreement with Dantzker et al (15). Figure (15) shows a critical value at 0.05 for these particular conditions. As the value of the second gas of uptake was increased, the critical value was also seen to increase, reaching the $\dot{V}_{IA/\dot{Q}}$ ratio of 0.13. These results confirmed the findings of Dantzker et al (15).

6.7 Enhancement In Uptake

The special findings of this research were that the uptake was enhanced and this contradicts the previous research which suggested that the gas exchange is impaired.

The enhancement of uptake was observed for the values of solubility of uptake (λ_2) = 0.01, 0.1, 1.0 and 10.0 Figure (39). It was found that there was no enhancement in uptake for the value of λ_2 = 0.001 which was in agreement with West (16), West (77). Enhancement in uptake was also observed, Figure (40) for the values of λ_2 = 0.1 and 1.0; there was no enhancement in uptake for λ_2 = 0.001, 0.01 and 10.0. In total, the enhancement was only observed for six particular values of solubilities compared with the total number of possibilities of 25. The rest of the curves followed the pattern found by previous researchers.

6.7.1 Constant Ventilation λ_2 = 0.01, 0.1 Figure (41)

For this condition, it was found that the maximum value of P_{aG} was 2.67 mmHg, i.e. a total enhancement in uptake of 0.17 mmHg while in curve 1, the enhancement was by a maximum value of pressure of 0.45 mmHg, i.e. by a factor almost 20% of its original value.

6.7.2 Constant Perfusion λ_2 = 0.01, 0.1 Figure (42)

The enhancement in this case was by 0.43 mmHg at the most, which was again almost 19% of its original value. The value of enhancement was somewhat reduced for the uptake of $\lambda_2 = 0.01$, it was found to be 2%.

In general, the maximum enhancement in uptake was by 20% which is quite large considering that previously, only impairment of gas exchange was observed.

6.8 Enhancement In Uptake for $\dot{V}_{A/Q}$ Model

The maximum rise in uptake was found to be 0.6 mmHg surprisingly enough, the total enhancement was by almost 45% of the original value of uptake. It was considered to be a large enough enhancement to warrant further investigation using experimental techniques.

6.9 General Conditions for Enhancement In Uptake

Looking at the curves, a set of inequalities was derived similar to Farhi and Yokoyama (37). It was found that the uptake was enhanced if only the following inequality was satisfied (derived in 4.7):

$$\frac{\lambda_3}{\lambda_2} < 1 \qquad (96)$$

The uptake for the gas with solubility λ_2 is enhanced if the above inequality is satisfied.

Example: $\lambda_1 = 0.001$ filler gas Stoetling (24)

$\lambda_2 = 0.01$ gases being taken up

$\lambda_3 = 0.001$ gas being eliminated

then $\frac{\lambda_3}{\lambda_2} = 0.01$

which satisfies the above inequality.

Therefore the above is satisfied offering conclusive proof of enhancement in uptake. The analysis is similar to the one shown by Farhi and Yokoyama (37) - that the shape of their $\dot{V}_{A/\dot{Q}}$ line for various pairs of gases was dictated only by the ratio λ_3/λ_2 regardless of the absolute values of λ_3 and λ_2. This research contradicts Farhi's and Yokoyama's (37) findings, that uptake is always impaired.

TABLE II

APPROXIMATE COMPOSITION OF THE ATMOSPHERE

Substance	Symbol	Molecular wt.	Vol % in Dry Air
Nitrogen	(N_2)	28·016	78·09
Oxygen	(O_2)	32.000	20·95
Carbon Dioxide	(CO_2)	44·011	0·03
Argon	(Ar)	39·944	0·93
Neon	(Ne)	20·183	0·0018
Helium	(He)	4·003	0·000524
Krypton	(Kr)	83·80	0·0001
Hydrogen	(H_2)	2·016	0·000050
Xenon	(Xe)	131·30	0·000008

Compiled from Documenta Geigy, Scientific Tables (6th Ed) edited by Konrad Diem; published by Geigy Pharmaceuticals Ardsley N.Y. 1962.

CHAPTER 7

CONCLUSIONS

The mathematical model presented in this thesis questions the findings of early researchers-that the presence of regional ($\dot{V}_{A/Q}$) inequality always reduces the efficiency of pulmonary gas exchange, Riley and Cournand (6), Rahn (7). It further questions the fact that both elimination and uptake are impaired as demonstrated in the work of Farhi (12), Scrimshire (11), West (16, 17).

West (16) showed that the output of Carbon Dioxide (CO_2) was impaired by 45% of its original value. While Scrimshire (11) showed that impairment of breathing efficiency is substantially influenced by the manner in which ventilation or blood flow is altered in disease. It was also shown in their work,that any imbalance in the normal relationship between blood flow and ventilation must impair overall gas exchange.

The results of this thesis contradict the findings of West (16) and demonstrate,that for some values of solubilities there is a definite enhancement in uptake. The enhancement in uptake may be as high as 20% of its original value, and it was neither ventilation dependent nor perfusion dependent, as was suggested by West (16).

Enhancement in uptake was observed for the values of solubility of uptake (λ_2) = 0.01, 0.1, 1.0 and 10.0 Figure (39). It was found that there was no enhancement for the other values of solubility which was in agreement with West (16) West (77). The maximum enhancement observed in this work was by a factor of 20%.

CHAPTER 8

FUTURE WORK

It has been proved conclusively that there is a definite enhancement in the uptake of gas for some of the values of solubility; when subjected to the mathematical model presented here for a simulated set of inert gases.

An experimental protocol should be drawn using the guidelines detailed below:

1. The subjects should be required to undergo routine lung function tests which should be non-invasive and simple to perform, similar to the ones already carried out routinely in hospitals. During single breath tests (which should be investigated specifically),the subject should be required to inhale and exhale once per test, but may be asked to alter the rate and depth of breathing, position, or gas mixtures.

2. Most of the gas combination mixtures should be mixtures of air or oxygen, plus a small concentration of an inert gas, such as helium or argon. The only potentially dangerous gases to be used in such mixtures will be Carbon Monoxide and Nitrous Oxide.

3. To avoid any harm coming to the subject, Nitrous Oxide should be used at 5% concentration, which is well below analgesic levels. The concentration of Carbon Monoxide should be 0.25% or less. The tests involving these gases should be rapidly performed and should involve only one or two inhalations.

4. The volunteers should be given a detailed typed description of the single breath tests and instructions explaining the procedure.

5. The results for different tracers should be noted and it should be determined what percentage of uptake is enhanced. A theoretical parallel should be drawn.

APPENDIX A

Computer Simulation of the Model

APPENDIX A1

LIST OF VARIABLES USED IN THE SIMULATION

GWENT – Subroutine to simulate gas exchange for uneven vetilation.

GPERF – Subroutine to simulate gas exchange for uneven blood flow.

GHOMO – Subroutine to simulate gas exchange for a homogeous lung.

VIAQ – $\dot{V}_{IA/\dot{Q}}$ ratio

PV – Venous gas tension.

PG – Inspired gas tension.

SO – Solubility of the gas.

UP – Gas uptake.

VQ – $\dot{V}_{A/\dot{Q}}$ ratio

NC – Number of compartments. (ten in this case)

NG – Number of inert gases present.

IO – Data options choosen
1. GWENT
2. GPERF
3. GHOMO

PT – Total alveolar gas pressure.

QT – Cardiac output.

VT – Minute volume.

PI – Inspired gas pressure.

B – Degrees of inequality.

VIAT – Total inspired volume of the gas.

BI – Alveolar ventilation.

Q – Perfusion.

VF – $\dot{V}_{IA/Q}$ ratio

AR – Arterial tension.

VI – Inspired tidal volume.

CVIAQ – Subroutine to calculate $\dot{V}_{IA/Q}$ ratio

A – 2 Parameters for

R – 1 a G.P

B – Degrees of inequality

(0-2.0)

APPENDIX A2

Flowchart for Simulation of The Model

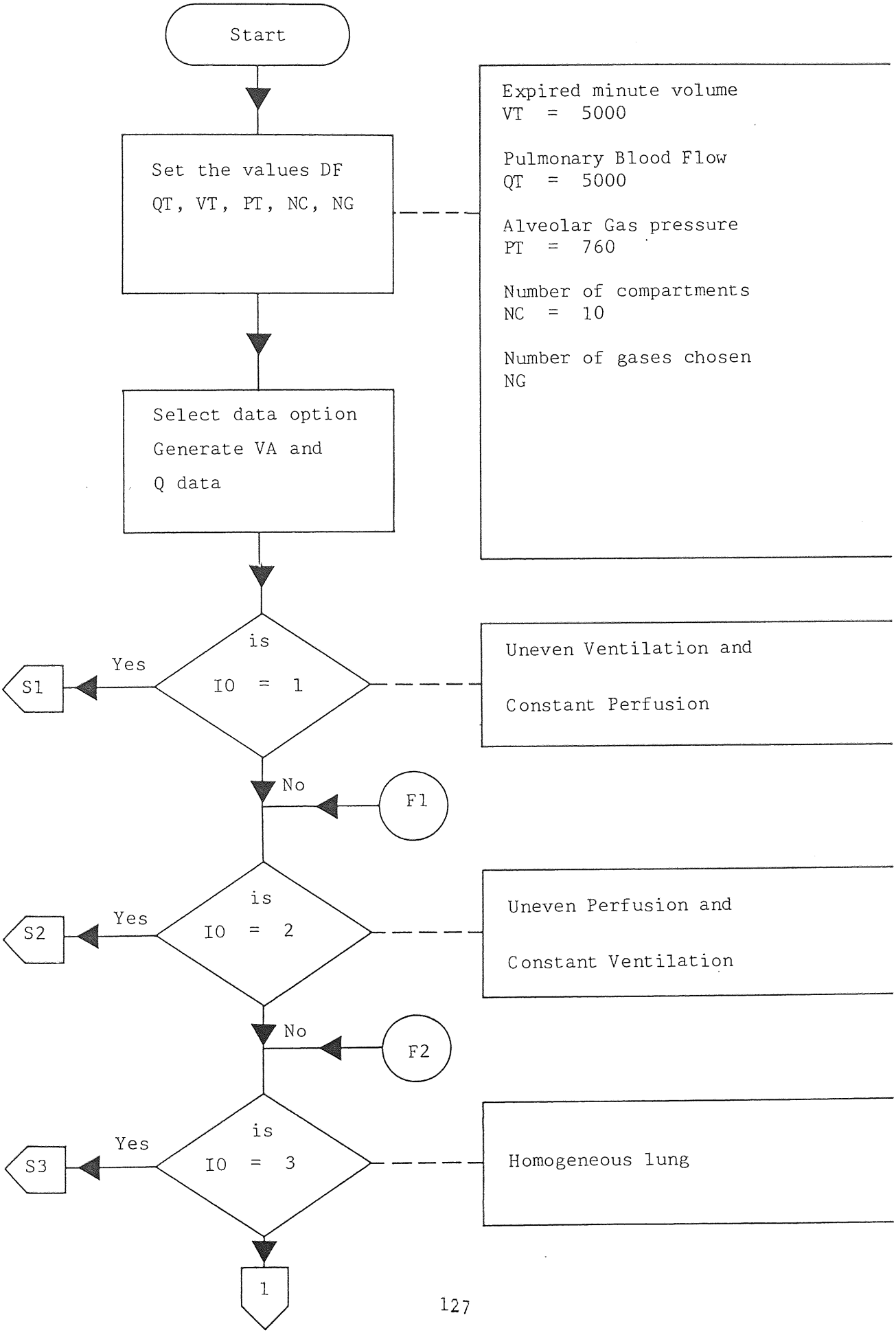

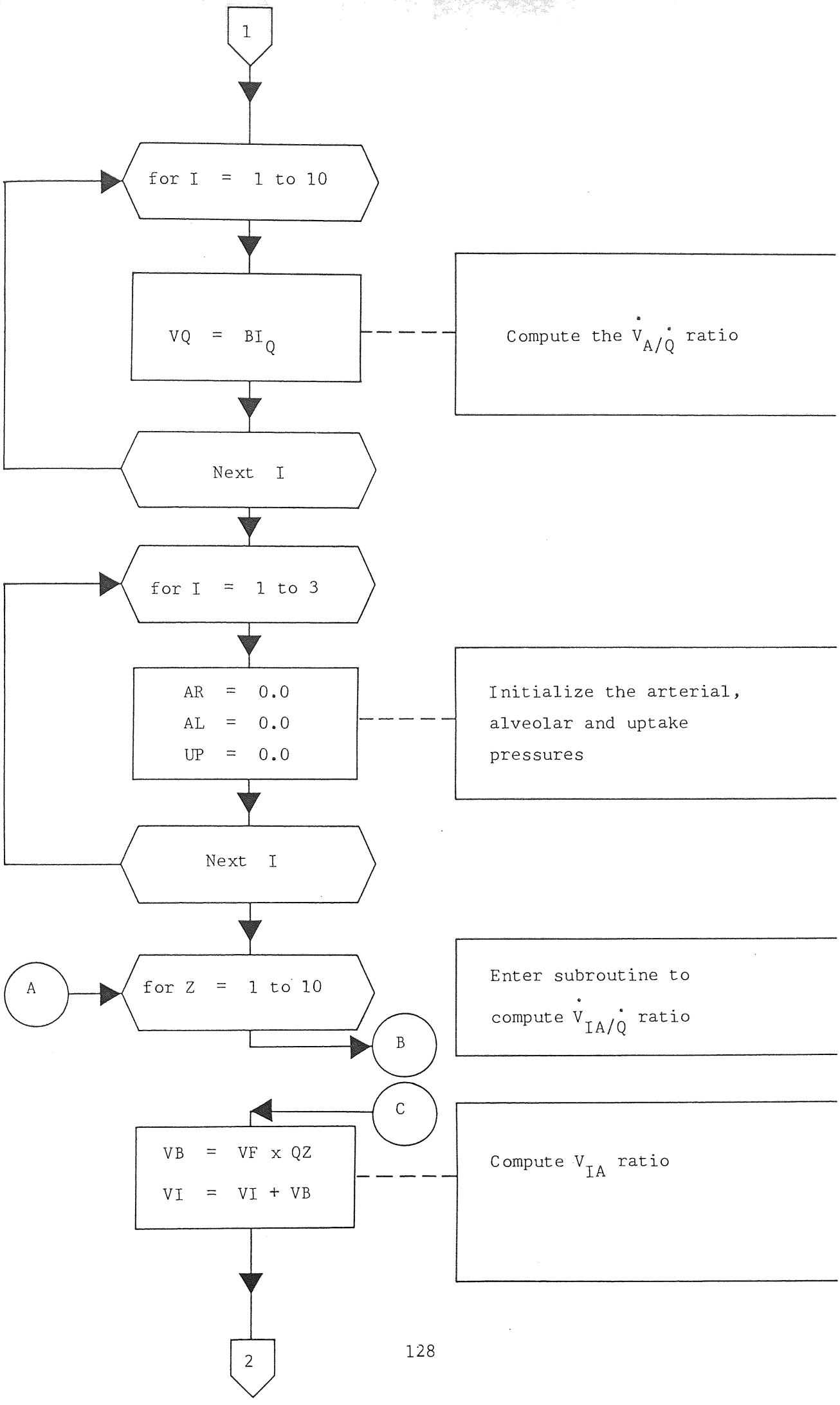
1
for I = 1 to 10
VQ = BI_Q
Compute the V̇A/Q̇ ratio
Next I
for I = 1 to 3
AR = 0.0
AL = 0.0
UP = 0.0
Initialize the arterial, alveolar and uptake pressures
Next I
A
for Z = 1 to 10
Enter subroutine to compute V̇IA/Q̇ ratio
B
C
VB = VF x QZ
VI = VI + VB
Compute VIA ratio
2

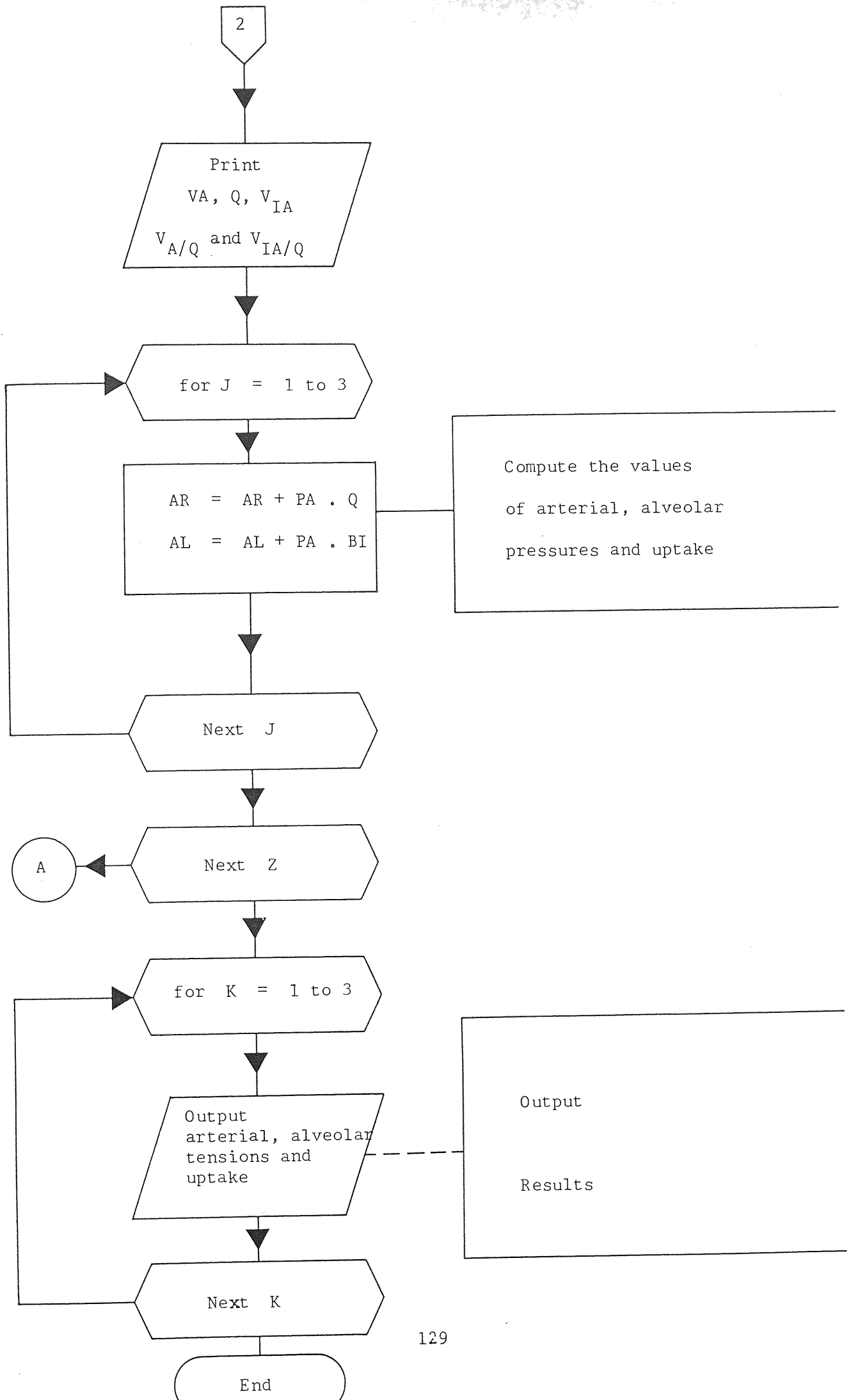
2
Print
VA, Q, V_{IA}
$V_{A/Q}$ and $V_{IA/Q}$
for J = 1 to 3
AR = AR + PA . Q
AL = AL + PA . BI
Compute the values
of arterial, alveolar
pressures and uptake
Next J
A
Next Z
for K = 1 to 3
Output
arterial, alveolar
tensions and
uptake
Output
Results
Next K
End

Subroutine (g vent)

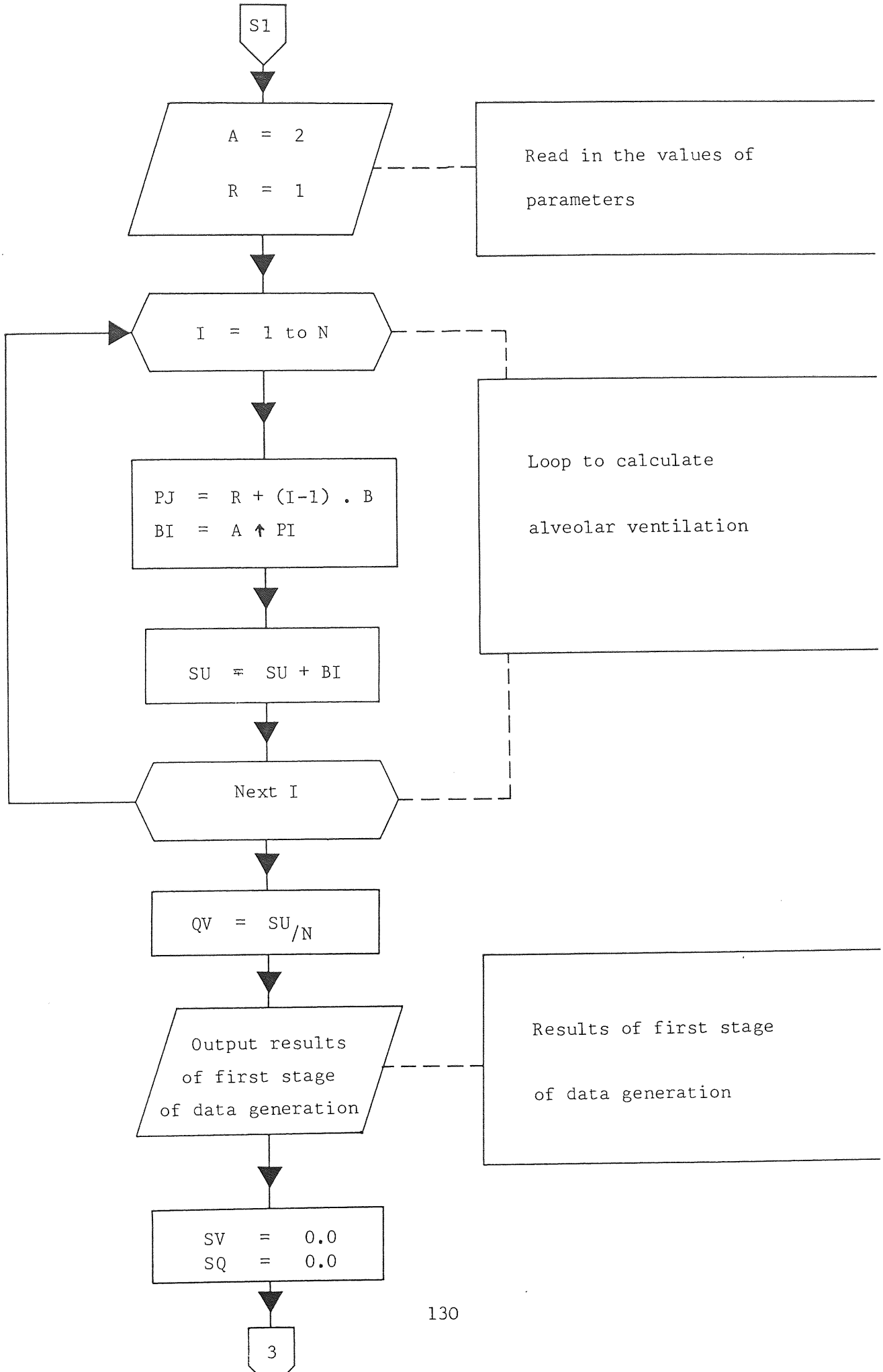

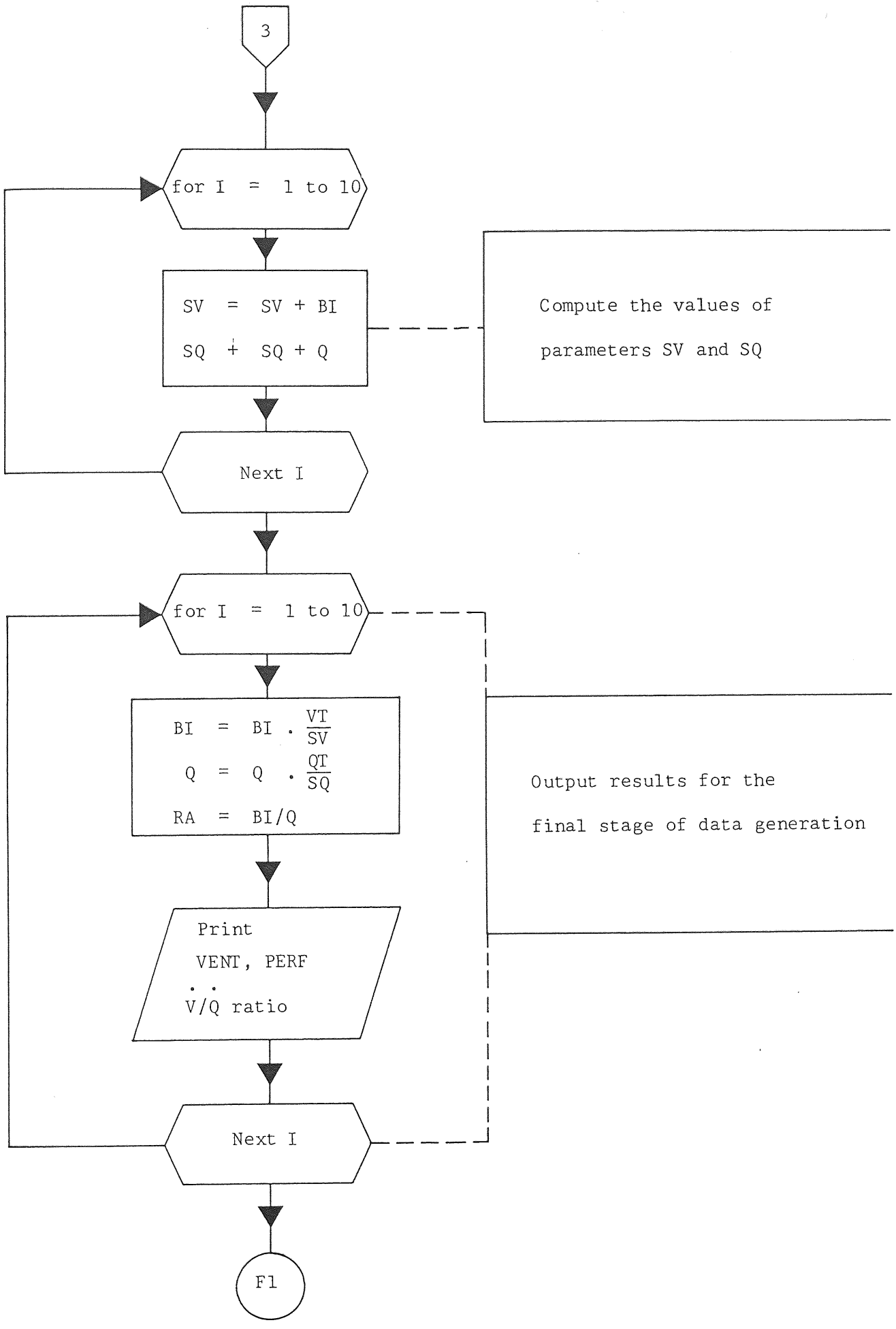
3
for I = 1 to 10
SV = SV + BI
SQ + SQ + Q
Compute the values of
parameters SV and SQ
Next I
for I = 1 to 10
BI = BI . VT/SV
Q = Q . QT/SQ
RA = BI/Q
Output results for the
final stage of data generation
Print
VENT, PERF
. .
V/Q ratio
Next I
F1

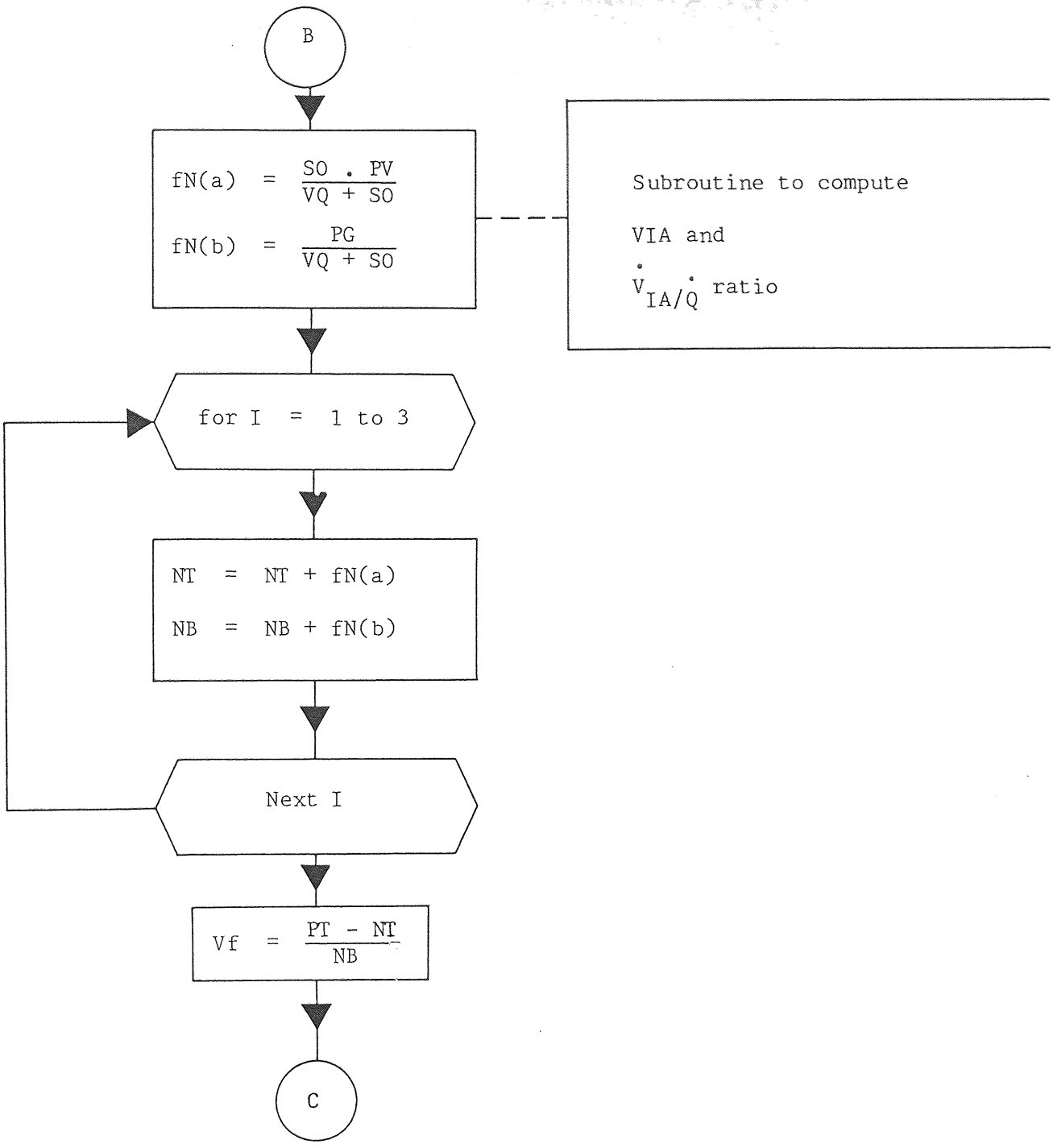
B
$fN(a) = \frac{SO \cdot PV}{VQ + SO}$
$fN(b) = \frac{PG}{VQ + SO}$
Subroutine to compute
VIA and
$\dot{V}_{IA/\dot{Q}}$ ratio
for I = 1 to 3
NT = NT + fN(a)
NB = NB + fN(b)
Next I
$Vf = \frac{PT - NT}{NB}$
C

Subroutine (GPERF), GHOMO)

These subroutines are similar to the previous one (g vent).

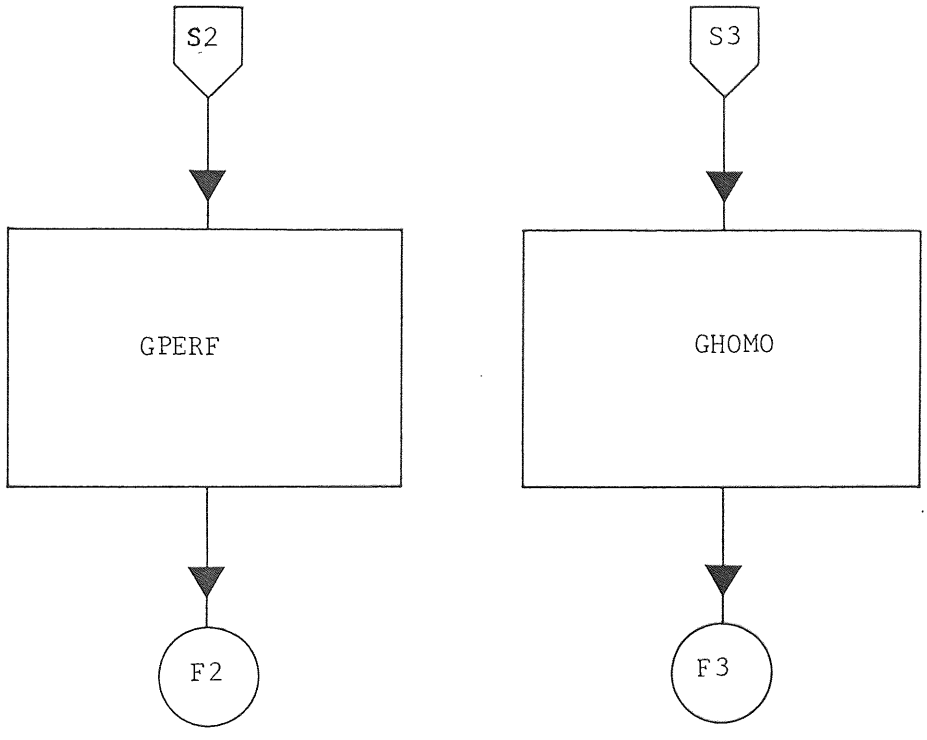

APPENDIX A3

```
2 print"3"
3 print" master multigas"
4 print:print
5 print"this program simulates the simultaneous exchange of"
6 print"several inert gases"
7 print"under pseudo steady-state conditions in non homogeneous"
8 print"lung-model"
9 print"having either unequal ventilation or unequal blood flow"
10 print"data options choosen"
11 print"data options choosen"
12 print"1.....gvent  uneven ventilation"
13 print"2.....gperf  uneven perfusion"
14 print"3.....ghomo  homogeneous lung"
15 print:print
18 print"press any key to start"
19 get x$:if x$=""then 19
20 print"3"
21 print chr$(27)chr$(15)"e l i m i n a t i o n /u p t a k e"
22 print"press any key to start"
23 get x$:if x$=""then 23
24 print"3"
25 print"this model is for gas elimination/uptake(viaq)"
26 print"venous gas tension pv(i)=380.0"insp gas tension pg(i)=0
27 print"press any key to start"
28 get x$:if x$=""then 28
29 print"3"
30 dim va(10),q(100),vq(10),so(10),pg(10)
31 dim pv(10),ar(10),al(10),pa(10),up(10)
32 qt=5000.0
33 vt=5000.0
34 pt=760.0

ready.
```

```
 36 ng=3
 38 nc=10
 40 print:print:print
 45 b$="":for i=1 to 32:b$=b$+" ":next i
 50 print"number of model compartments2 nc="; nc
 60 print"number of inert gases present2 ng=";ng
 70 input"data options       io=";io
 72 print"data option chosen  io=";io
 80 if nc<=0 then print"end of data pack":goto 5080
 90 print"total alveolar pressures2 pt=";pt
100 print"minute volume vt=";vt
102 print"cardiac output q=";qt
105 open4,4
107 cmd4
110 printchr$(27)chr$(15)"e l i m i n a t i o n / u p t a k e"
120 print"simulation of inert gas exchange"
121 print""""""""""""""""""""""""""""""""""""""""
122 print:print:print
123 print"number of gases              ng="ng
124 print"total alveolar gas pressure pt="pt
126 print"expired minute volume ......vt="vt
128 print"pulmonary blood flow  ......qt="qt
132 rem input sol of each gas(so)
134 rem inspired tension(pi),ven ten(pv)
135 print:print:print
136 print#4
138 close4
143 input"b=";b
144 input"so(1)=";so(1):input"so(2)=";so(2)
145 so(3)=0.001
147 pg(1)=380:pg(2)=380:pg(3)=0
150 pv(1)=0  :pv(2)=0  :pv(3)=760
156 open4,4
157 cmd4
158 for i=1to ng step 1

ready.
```

```
158 for i=1to ng step 1
159 print"gas i.........................="i
160 print"blood gas sol at 37 deg c=so(i)="so(i)
161 print"inspired gas tension......pg(i)="pg(i)
162 print"venous tension............pv(i)="pv(i)
164 print:print:print
166 next i
180 rem select data options and generate        va and q data
188 n=nc
190 if io=1 then gosub 3000
200 if io=2 then gosub 4000
210 if io=3 then gosub 5000
220 rem calculate the va/q ratio for each compartment
222 print:print:print
230 for i=1 to nc step 1
240 vq(i)=bi(i)/q(i)
245 next i
250 rem initialize arterial(art)
251 rem alveolar(alv) average values,andtotal inspired volume(viat)
260 vi=0.0
270 for i= 1 to ng step 1
280 ar(i)=0.0
290 al(i)=0.0
300 up(i)=0.0
312 next i
320 rem compute gas exchange for the ithcompartment
330 rem compute alveolar tension of the jth gas
332 print"       va          q          via          va/q       via
334 print:print:print
340 for z= 1 to nc step1
342 gosub 2000
350 vb=vf*q(z)
352 vi=vi+vb
354 f=bi(z):a=5:b=6:gosub 6000:p$=s$
356 f=q(z):a=0:b=8:gosub 6000:p$=p$+s$

ready.
```

```
357 f=vb:a=5:b=13:gosub 6000:p$=p$+s$
358 f=vq(z):a=7:b=7:gosub 6000:p$=p$+s$
360 f=vf:a=7:b=8:gosub 6000:p$=p$+s$
362 f=z:a=0:b=6:gosub 6000:p$=p$+s$
364 printp$
380 for j=1 to ng step 1
390 pa(j)=(vf*pg(j)+so(j)*pv(j))/(vq(z)+so(j))
400 ar(j)=ar(j)+pa(j)*q(z)
410 al(j)=al(j)+pa(j)*bi(z)
420 up(j)=up(j)+q(z)*so(j)*(pa(j)-pv(j))*0.0013157
428 print"gas tension"pa(j)
432 next j
434 next z
450 rem determine average arterial and alveolar tension
452 open4,4:cmd4
460 for k=1to ng step 1
470 ar(k)=ar(k)/qt
480 al(k)=al(k)/vt
481 print:print:print
482 print".....gas="k
484 print".....arterial ten="ar(k)
486 print".....alveolar ten="al(k)
488 print".....uptake.....="up(k)
502 next k
510 ra=vi/vt
511 print:print:print
512 print"expired minute volume vt=";vt
514 print"inspired tidal volume vi=";vi
516 print"inspired /expired vol ra=";ra
530 print#4:close4
540 end
2000 rem subroutine cviaq(pt,sol,vaq,pig,pvg,ng,viaq)
2010 rem routine to determine via/q ratio
2020 def fnt(i)=so(i)*pv(i)/(vq(z)+so(i))
2030 def fnb(i)=pg(i)/(vq(z)+so(i))

ready.
```

```
2032 nt=0.0
2034 nb=0.0
2060 for i=1 to ng step 1
2070 nt=nt+fnt(i)
2080 nb=nb+fnb(i)
2090 next i
2100 vf=(pt-nt)/nb
2110 return
3000 rem subroutine to generate ventilation and blood flow data
3020 rem allexpressed as ml/breaths/compartements
3030 dim bi(100),ra(100)
3040 rem read parameters a,r and b for
3050 a=2
3052 r=1
3056 print"distribution of ventilation chosen (g vent)"
3058 print""""""
```

```
3180 next i
3182 print#4:close4
3190 rem write results of first stage of calculation
3193 print"first stage of data generation"
3194 print""""""""""""""""""""""""""""""""""""""""""""
3195 print:print:print
3196 print"  i       vent       perfusion     v/q-ratio"
3197 print "   "chr$(10);chr$(13)
3198 for i= 1 to n step 1
3199 f=i:a=0:b=3:gosub 6000:p$=s$
3200 f=bi(i):a=5:b=6:gosub 6000:p$=p$+s$
3201 f=q(i):a=2:b=9:gosub 6000:p$=p$+s$
3202 f=ra(i):a=7:b=9:gosub 6000:p$=p$+s$
3204 printp$
3208 next i
3209 print:print:print
3210 rem calculate abs vent and perf
3220 sv=0.0
3230 sq=0.0
3240 for i=1 to n step 1
3250 sv=sv+bi(i)
3260 sq=sq+q(i)
3272 next i
3280 rem scale each v(i) & q(i) such that tot=tidal value
3282 print"final  stage of data generation"
3284 print""""""""""""""""""""""""""""""""""""""""""""
3286 print:print:print
3287 print"  i       vent       perfusion     v/q-ratio"
3288 printchr$(10);chr$(13)
3290 for i=1 to n step 1
3300 bi(i)=bi(i)*vt/sv
3310 q(i)=q(i)*qt/sq
3320 ra(i)=bi(i)/q(i)
3340 rem write scaled vent & perf data
3342 f=i:a=0:b=3:gosub 6000:p$=s$

ready.
```

```
3344 f=bi(i):a=5:b=6:gosub 6000:p$=p$+s$
3345 f=q(i):a=2:b=9:gosub 6000:p$=p$+s$
3346 f=ra(i):a=7:b=9:gosub 6000:p$=p$+s$
3347 printp$
3352 next i
3354 return
3386 print:print:print
4000 rem gperf,routine to generate vent and blood flow data
4010 rem gperf generates a g.p of perf with const vent
4020 rem all expressed as ml of breath/comp
4030 dim  bi(100),ra(100)
4040 rem read parameters a,r,b for g.p  a**(r+(i-1)*b)
4050 a=2
4052 r=1
4056 print"distribution of ventilation chosen (g perf)"
4058 print""""""
```

```
4150 next i
4155 print#4:close4
4160 rem write results of first stage of calculation
4161 print"first stage of data generation"
4162 print""""""""""""""""""""""""""""""""""""""""
4163 print:print:print
4166 print"  i        vent        perfusion      v/q-ratio"
4168 for i=1to n step 1
4169 f=i:a=0:b=3:gosub 6000:p$=s$
4170 f=bi(i):a=5:b=6:gosub 6000:p$=p$+s$
4171 f=q(i):a=2:b=9:gosub 6000:p$=p$+s$
4172 f=ra(i):a=7:b=9:gosub 6000:p$=p$+s$
4174 printp$
4178 next i
4180 rem calculate abs vent and perf
4190 sq=0.0
4200 sv=0.0
4210 for i=1 to n step 1
4220 sq=sq+q(i)
4230 sv=sv+bi(i)
4242 next i
4250 rem scale each v(i) and q(i) such  that the total=tidal value
4251 print"final stage of data generation"
4252 print""""""""""""""""""""""""""""""""""""""""
4253 print:print:print
4254 print"  i        vent        perfusion      v/q-ratio"
4260 for i=1 to n step 1
4270 q(i)=q(i)*qt/sq
4280 bi(i)=bi(i)*vt/sv
4290 ra(i)=bi(i)/q(i)
4400 rem write scaled ventilatio and perfusion data
4402 f=i:a=0:b=3:gosub 6000:p$=s$
4404 f=bi(i):a=5:b=6:gosub 6000:p$=p$+s$
4406 f=q(i):a=2:b=9:gosub 6000:p$=p$+s$

ready.
```

```
4408 f=ra(i):a=7:b=9:gosub 6000:p$=p$+s$
4410 printp$
4412 next i
4420 return
5000 rem subroutine gjoint
5010 rem temporary routine to generate data for a homogeneous lung
5011 print"homogeneous lung option chosen"
5012 print""""""""""""""""""""""""""""""""""""""""""
5013 print:print:print
5014 print"final stage of data generation"
5015 print""""""""""""""""""""""""""""""""""""""""""""""""""
5016 print"  i         vent       perfusion        v/q-ratio"
5020 for i=1 to n step 1
5030 bi(i)=vt
5040 q(i)=qt
5050 ra(i)=bi(i)/q(i)
5055 next i
5060 print i,     bi(1),   q(1),    ra(1)
5070 return
5075 print#4
5077 close4
5080 end
6000 s$=right$(b$+str$(sgn(f)*int(abs(f))),b)
6010 v=abs(f)-int(abs(f))
6020 if a=0 then return
6030 s$=s$+"."
6035 forl=1toa
6040 v=v*10
6050 s$=s$+right$(str$(int(v)),1)
6060 nextl
6070 return
ready.
```

APPENDIX A4

e l i m i n a t i o n / u p t a k e

simulation of inert gas exchange

number of gases ng= 3
total alveolar gas pressure pt= 760
expired minute volume .....vt= 5000
pulmonary blood flow .....qt= 5000

gas i.....= 1
blood gas sol at 37 deg c=so(i)= 1
inspired gas tension.....pg(i)= 380
venous tension.....pv(i)= 0

gas i.....= 2
blood gas sol at 37 deg c=so(i)= 10
inspired gas tension.....pg(i)= 380
venous tension.....pv(i)= 0

gas i.....= 3
blood gas sol at 37 deg c=so(i)= 1e-03
inspired gas tension.....pg(i)= 0
venous tension.....pv(i)= 760

distribution of ventilation chosen (q vent)

.....a= 2

.....r= 1

.....b= 1

first stage of data generation

i	vent	perfusion	v/q-ratio
1	2.00000	204.60	0.0097751
2	4.00000	204.60	0.0195503
3	8.00000	204.60	0.0391006
4	16.00000	204.60	0.0782013
5	32.00000	204.60	0.1564027
6	64.00000	204.60	0.3128054
7	128.00000	204.60	0.6256109
8	256.00000	204.60	1.2512218
9	512.00000	204.60	2.5024437
10	1024.00000	204.60	5.0048875

final stage of data generation

i	vent	perfusion	v/q-ratio
1	4.88758	500.00	0.0097751
2	9.77517	500.00	0.0195503
3	19.55034	500.00	0.0391006
4	39.10068	500.00	0.0782013
5	78.20136	500.00	0.1564027
6	156.40273	500.00	0.3128054
7	312.80547	500.00	0.6256109
8	625.61094	500.00	1.2512218
9	1251.22189	500.00	2.5024437
10	2502.44379	500.00	5.0048875

va	q	via	va/q
4.88758	500	832.11879	0.0097751

gas tension 626.288208
gas tension 63.1792694
gas tension 70.5325229

9.77517	500	880.35638	0.0195503

gas tension 656.241113
gas tension 66.7765347
gas tension 36.9823527

19.55034	500	918.15448	0.0391006

gas tension 671.539745
gas tension 69.50796
gas tension 18.9522951

39.10068	500	961.70172	0.0782013

gas tension 677.882009
gas tension 72.5221975
gas tension 9.5957938

78.20136	500	1031.59867	0.1564027

gas tension 677.97746
gas tension 77.1941613
gas tension 4.82837856

156.40273	500	1160.84771	0.3128054

gas tension 672.029693
gas tension 85.5484245
gas tension 2.42188255

312.80547	500	1407.65906	0.6256109

gas tension 658.103891
gas tension 100.683236
gas tension 1.2128738

625.61094	500	1874.38438	1.2512218

gas tension 632.781752
gas tension 126.611327
gas tension .606921187

1251.22189	500	2734.89050	2.5024437

gas tension 593.447578
gas tension 166.248841
gas tension .303581811

2502.44379	500	4287.75001	5.0048875

gas tension 542.672942
gas tension 217.175237
gas tension .151821228

```
.....................gas= 1
.............arterial ten= 640.896439
.............alveolar ten= 581.902653
.............uptake......= 4216.13722


.....................gas= 2
.............arterial ten= 104.544719
.............alveolar ten= 177.351905
.............uptake......= 6877.47432


.....................gas= 3
.............arterial ten= 14.5588424
.............alveolar ten= .745441158
.............uptake......=-4.90388466


expired minute volume vt= 5000
inspired tidal volume vi= 16089.4618
inspired /expired vol ra= 3.21789235
```

APPENDIX B

Solution of The Cubic Equation

Using Newton Raphson Technique

APPENDIX B1

List of Variables

P(0) - Coefficient of x^3

P(1) - Coefficient of x^2

P(2) - Coefficient of x

P(3) - Constant

r(1,?) - Real part of the root

r(2,?) - Imaginary part of the root

APPENDIX B2

Flowchart for Solving A Cubic

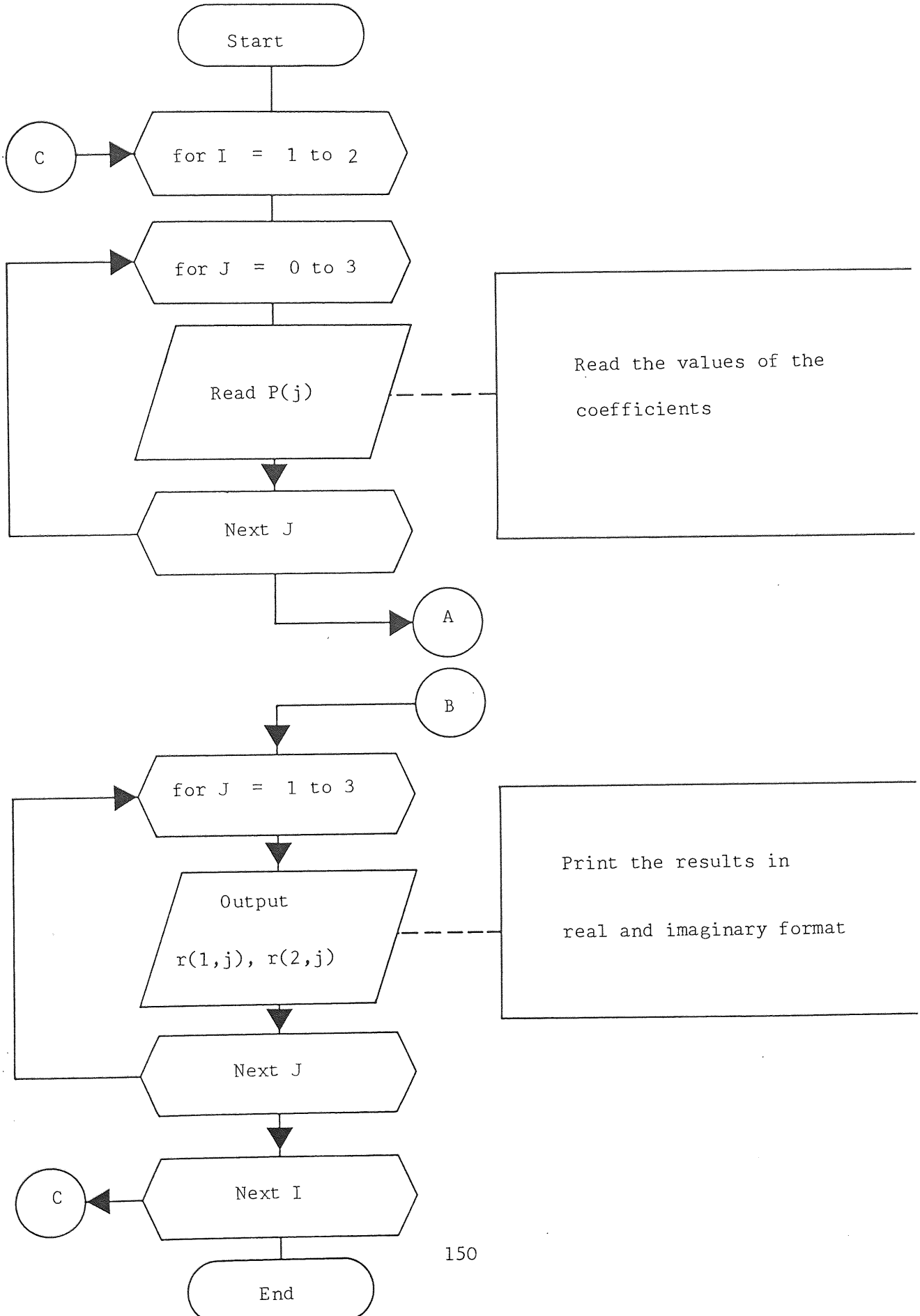

Subroutine To Solve A Cubic Equation

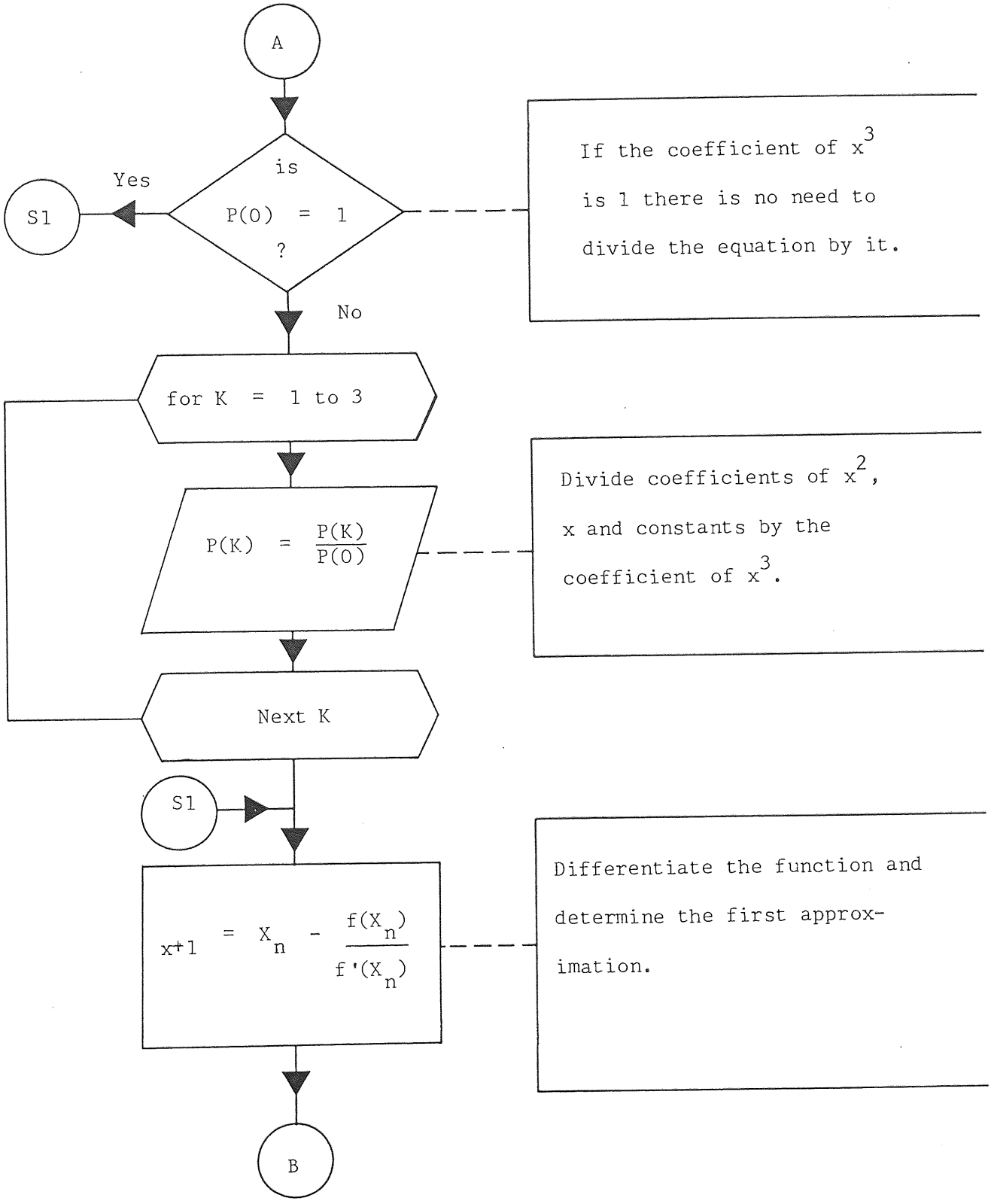

APPENDIX B3

```
50000 rem==cubic
50002 rem "PROGRAM TO SOLVE A CUBIC EQUATION"
50010 rem  written: 09/06/82, naqvi
50020 rem  updated: 09/06/82, naqvi
50030 rem--driver
50040 dim r(2,3),p(3)
50050 for i=1 to 2
50060 rem  get the data
50070 for j=0 to 3
50080 read p(j)
50090 if p(j)>=0 then print"+";
50100 print p(j);"x^";chr$(j+48);" ";
50110 next j
50120 print " = 0"
50130 gosub50250:rem  solve the cubic
50140 rem  print the solution
50150 print"Solutions are
50160 for j=1 to 3
50170 print r(1,j);:ifr(2,j)>=0thenprint"+";
50180 print r(2,j);"j"
50190 next j
50200 print""
50210 next i
50220 end
50230 data 1,4,1,4
50240 data 1,1,-9,-9
50250 rem==solve a cubic
50270 rem  algorithm 326
50280 rem  roots of low order polynomial equations
50290 rem  t.r.f. nonweiler
50300 rem  cacm 11:4, april 1968, 269-270
50310 rem
50320 rem  failure occurs if p(0)=0.
50325 rem assume that 0<atn(x)<pi/2 for x>0
50330 rem  input should be such that
```

ready.

```
50350 rem     p(0).x^3 + p(1).x^2 + p(2).x + p(3) = 0
50370 rem  output is in the array r where
50390 rem     r(1,?) is the real part
50400 rem     r(2,?) is the imaginary part
50410 if p(0)<>1 then for k=1 to 3: p(k)=p(k)/p(0): next k
50420 s=p(1)/3:t=s*p(1):b=0.5*(s*(t/1.5-p(2))+p(3)):t=(t-p(2))/3
50430 c=t^3:d=b*b-c
50440 if d<0 goto50530
50450 d=(sqr(d)+abs(b))^(1/3)
50460 ifd=0goto50490
50470 b=d:ifb>0thenb=-d
50480 c=t/b
50490 d=sqr(.75)*(b-c):r(2,2)=d:b=b+c:c=-0.5*b-s:r(1,2)=c
50500 if(b>0)=(s<=0)thenr(1,1)=c:r(2,1)=-d:r(1,3)=b-s
50502 r(2,3)=0:goto50520
50510 r(1,1)=b-s:r(2,1)=0:r(1,3)=c:r(2,3)=-d
50520 return
50530 ifb=0thend=atn(1)/1.5:goto50550
50540 d=atn(sqr(-d)/abs(b))/3
50550 ifb<0thenb=sqr(t)*2:goto50570
50560 b=-sqr(t)*2
50570 c=cos(d)*b
50580 t=-sqr(.75)*sin(d)*b-.5*c
50590 d=-t-c-s:c=c-s:t=t-s
50600 ifabs(c)>abs(t)thenr(1,3)=c:goto50620
50610 r(1,3)=t:t=c
50620 ifabs(d)>abs(t)thenr(1,2)=d:goto50640
50630 r(1,2)=t:t=d
50640 r(1,1)=t
50650 fork=1to3:r(2,k)=0:next
50660 return
63998 rem      scratch"cubic",d0:dsave"cubic",d0:verify"*",8
63999 rem      scratch"cubic",d1:dsave"cubic",d1:verify"*",8
ready.
```

REFERENCES

1. Nunn, J.F.
The lung as a black box
Can Anaesthetists Soc. J. 13: 81 - 97, 1966

2. Miller, W.S.
The lung
Springfield, III., Charles C Thomas, 1937

3. Bohr, C.
Ueber die lungenathmug
Skand Arch Physiol 2: 236, 1891
(as quoted by Scrimshire thesis ref (23))

4. Brink, F., Jr.
Handbook of Respiratory Data in Aviation
Washington, D.C; subcommittee on Oxygen and Anoxia of the committe in Aviation Medicine, Division of Medical Sciences, National Research in Aviation Medicine, Division of Medical Sciences, National Research counsil acting for the committe on Medical Research, office of Scientific Research and Development,1944.

5. Helmholz, H.E., Jr., J.B. Bateman and W.M. Boothby.
The effects of altitude anoxia on the respiratory process
J. Aviation Med 15: 366, 1944.

6. Riley, R.L. and A. Cournand.
'Ideal' alveolar air and the analysis of ventilation - perfusion relationships in the lungs.
J. Appl. Physiol 1: 825 , 1949

7. Rahn, H
A concept of mean alveolar air and the ventilation - bloodflow relationships during pulmonary gas exchange.
Am. J. Physiol. 158: 21, 1949.

8. Farhi., L.E., and Rahn, H.
A theoretical analysis of the alveolar - arterial oxygen difference with special reference to the distribution effect.
J. Appl. Physiol. 7: 699, 1955

9. West, J.B.
Regional differences in gas exchange in the lung of erect man
J. Appl. Physiol. 17: 893, 1962.

10. Kelman, G.R.
Digital Computer sub Routines for the conversion of Oxygen tension into saturation.
J. Appl. Physiol 21: 1375, 1966.

11. Scrimshire, D.A
Theoretical analysis of independent $\dot{V}_A$ and $\dot{Q}$ inequalities upon pulmonary gas exchange
Respir Physiol. 29: 163, 1977.

12. Farhi, L.E.
Elimination of inert gas by the lung
Respir. Physiol 3:1, 1967.

13. Shah, J., J.G. Jones, J. Galvin and P.J. Tomlin.
Pulmonary gas exchange during induction of anaesthesia with nitrous oxide in seated subjects.
Brit. J. Anaesth. 43: 1013, 1971.

14. Farhi, L.E., A.J. Olszowka.,
Analysis of alveolar gas exchange in the presence of soluble inert gases.
Respir. Physiol. 5:53, 1968.

15. Dantzker, D.R., P.D. Wagner., J.B. West.,
Instablity of lung units with low $\dot{V}_{A/Q}$ ratios during O_2 breathing.
J. Appl. Physiol 38: 886, 1975.

16. West, J.B.,
Ventilation - perfusion inequality and overall gas exchange in computer models of the lung.
Respir. Physiol. 7: 88, 1969.

17. West., J.B.,
Ventilation/blood flow and gas exchange
2nd ed. Oxford: Blackwell Scientific publications, 1970.

18. Wagner., P.D.,
Susceptibility of different gases to ventilation - perfusions inequality.
Am. Phys Science: 372, 1979.

19. Gurtner, H.P., W.A. Briscoe and A. Cournand
studies of the $V_{A/\dot{Q}}$ relationships in the lungs of subjects with chronic pulmonary emphysema, following a single intravenous injection of radioactive Krypton (Kr^{85}) I. Presentation and Validation of a theoretical model.
J. Clin. Invest 39: 1080 - 1089, 1960.

20. Briscoe, W.A. and A. Cournand.
The degree of ventilation of blood perfusion and of ventilation within the emphysematous lung, and some related considerations.
In: Ciba foundation symposium on Pulmonary Structure and function.
London: J.S.A Churchill LTD., 1962.

21. Rochester, D.F., R.A. Brown, W.A. Wichern and H.N. Frilts,
Comparison of alveolar and arterial concentration of Kr^{85} and ^{133}Xe infused intravenously in man.
J. Appl. Physiol 22, 423 - 430: 1967.

22. Scrimshire, D.A. and P.J. Tomlin.
Gas exchange during the initial stages of N_2O uptake and elimination in a lung model.
J. Appl. Physiol. 775 - 789: 1973.

23. Scrimshire, D.A.
Theoretical analysis of gas exchange in a lung model
PhD Thesis University of Aston in Birmingham, England: 1973.

24. Stoelting, R.K., and Edmond I. E, II
An additional explanation for the second gas effect: a concentrating effect.
Anesth. 30: 273 - 277, 1969.

25. Nunn, J.F.
Applied Respiratory Physiology with special reference to Anaesthesia
London: Butterworths, 1969.

26. Weibel, E.R. and D.M. Gomez.
Architecture of the Human Lung
Science 137: 577, 1962.

27. Weibel, E.R.
Marphometry of the Human Lung
Berlin: Springer, 1963.

28. Angus G.E. and W.M. Thurlbeck.
Number of alveoli in the human lung.
J. Appl Physiol 32, 483-485: 1972

29. Klocke, R.A.
Carbon Dioxide transport in "Extrapulmonary Manifestation of Respiratory Disease"
(E.D. Robin Ed) 31 - 343. Dekker, New York, 1978

30 Holland, R.A.B. and Forster, R.E.
Effect of temperature on rate of CO_2 uptake by human red cell suspensions.
Am. J. Physiol 228, 1589 - 96: 1975.

31. McClintic, J.R.
Physiology of the human body,
2nd edition, John Wiley & sons (publishers): 1978

32. Adair, G.S
The haemoglobin system. VI. The oxygen dissociation curve of haemoglobin.
J. Biol. Chem 63: 529, 1925.

33. Staub, N.C.
A simple small oxygen electrode
J. App. Physiol 16: 192, 1961.

34. Staub, N.C.
Alveolar - arterial oxygen tension gradient due to diffusion
J. App. Physiol, 18: 673, 1963.

35. Colburn, W.E., J.W. Evans, and J.B. West
Analysis of effect of the solublity on gas exchange in nonhomogenous lungs.
J. Appl. Physiol 37: 547 - 551, 1974.

36. Evans, J.W., P.D. Wagner and J.B. West.
Conditions for reduction of pulmonary gas transfer by ventilation-perfusion inequality.
J. Appl. Physiol 36: 533 - 537, 1974.

37. Farhi, L.E., and T. Yokoyama
Effects of ventilation - perfusion inequality on elimination of inert gases.
Resp. Physiol, 3: 12 - 20, 1967.

38. Yokoyama, T., L.E. Farhi
Study of ventilation - perfusion ratio distribution in the anaesthetized dog by multiple inert gas washout.
Resp, Physiol. 3: 166 - 176, 1967

39. Wagner, P.D., P.F. Naumann; and R.B. Lavavuso
Simultaneous measurement of eight foreign gases in blood gas chromatography.

J. Appl. Physiol. 36, 600 - 605: 1974.

40. Wagner, P.D., H.A. Saltzman and J.B. West,
Measurement of continuous distributions of ventilations - perfusion ratios: Theory.
J. App. Physiol: 36, 588 - 599: 1974.

41. Olszowka, A.J.
Can $\dot{V}_{A/Q}$ distribution in the lung be recovered from inert gas retention data.
Respir. Physiol, 25, 191 - 198: 1975.

42. Jaliwala, S.A., R.E. Mates., and F.J. Klocke.,
An efficient optimization technique for recovering ventilation-perfusion distributions from inert gas data.
Effects of random experimental error.
J. Clin. Invest. 55, 188 - 192: 1975.

43. Evans, J.W., and P.D. Wagner.
Limits on $\dot{V}_{A/Q}$ distributions from analysis of experimental inert gas elimination.
J. Appl Physiol. 42, 889 - 898: 1977.

44. Canfield, R.E., and Rahn, H
Arterial - alveolar Na gas pressure differences due to ventilation-perfusion variations.
J. Appl. Physiol. 10, 165 - 172: 1957.

45. Fink, B.R.
Diffusion anoxia,
Anaesthesiology 16, 511 - 519: 1955.

46. Epstein, R.M., H. Rackon; E. Salantire.,
and L.L, Woff.,
Influence of the concentration effect on the uptake of anaesthetic mixture: the second gas effect.
Anaesthesiology 25, 364 - 371: 1964.

47. Haldane, J.S.
"Methods of Air Analysis"
3rd ed. Griffin, 1920.

48. Krogh, A.
On the mechanism of gas exchange in the lungs.
Skand Arch Physiol 23, 248 - 278: 1910.

49. Evans, J.W.
On steady state inert gas exchange
Math. Biosci. 46, 209 - 222, 1979.

50. Zuntz, N
Physiologie der Blutgase and des respiratorischen gaswechsels.
In: "Handbuch der Physiologie "
(L. Hermann, ed), Vol. 4, part 2, 1 - 162 vogel Leipzig: 1882.

51. Rohrer, F.
Der Stromungswiderstand in den menschlichen Atemwegen und der Einfluss der unregelmassigen verzweigung des Bronchialsystems auf den Atmungsverlauf in verschiedenen Lungenbezirken.
Pfluegers Arch. gas physiol. 162, 225 - 229: 1915
(Engl. transl in "Translations in Respiratory Physiology")
(J.B. West ed) 3 - 66. Dawden, Hutchiuson & Ross, Strandsbury, Pennsylvania, 1975).

52. Fowler, W.S.
Lung function studies II. The respiratory dead space
Am. J. Physiol 154, 405 - 416: 1948.

53. Enghoff, H.
Volume inefficax. Bemerkungen zur Frage des Schadlichen Raumes.
Upsala Laekarefoeren. Foerh. 44, 191 - 218: 1938.

54. Riley, R.L., J.L. Lilienthal , D.D, Proemmel, and R.E. Franke,
On the determination of the physiologically effective pressures of oxygen and Carbon Dioxide in alveolar air.
Am. J. Physiol. 147, 191 - 198: 1946.

55. Lilienthal, J.L., Jr. R.L. Riley. D.D. Proemmel., and R.E. Franke.,
An experimental analysis in man of the oxygen pressure gradient from alveolar air to arterial blood during rest and exercise at sea level and at altitudes.
Am. J. Physiol: 147, 199 - 216: 1946.

56. Riley, R.L. and H.S. Permutt.,
Venous admixture component of the $AaPo_2$ gradient
J. Appl. Physiol 35, 430 - 431, 1973.

57. Ball , W.C., P.B. Stewart, L.G.S. Newham and D.V. Bates.
Regional pulmonary dunction studied with $Xenon^{133}$
J. Clin. Jnvert. 41,519 - 531: 1962

58. West; J.B. and C.T. Dollery
Distribution of blood flow and ventilation - perfusion ratio in the lung, measured with radioactive CO_2.
J. Appl. Physiol. 15, 405 - 410, 1960

59. Forster, R.E.
Rate of gas uptake by red cells.
In: Handbook, of physiology, Respiration Volume I.
Washington, D.C.: American Physiology Society, 1964.

60. Bates, D.V. and R.V. Christie.
Respiratory function in Disease.
Philadelphia: W.B. Saunders Company, 1964.

61. Noehren, T.H.
Pulmonary clearence of inert gases with particular reference to ethyl - ether.
J. Appl. Physiol. 17: 795 - 798: 1962.

62. Kety, S.S
Theory and applications of exchange of inert gases at lungs and tissues.
Pharmacol. Rev. 3:1, 1951.

63. Severinghaus, J.W.
Role of lung factors. In: uptake and distribution of anaesthetic agents. New York: Mc. Grew - H:II Book Company, Inc., 1962.

64. Wagner, P.D., and J.W. Evans conditions for equivalance of gas exchange in series and parallel models of the lungs.
Respir. Physiol. 31, 117 - 138: 1977.

65. Briscoe, W.A
A method for dealing with data concerning uneven ventilation of the lung and its effect on blood gas transfer.
J. Appl. Physiol. 14, 291 - 298: 1959.

66. Briscoe, W.A.
Comparison between alveolar arterial gradient predicted from mixing studies and the observed gradient
J. App. Physiol. 14, 299 - 304: 1959.

67. Wagner, P.D., H.A. Saltzman., J.B. West
Measurement of continuous distributions of ventilation - perfusion ratios: Theory
J. Appl. Physiol. 36, 588 - 599: 1974.

68. Farhi. L.E., and H. Rahn
A theorerical analysis of the alveolar - arterial O_2 difference with special reference to the distribution effect.
J. Appl. Physiol. 7, 699 - 703: 1955.

69. Kelman, G.R.
A new lung model: An Investigation with the aid of a digital computer.
Computers an Biomedical Research 3; 241: 1970.

70. Pappenheimer, J.R., J. Comroe, A. Cournand, J.K. W. Ferguson, G.F. Filley, W.S. Fowler, J.S. Gray, J.F. Helmholtz, A.B. Otis, H. Rahn and R.L. Riley.
Standardization of definition and symbols in respiratory physiology.
Fedn. Proc. 9: 602, 1950

71. Scrimshire, D.A and Naqvi, K.A
Quantitative modelling of pulmonary gas exchange In: Conference proceedings of the first international conference on Applied Modelling and Simulation volume V Lyon France, 82 - 86, 1981.

72. West, J.B
Topographical distribution of blood flow in the lung.
In; Handbook of physiology, Respiration Volume II.
American physiological society, Washington, D,C., 1965.

73. West, J.B., P.D. Wagner, and C.M.W. Derks.,
gas exchange in distribution of $\dot{V}_{A/Q}$ ratios:
partial pressure - solubility diagram
J. Appl. Physiol. 37: 533 - 540, 1974.

74. Suskind, M., H. Rahn.,
Relationship between caridiac output and ventilation and gas transport, with particular reference to anaesthesia;
J. Appl. Physiol: 7:59, 1954.

75. Rahn, H.,
Role of N_2 in various biological processes with particular reference to the lung.
In: Harvey Lectures, series 55, New York, Academic Press
pp. 173 - 199: 1961.

76. Farhi, L.E
Atmospheric Nitrogen and its role in modern medicine
J. Am. Med Assoc 188, 984 - 993: 1964.

77. West J.B.,
Effect of slope and shape of dissociation curve on pulmonary gas exchange.
Resp. Physiol. 8, 66 - 85: 1969/1970.